AD_____

Award Number: DAMD17-01-1-0423

TITLE: Assessing Vascular Oxygen Dynamics for Breast Tumor Prognosis: Comparison Between MR BOLD and Near Infrared Method

PRINCIPAL INVESTIGATOR: Yueqing Gu, Ph.D.

CONTRACTING ORGANIZATION: The University of Texas at Arlington
Arlington, Texas 76019

REPORT DATE: September 2003

TYPE OF REPORT: Annual Summary

PREPARED FOR: U.S. Army Medical Research and Materiel Command
Fort Detrick, Maryland 21702-5012

REPORT DOCUMENTATION PAGE

Form Approved
OMB No. 074-0188

1. AGENCY USE ONLY (Leave blank)	2. REPORT DATE	3. REPORT TYPE AND DATES COVERED
	September 2003	Annual Summary (1 Sep 2002 - 31 Aug 2003)

4. TITLE AND SUBTITLE
Assessing Vascular Oxygen Dynamics for Breast Tumor Prognosis: Comparison Between MR BOLD and Near Infrared Method

5. FUNDING NUMBERS
DAMD17-01-1-0423

6. AUTHOR(S)
Yueqing Gu, Ph.D.

7. PERFORMING ORGANIZATION NAME(S) AND ADDRESS(ES)
The University of Texas at Arlington
Arlington, Texas 76019

E-Mail: guyueqing_99@yahoo.com

8. PERFORMING ORGANIZATION REPORT NUMBER

9. SPONSORING / MONITORING AGENCY NAME(S) AND ADDRESS(ES)
U.S. Army Medical Research and Materiel Command
Fort Detrick, Maryland 21702-5012

10. SPONSORING / MONITORING AGENCY REPORT NUMBER

11. SUPPLEMENTARY NOTES
Original contains color plates: All DTIC reproductions will be in black and white.

12a. DISTRIBUTION / AVAILABILITY STATEMENT
Approved for Public Release; Distribution Unlimited

12b. DISTRIBUTION CODE

13. ABSTRACT (Maximum 200 Words)
The goal of this research is to investigate breast tumor vascular oxygenation, $[HbO_2]$, and total hemoglobin concentration, $[Hb]_{total}$, with respect to different interventions by correlating the results of Near Infrared Spectorscopy (NIRS) with BOLD in MRI. Up to now, I have demonstrated the capability and accuracy of NIRS as a non-invasive real time monitoring tool for tumor vascular oxygenation and blood volume by comparing the simultaneous measurements among three oxygen-related indicators and using ^{19}F MRS of PFOB for blood volume measurement, respectively. Hyperoxic gases and hydralazine interventions have been intensively investigated by NIRS. Results showed that carbogen and oxygen breathing significantly elevate breast tumor oxygenation without difference in terms of magnitude, but with sluggish response in carbogen breathing. CO_2 contributes a small portion to the elevation of $\Delta[HbO_2]$. Only ~40% of the breast tumors have good response in $\Delta[Hb]_{total}$ with respect to hyperxoci intervention. Administration of hydralazine effectively reduced both $\Delta[HbO_2]$ and $\Delta[Hb]_{total}$ in all the breast tumors. Meanwhile, I performed simultaneous measurements of tumor vascular oxygenation by NIRS and BOLD MRI, respectively. Results indicated the consistency of tumor global oxygenation obtained form the two simultaneous, independent measurements, with heterogeneous response displayed inside breast tumors in BOLD MR images, which may help us better understand, and further, interpret the mechanism of BOLD MRI.

14. SUBJECT TERMS
Technology development, radiologic sciences, tumor therapy planning and prognosis, tumor physiology monitoring

15. NUMBER OF PAGES
87

16. PRICE CODE

17. SECURITY CLASSIFICATION OF REPORT	18. SECURITY CLASSIFICATION OF THIS PAGE	19. SECURITY CLASSIFICATION OF ABSTRACT	20. LIMITATION OF ABSTRACT
Unclassified	Unclassified	Unclassified	Unlimited

Table of Contents

Cover.....1

SF 298.....2

Table of Contents.....3

Introduction.....4

Objective 4

Body of Report 4

Key Research Accomplishments.....12

Reportable Outcomes.....12

Conclusions.....13

References.....14

Appendices.....

2002-2003 ANNUAL PROGRESS REPORT (YEAR 2)

This report presents the specific aims and accomplishments of our breast cancer research project during the second year of funding sponsored by the U.S. Department of the Army. It covers our activities from November 1, 2002 to October 31, 2003.

Introduction

It is generally recognized that hypoxic or even anoxic regions in solid- growing tumors may limit the efficacy of non-surgical therapy, including radiotherapy, photodynamic therapy, and chemotherapy[1,2,3,4]. Inhalation of hyperoxic gases was considered to be one of the most effective methods to reduce tumor hypoxia, and thus, to enhance the efficiency of standard therapies in experimental malignancies as well as in human tumors. However, the therapeutic benefits of respiratory hyperoxic gases are diverse, depending on the tumor types and individuals[5,6,7]. Accordingly, accurate assessment of tumor oxygenation at various stages of tumor growth and in response to interventions may provide a better understanding of tumor development and may serve as a prognostic indicator for treatment outcome, potentially allowing therapy to be tailored to individual characteristics. MRI BOLD (Blood Oxygenation Level Dependent) is a clinically accepted modality for *in vivo* non-invasively imaging the dynamic changes of vascular oxygenation based on the intrinsic agent, deoxygenated hemoglobin[8]. However, interpretation of the BOLD signal is confounded by variation in hemoglobin concentration, saturation and blood flow[9]. Near Infrared Spectroscopy (NIRS) offers a noninvasive real time monitoring way to differentiate the changes in hemoglobin saturation and concentration in breast tumors caused by respiratory intervention[10,11,12]. Simultaneous measurements between NIRS and MRI BOLD proposed in this project may allow better investigating and understanding of the physiological mechanism in the breast tumors under respiratory interventions, and further, to interpret the BOLD signals. .

Objective:

The overall project has three specific aims:

Aim 1: To investigate heterogeneity of SO_2 in the tumor vascular bed of breast tumors, using a NIRS system against the fiber optic needle measurements.

Aim 2: To compare and correlate the measurement results of the breast tumors under 100% O_2 intervention taken simultaneously from the NIR oximeter and from the BOLD method.

Aim 3: To study the influence of five interventions on SO_2 and BOLD on breast tumors with various sizes using both the NIR oximeter and the MRI BOLD method.

Specifically, Task 3 was planned for months 12-18 to accomplish Aim 2, and Task 4 was planned for months 18-36 to accomplish Aim 3:

Task 3: To compare/correlate the experimental results of the breast tumors under 100% O_2 intervention from the 3-channel NIR oximeter and from the BOLD method ***(months 12-18)***:

Task 4: To study the influence of five interventions on SO_2 and the BOLD effects of breast tumors with various sizes using both the 3-channel NIR oximeter and the MRI BOLD method. ***(months 18-36)***:

Body of the Report

The PI has made significant efforts to accomplish the tasks. The overall purpose of this project is to investigate vascular oxygen dynamics in breast tumors by correlating two methods: NIRS and BLOD in

MRI. In the first year, I have obtained the specific skills for handing laboratory animals and appropriate knowledge of tumor physiology, NIR Oximeter and BOLD MRI. Meanwhile, I have conducted primary experiments on both phantom and breast tumors for evaluating NIRS system and assessing the dynamic response of breast tumor oxygenation with respect to respiratory challenges (See the annual report in year 1). During the second year (Nov.1, 2002~Oct.31,2003), I performed intensive study on tumor vascular oxygenation and total blood volume with respect to different external interventions. Also, I conduct the simultaneous measurement between NIRS and MRI BOLD. I have mainly accomplished the task proposed in this period, as reported below:

1. Evaluation of tumor total hemoglobin concentration acquired from NIRS by using ^{19}F MRS of PFOB

1.1 Motivation of this study

Near infrared spectroscopy (NIRS) possess the feature for *in vivo* non-invasive real time monitoring of tumor vascular oxygenation and total hemoglobin concentration. Previously, we have demonstrated the practicability and accuracy of NIRS for the measurement of tumor vascular oxygenation changes (HbO_2), under various therapeutic interventions, by comparative measurements with a pulse oximeter[10], needle electrode, MRI[11] and multi-channel FOXY™ oxygen needle probe[12]. However, unlike the often observed, highly repeatable tumor HbO_2 changes caused by hyperoxic gas inhalations, tumor vascular hemoglobin concentrations, $[Hb]_{total}$, measured by NIRS were often largely variable from tumor to tumor, without consistent patterns[13]. Because of the inconclusive observations in $\Delta[Hb]_{total}$, we have wondered whether the methodology of NIRS is reliable for quantification of tumor total hemoglobin concentration. Thus, we conducted this study to validate the NIRS as an accurate means to quantify changes in tumor vascular blood volume through another independent method, ^{19}F MRS of PFOB.

1.2 ^{19}F MRS of PFOB for the Measurement of Tumor Blood Volume

Perfluorooctylbromide (PFOB) ($C_8F_{17}Br$) emulsions (Alliance pharmaceutical Corp., San Diego,CA), with inert characteristic in chemical and biochemical reactions, and usually acted as artificial blood substitutes[14], was used here as blood volume indicator for ^{19}F magnetic resonance spectroscopy (MRS) measurements. Before the ^{19}F MRS measurement, 2ml PFOB emulsion was intravenously infused into the blood stream of breast tumor bearing rat and circulate to reach an equilibrium state. Then the rats were positioned in an Omega CSI 4.7-Telsa, superconducting magnet system (Acustar™, Bruker Instrument, Inc., Fremont, CA). The breast tumors were placed within a frequency-tunable ($^1H/^{19}F$), single-turn, solenoid coil at the isocenter of the magnet, accompanying with a sealed capillary containing sodium trifluoroacetate (TFA), used as an external standard for quantifying tumor blood volume. The 90^0 pulse width (pw) was determined from a 180^0 null of the whole tumor. Shimming was performed on the tumor tissue water proton FID (200.1 MHz at 4.7) to a typical line width of 60 Hz. The rats were exposed to hyperoxic respiratory, and spectra were acquired with a long repetition time (TR = 30 s) to ensure that changes in T1 due to variable oxygenation would not interfere with volume measurements[15].

Given a set of NMR spectra acquired with chosen system parameters, it has been shown that the integration of ^{19}F signal from a tumor was linearly proportional to the total number of ^{19}F nuclear spins of PFOB in the tumor, which, in turn, was linearly proportional to the total blood volume in the tumor, assuming that the PFOB emulsion had reached an equilibrium state with the blood throughout the tumor. Thus, the areas under spectral peaks of PFOB were integrated in the data post-processing.

After the tumor measurement, rats were removed from the RF coil, with the reference TFA capillary still left in the original position. Amount of 0.5 ml blood sample was then drawn by tail vein from the rats and was placed into the RF coil without disturbing the reference TFA capillary. While keeping the same system acquisition parameters, another set of ^{19}F spectrum from the rat blood sample was acquired, and

the corresponding integrations of ^{19}F signals were calculated. It follows that the blood volume in tumor vasculature can be calculated based on the following equation:

$$V_{T\_blood} = V_{S\_blood} \cdot \left(\frac{I_{T\_blood}}{I_{S\_blood}}\right) \cdot \left(\frac{I_{S\_TFA}}{I_{T\_TFA}}\right), \qquad (4)$$

where V_{T_blood} and V_{S_blood} were the tumor vascular blood volume and blood sample volume (ml), respectively, and I_{T_blood} and I_{S_blood} were the integrated NMR signals from the ^{19}F peaks of PFOB in the rat tumor and in the blood sample, respectively. I_{blood_TFA} and I_{Tumor_TFA} were the respective integrations of ^{19}F NMR signals from the TFA capillary, which was used as a calibration standard to accompany with the blood sample and the tumor measurement.

1.3 Results of tumor vascular $[Hb]_{total}$ and blood volume

Breast tumor (mammary adenocarcinomas 13762NF) bearing Fisher rats experienced alternative carbogen (5% CO_2 and 95% O_2) and oxygen interventions, i.e., air-oxygen-air-carbogen-air. Changes in $[HbO_2]$ and $[Hb]_{total}$ with respect to hyperoxic gas interventions were monitored by NIRS. If the hyperoxic gases regulated $\Delta[Hb]_{total}$ significantly, the same rat was re-anesthetized in the next day and i.v. infused with 2 ml of PFOB emulsion. The ^{19}F MRS measurement for tumor blood volume was performed 30 min later to give sufficient time for the PFOB emulsion to reach an equilibrium state within the blood stream. The protocol of the inhaled gas was the same as that used in the NIRS measurements.

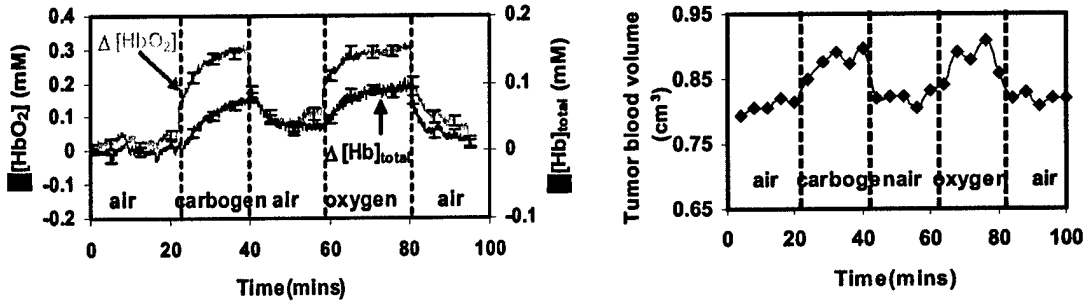

(a) (b)

Figure 1 (a) Time course profiles of tumor vascular $\Delta[Hb]_{Total}$ and $\Delta[HbO_2]$ monitored by NIRS for a representative breast tumor (2.6 cm^3), with inhaled gas sequence of air-carbogen-air-oxygen-air. (b) Time course of tumor blood volume, $V_{T\text{-}blood}$, measured by ^{19}F MRS of PFOB for the same breast tumor(2.6 cm^3), with gas breathing sequence of air-carbogen-air-oxygen-air.

Fig. 1(a) and (b) show the time course profiles of $\Delta[Hb]_{total}$, $\Delta[HbO_2]$ and blood volume ($V_{T\text{-}blood}$) in response to hyperoxic gas interventions, monitored by NIRS and ^{19}F MRS of PFOB, respectively. In spite of fluctuation, the overall trend of $V_{T\text{-}blood}$ was similar to that of $\Delta[Hb]_{Total}$. 8 of the Fisher rats, with good response to gas intervention in $\Delta[Hb]_{Total}$, were performed MRS measurement the next day after the NIRS monitoring. The linear correlation (R^2 =0.7) between tumor vascular $\Delta[Hb]_{Total}$ obtained from NIRS and $\Delta V_{T\text{-}blood}$ from MRS among the 8 breast rat tumors was revealed in Fig.2, demonstrating the practicability and reliability of near infrared spectroscopy as an *in vivo* non-invasive real time monitoring tool for tumor

vascular total hemoglobin concentration.(see the appendix manuscript).

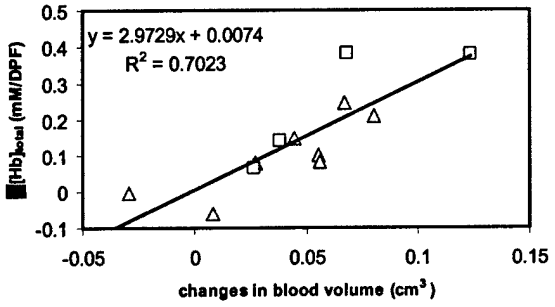

Figure 2 Correlation between the maximal changes in $\Delta[Hb]_{Total}$ and $V_{T\text{-}blood}$ for hyperoxic gases inhalation in the 9 breast tumors. Triangle : carbogen intervention. Square: oxygen intervention.

2. Intensive study of dynamic response of tumor vascular $\Delta[HbO_2]$ and $\Delta[Hb]_{total}$ with respect to different interventions.

Hyperoxic gas intervention was thought to be one of the most effective methods to reduce tumor hypoxia, and thus, to enhance the efficiency of standard therapies in experimental malignancies as well as in human tumors. Carbogen has been favored over oxygen in clinical application. Our concern is which gas will have more benefit on breast tumors treatment. Previously, we reported some primary results on hyperoxic gas intervention. Here we provide a considerable extension of our previous NIR studies of breast tumors, in terms of numbers of animals, range of interventions, and extent of analysis.

2.1 Comparison of carbogen and oxygen respiratory on $\Delta[HbO_2]$ and $\Delta[Hb]_{total}$

Breast tumor bearing rats were exposured to alternative gas inhalation, i.e., air-carbogen-air-oxygen-air, and the reversed gas inhalation sequence. $\Delta[HbO_2]$ and $\Delta[Hb]_{total}$ were monitored by NIRS. Fig.3 is a typical time profile of $\Delta[HbO_2]$ and $\Delta[Hb]_{total}$ with respect to gas intervention. $\Delta[HbO_2]$ has good response to hyperoxic gas respiratory, and $\Delta[Hb]_{total}$ has no corresponding change with gas respiratory in this case. We did extensive analysis on $\Delta[HbO_2]$ among 7 rats under the gas sequence as air-carbogen-air-oxygen-air.

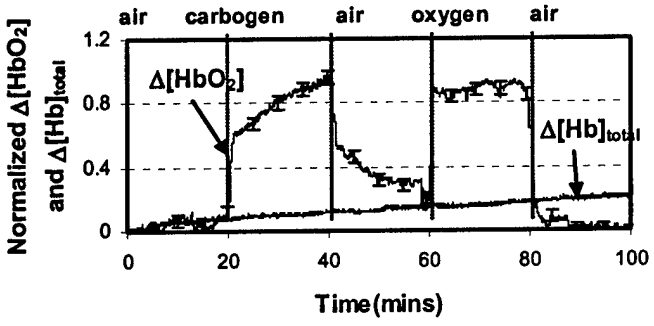

Fig.3 Time course profile of $\Delta[HbO_2]$ and $\Delta[Hb]_{total}$ with respect to carbogen and oxygen intervention in the sequence of air-carbogen-air-oxygen-air

Results showed there is no significant difference in terms of amplitude for carbogen and oxygen respiratory (Fig.4 (a)), but there is significant difference between the response time, namely, carbogen breathing displayed longer response or decline time than the oxygen breathing (Fig.4(b)) (See attached manuscript for detail).

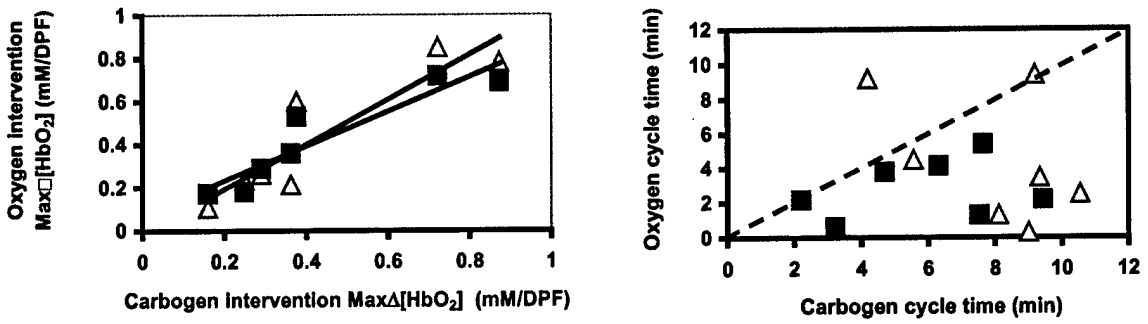

Fig. 4 (a) Comparison of maximal changes of tumor vascular oxygen hemoglobin concentration, $\Delta[HbO_2]$, caused by carbogen and oxygen interventions, respectively, under the inhalation sequence of air-carbogen-air- oxygen-air. ■ Comparison of the rising parts for each intervention; Δ Comparison of the rising part for carbogen versus the falling part for oxygen. In both cases $R^2>0.8$. (b) Comparison of response times to each gas intervention. Here, the time to 80% maximum response to each intervention is compared for carbogen versus oxygen: □ rising parts (onset of hyperoxia) ■ falling parts (return to normoxic gas breathing). The line of unity shows that the time for carbogen was almost always longer than for oxygen.

2.2 Effect of CO_2 on tumor vascular $\Delta[HbO_2]$ and $\Delta[Hb]_{total}$

To further explore the vasoactive contribution of the CO_2, air mixture (air + 5% CO_2) and carbogen (95% O_2 +5% CO_2) were applied to 5 breast tumor bearing rats in the sequence of air-air mixture-carbogen-air. Fig. 5a is the corresponding time course of $\Delta[HbO_2]$ and $\Delta[Hb]_{total}$ for a representative 13762NF breast tumor (1.2 cm^3). When the inhaled gas was switched from air to air mixture, $\Delta[HbO_2]$ increased immediately ($P<0.05$), then kept a plateau. Upon the administration of carbogen, $\Delta[HbO_2]$ elevated quickly within the first minute, followed by a gradual and significant increase to a maximum over the next 19 minutes, then decreased to the baseline when the inhaled gas was switched back to air. The percentage of increase in $\Delta[HbO_2]$ caused by 5% CO_2 in air is about 19% of that caused by carbogen. The changes in $\Delta[HbO_2]$ caused by both air mixture and carbogen in 5 rats are summarized in Fig.5b, the contributions of CO_2 to the elevation of $\Delta[HbO_2]$ are all less than 20%. Also, $\Delta[Hb]_{total}$ showed response to gas respiratory in this case.

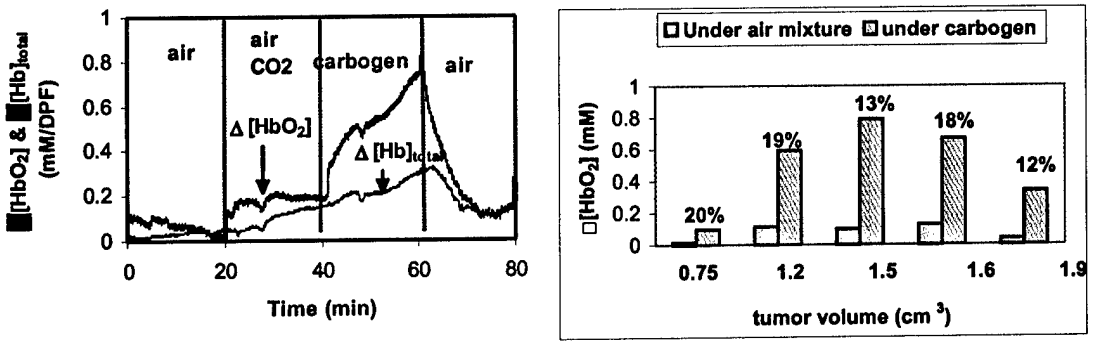

(a) (b)

Figure 5 (a) Time course of tumor vascular $\Delta[HbO_2]$ and $\Delta[Hb]_{total}$ for a representative 13762NF rat breast tumor (1.2 cm^3), with the inhaled gas under the sequence of air-air mixture-carbogen-air. **(b)** Maximal changes of tumor vascular oxygen hemoglobin concentration, $\Delta[HbO_2]$, caused by air mixture and carbogen interventions, respectively, in the 5 breast rat tumors under the inhalation sequence of air-air mixture- carbogen-air. The percentage of $\Delta[HbO_2]$ caused by air mixture over that produced by carbogen are labeled in each of the tumor data.

2.3 Comparison of different interventions on tumor vascular $\Delta[HbO_2]$ and $\Delta[Hb]_{total}$

We applied different interventions on the breast tumor bearing rats to compare the response of $\Delta[HbO_2]$ and $\Delta[Hb]_{total}$ to the challenges. The intervention sequence is: air-air mixture-carbogen-air-oxygen-air-hydralazine. Fig.6 is a typical time course of tumor vascular $\Delta[HbO_2]$ and $\Delta[Hb]_{total}$ for a representative 13762NF breast tumor (1.5 cm^3). Carbogen and oxygen breathing elevated $\Delta[HbO_2]$ significantly, air mixture just contribute small potion of elevation. And $\Delta[Hb]_{total}$ doesn't show any response to hyperoxic gas intervention in this case. However, infusion of hydralazine reduced both $\Delta[HbO_2]$ and $\Delta[Hb]_{total}$ significantly (see the attached manuscript for detail).

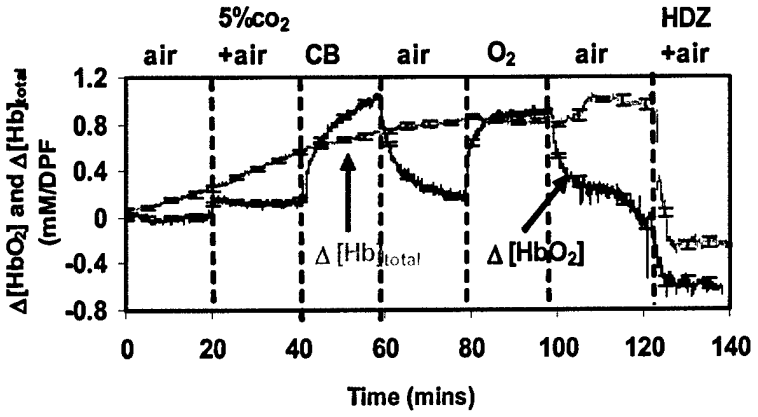

Fig 6 Time course of tumor vascular $\Delta[HbO_2]$ and $\Delta[Hb]_{total}$ for a representative 13762NF breast tumor (1.5 cm^3). Intervention sequence: air-air mixture-carbogen-air-oxygen-air-hydralazine

2.4 Statistic results

39 breast tumor bearing Fisher rats experienced alternative carbogen and oxygen interventions. Among them, 5 of rats were exposure to air mixture respiratory, and 19 of rats were infused with hydralazine either under air breathing or carbogen breathing. $\Delta[HbO_2]$ and $\Delta[Hb]_{total}$ were monitored by NIRS. Meanwhile, we compared the response of $\Delta[HbO_2]$ and $\Delta[Hb]_{total}$ in breast tumors to that in prostate tumors. Results in Table **1** have shown that hyperoxic gas breathings can effectively elevate tumor vascular oxygen status in all of the breast tumors (39/39), but only in ~50% (10/21) of the prostate tumors, while such respiratory interventions lead to increases in total vascular volume for some of the breast tumors (~40%, 15/39) but little changes for the prostate tumors (1/21). Administration of hydralazine can significantly reduce $\Delta[HbO_2]$ and $\Delta[Hb]_{total}$ in both breast tumors and prostate tumors. Tumor physical volume was involved in the response behavior, namely, small tumor (<2.5 cm^3 in volume) has better response than big tumor (> 2.5 cm^3),see the manuscript for the detail.

Table 1 Statistic results of $\Delta[HbO_2]$ and $\Delta[Hb]_{total}$ with respect to different interventions

Tumor model	Total tumors	Response to hyperoxic gases in $\Delta[HbO_2]$	Response to hyperoxic gases in $\Delta[Hb]_{total}$	No. of tumors measured by ^{19}F MRS of PFOB	Response to HDZ administration in $\Delta[HbO_2]$	Response to HDZ administration in $\Delta[Hb]_{total}$
Breast tumor 13762 NF	39	39/39	15/39	8	19/19	19/19
Prostate tumor	21	10/21	1/21	3	5/6	6/6

3. Simultaneous measurement of changes in tumor oxygenation by NIRS and MRI BOLD.

3.1 BOLD MRI and experimental setup

As demonstrated previously, the changes of deoxygenated and oxygenated hemoglobin concentrations can be quantified by NIR spectroscopy based on their absorption properties. In the other hand, deoxyhemoglobin possess magnetic feature. The paramagnetic deoxyhemoglobin creates local magnetic field variations in the proximity of blood vessels, which produces additional phase dispersion of water proton signals in the surrounding tissue. Gradient recalled echo (GRE) ^1H MR imaging sequence are sensitive to these local susceptibility variations near the vessels and, hence, the increasing in the concentration of deoxyhemoglobin, due to the desaturation of O_2 or blood flow, lead to signal attenuation in gradient echo or T_2^* (apparent spin-spin relaxation time)-weighted image. The intensity of T_2^*-weighted image is directly related to the amount of deoxygenated hemoglobin, and thus, related to oxygenated hemoglobin, which is comparable with $\Delta[HbO_2]$ obtained from NIRS system. The parameters for data acquisition of T_2^*- weighted image are optimized as: TR(Recycle time)=300ms, TE(Echo time)=30ms, Flip angle=20^0.

Figure 7 is the experimental setup for the simultaneous measurements of NIR and MRI. The rat breast tumors were shaved and placed in the frequency tunable ($^1H/^{19}F$) single turn solenoid RF coil inside the magnetic system. The delivering and detecting fiber bundles (~ 5 m long) of the NIRS were touched firmly to the surface of the shaved tumors (without compression of tumor) for the measurement of $\Delta[Hb]_{Total}$ and $\Delta[HbO_2]$. The coil was tuned at proton resonance frequency (200.13 MHz at 4.7 T). BOLD MRI was performed simultaneously with NIRS during hyperoxic gas interventions.

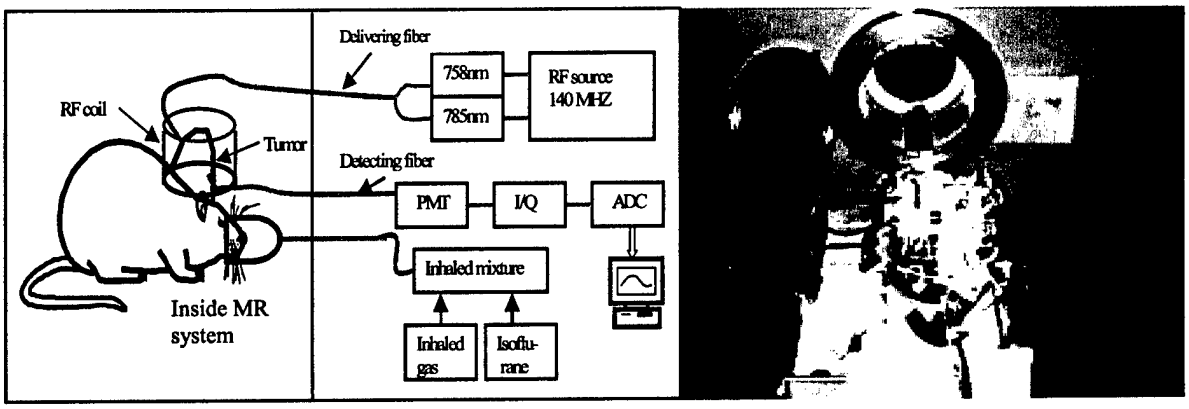

(a) (b)

Figure 7 (a) Experimental setup for simultaneous measurements by NIRS and MR. Tumor was placed in the RF coil. Two fiber bundles of the NIRS system deliver and detect the laser light through the tumor. PMT represents a photomultiplier tube. I/Q is an in-phase and quadrature phase demodulator for retrieving amplitude and phase information. (b) Picture of the experimental setup

3.2 Consistence of tumor global oxygenation measured simultaneously by NIRS and BOLD MRI

Using the setup in Fig.7, we simultaneously monitored $\Delta[HbO_2]$ and T2*-weighted signal by NIRS and MRI. In order to compare the tumor global signal obtained by the two independent modalities, the whole tumor was selected as one thick slice in MRI image because the one-channel NIRS only can sample the global signal of the tumor. Fig.8 is the BOLD MR images of the whole rat breast tumor (4.8

cm ^{3}) with different gases inhalation. The whole tumor was selected as the Region of interest (ROI). Analysis of ROI gave rise to the mean values of each image, as shown in Fig.9 (a). During the first 20 minutes, the rat breath air as baseline, and the mean intensity of BOLD image (#1~5) is about 0.0162±0.0005. The carbogen intervention after air baseline breathing produced a significant increasing ($P<0.001$) in the intensity of BOLD MRI to about 0.0189±0.0008. Then the signal decreased significantly to 0.011±0.001 when the inhaled gas was switched back to air ($P<0.001$). Similar tendency in $\Delta[HbO_2]$ was observed by NIRS (Fig.9(b)), indicating the consistence of tumor vascular oxygen status measured by BOLD MRI and NIRS, respectively.

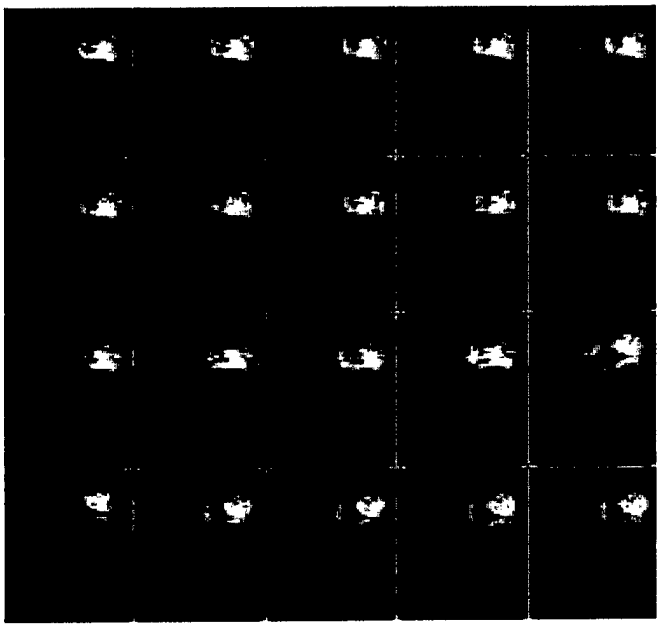

Fig.8 BOLD MR images of the whole rat breast tumor (No.# 2, 4.8 cm ^{3}) with different gases inhalation. Image #1~5 are during air breathing, #6~14 are under carbogen inhalation, and #15~20 return to air breathing.

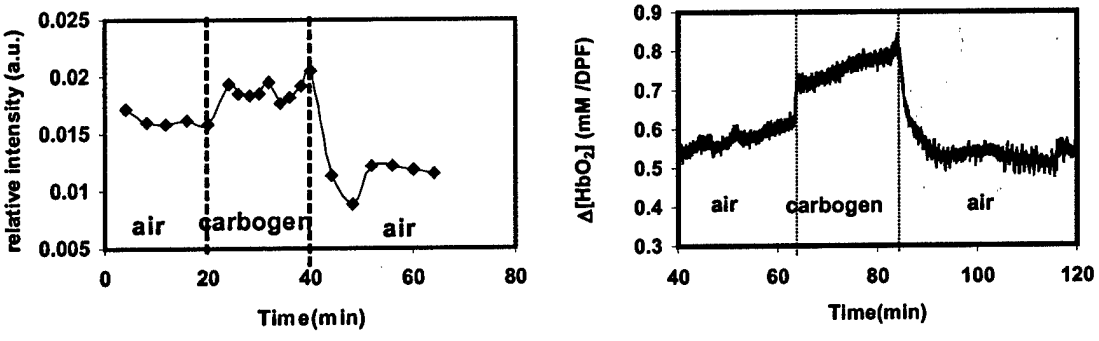

(a) (b)

Figure 9 Simultaneous measurements of rat breast tumor (4.8 cm ^{3}) vascular oxygenation status by BOLD MRI and NIRS. (a) The average intensity of BOLD MRI images within the tumor region. (b) The changes in oxygenated hemoglobin concentration, $\Delta[HbO_2]$, measured by NIRS.

3.2 Heterogeneity of the response of tumor oxygenation to hyperoxic gas intervention

Unlike the one-channel NIR spectroscopy, MRI can display the heterogeneity inside the tumors. Fig.10 shows three BOLD MRI cross-sectional intensity images in the 1st slice (~2mm thickness) of a

representative breast tumor under air-carbogen-air gas interventions. The images illustrate heterogeneous changes in BOLD MRI intensity in response to the gas interventions. Some locations exhibit increased signals (e.g., at the center region), and some remain unchanged (e.g., near the two side regions), when the gas was switched to carbogen and then back to air. The heterogeneous response of tumor oxygen to gas intervention displayed in almost all the tumors. Fig.11 is a time course profile of BLOD MRI intensity with respect to carbogen and hydralazine intervention in different Region of Interest (ROI) in one slice of a representative breast tumor. The curves indicated carbogen elevated tumor oxygenation in some regions. And some regions have no response to carbogen respiratory. However, hydralazine reduced the BOLD MRI signal in all the regions, which is consistent with our previous results from NIRS.

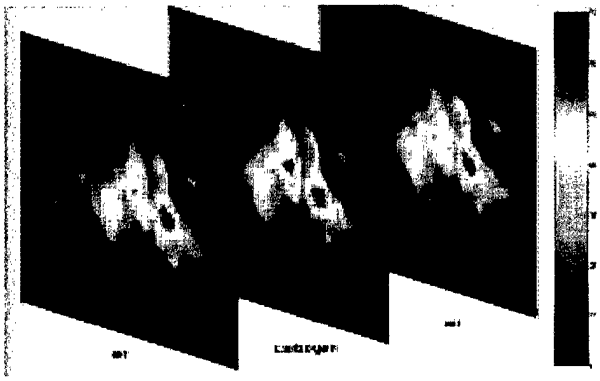

Fig. 10 BOLD MRI images of 1st slice on a breast tumor (#3) under a sequence of air-carbogen-air

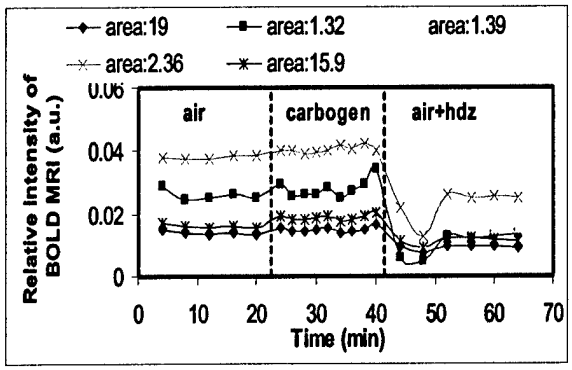

Fig. 11 Time course profile of relative MRI BOLD intensity at different Region of Interest under air-carbogen-air+hydralazine

Key Research Accomplishments (Oct. 31, 2002~Nov. 1, 2003):

a. Evaluated the practicability and accuracy of near infrared spectroscopy (NIRS) as a non-invasive monitoring tool for tumor blood volume by using ^{19}F MRS of PFOB.
b. Investigated intensively the dynamic response of tumor vascular $\Delta[HbO_2]$ and $\Delta[Hb]_{total}$ to hyperoxic gas (carbogen, oxygen, air mixture)respiratory and hydralazine administration . Results indicated that hyperoxic gas can significant elevate tumor vascular oxygenation in all the breast tumors, but only ~40% of them have good response in total blood volume. Administration of hydralazine can decrease both $\Delta[HbO_2]$ and $\Delta[Hb]_{total}$ all the breast tumors.
c. Performed simultaneous measurements in the changes of tumor vascular hemoglobin concentration by NIRS and BOLD MRI, revealing the consistent of the tumor global oxygenation obtained from the two independent modalities.
d. Displayed the heterogeneity of tumor vascular oxygenation with response to hyperoxic gas intervention by BOLD MR images

Reportable outcome (Oct. 31, 2002~Nov. 1,2003):

a. Peer review paper and manuscripts:

Y. Gu, V. Bourke, J. Kim, A. Constantinescu, R. P. Mason, H. Liu, "Dynamic response of breast tumor oxygenation to hyperoxic respiratory challenge monitored with three oxygen-sensitive parameters", Applied Optics, 42:1-8 (2003)

Y. Gu, Y. Song, A. Constantinescu, H.Liu, R.P.Mason, "Vascular oxygen dynamics of breast tumors in response to physiological interventions monitored by Near Infrared Spectroscopy", submitted to Int. J. Radiat. Oncol. Biol. Phys.

Y. Gu, H. Liu, Y. Song, W. Cui, A. Constantinescu, R. P. Mason, "Tumor Vascular Volume and Oxygenation in Response to Therapeutic Interventions: Assessed by Near Infrared Spectroscopy and ^{19}F MRS of PFOB", will be submitted to Cancer Research.

Y. Gu, R. P. Mason, H. Liu, "Estimation of optical path length in solid tumors: a combined study of near infrared spectroscopy and 19F magnetic resonant spectroscopy", in preparation, will be submitted to Optics Express.

b. Presentations and Proceeding papers:

Y. Gu, V. Kodibagkar, M. Xia, Z. Qian, J. G. Kim, A. Constantinescu, R. P. Mason, Hanli Liu. "Correlation of NIR spectroscopy with MR on assessing breast tumor vascular oxygen status and blood volume". Presented in international conference in San Joes, Jan 25~29,2003. *Optical tomograph and spectroscopy of tissue IV*, Chair: Britton Chance, *SPIE*

Y. Gu, V. Bourke, J. Kim, A. Constantinescu, R. P. Mason, H. Liu, "Vascular oxygenation dynamics of breast tumors in response to therapeutic interventions assessed by three oxygen-sensitive parameters", Presented in international conference in San Joes, Jan 25~29,2003. *Optical tomograph and spectroscopy of tissue IV*, Chair: Britton Chance, 4955, 416-423, *SPIE*

J. .G. Kim, **Y. Gu,** A. Constantinescu, R. P. Mason, H. Liu. "Non-uniform of breast tumor oxygenation monitored by three channel NIR spectroscopy", Presented in international conference in San Joes, Jan 25~29, 2003. *Optical tomograph and spectroscopy of tissue IV*, Chair: Britton Chance, 4955, 388-396, *SPIE*

Conclusion:

From the work that I have conducted during the period of Oct.31, 2002~Nov.1, 2003, the following conclusions can be drawn:

a.. Near Infrared Spectroscopy was evaluated as a reliable and accurate monitoring tool for non-invasive real time measurement of breast tumor vascular oxygenation and tumor blood volume, by using comparative measurements on the same tumors.

b. Hyperoxic gas respiratory can effectively elevate tumor oxygen level in all the breast tumors (100%). There is no significant difference in terms of magnitude in $\Delta[HbO_2]$ between carbogen and oxygen intervention. But the response time displayed more sluggish in carbogen intervention than in oxygen breathing. CO_2 contribute a small portion to the elevation of $\Delta[HbO_2]$. However, only ~40% of breast tumors have good response in $\Delta[Hb]_{total}$ with respect to hyperoxic gas intervention. Administration of hydralazine effectively reduced both $\Delta[HbO_2]$ and $\Delta[Hb]_{total}$ in all the breast tumors.

c. The global breast tumor oxygenation status showed consistence between the results obtained simultaneously from one-channel NIRS and BOLD MRI , respectively.

d. The heterogeneity of breast tumor vascular oxygenation with respect to hyperoxic gas interventions displayed obviously by BOLD MR images.

Appends:

One peer reviewed paper and two manuscripts.

Reference

[1] R. S. Bush, R. D. T. Jenkin, W. E. C Allt, F. A. Beale, A. J. Dembo, J. F. Pringle, "Definitive evidence for hypoxic cells influencing cure in cancer therapy". Br. J Cancer **37 (suppl 3)**, 302-306 (1978).

[2] E. J. Hall, Radiobiology for the radiologist. 4th ed.(Lippincott, Philadelphia, PA.,1994).

[3] M. Nordsmark, J. Overgaard , "A confirmatory prognostic study on oxygenation status and loco-regional control in advanced head and neck squamous cell carcinoma treated by radiation therapy". Radiother Oncol. **57**, 39-43 (2000).

[4] O. Thews, D. K. Kelleher, P. Vaupel, " Erythropoietin restores the anemia-induced reduction in cyclophosphamide cytotoxicity in rat tumors," Cancer Res, **61**,1358-1361 (2001).

[5] S. Dische, M. I. Saunders, R. Sealy, "Carcinoma of the cervix and the use of hyperbaric oxygen with radiotherapy:a report of a randomized controlled trial," Radiother Oncol. **53**, 93-98 (1999).

[6] V. M. Laurence, R. Ward, I. F. Dennis, N. M. Bleehen, "Carbogen breathing with nicotinamide improves the oxygen status of tumors in patients," Br. J Cancer **72**, 198-205 (1995).

[7] L. Martin, E. Lartigau, P. Weeger, "Changes in the oxygenation of head and neck tumors during carbogen breathing," Radiother Oncol, **27**,123-130 (1993).

[8] J. R. Griffiths, N. Taylor, F. Howe, M. Saunders, S. Robinson, P. Hoskins, "The response of human tumors to carbogen breathing monitored by gradient-recalled echo MRI," Int. J. Radiat. Oncol. Biol. Phys., **39**, 697-701(1997).

[9] S. P. Robinson, F. A. Howe, L. M. Rodrigues, M. Stubbs, and J. R. Griffiths, "Magnetic resonance imaging techniques for monitoring changes in tumor oxygenation and blood flow," Semin. Radiat. Oncol. **8**, 198-207(1998).

[10] H. Liu, Y. Song, K. L. Worden, X. Jiang, A. Constantinescu, and R .P. Mason, " Noninvasive investigation of blood oxygenation dynamics of tumors by near-infrared spectroscopy," Appl. Opt. **39**,5231-5243 (2000).

[11] J. G. Kim, Y.Song, D. Zhao, A. Constantinescu, R .P. Mason, and H. Liu, "Interplay of Tumor Vascular Oxygenation and pO_2 in Tumors Using NIRS, ^{19}F MR pO_2 Mapping, and pO_2 Needle Electrode," J. Biomed. Optics. **8**,53-62 (2003).

[12] Y .Gu, V. Bourke, J. Kim, A. Constantinescu, R. P .Mason, H. Liu, "Dynamic response of breast tumor oxygenation to hyperoxic respiratory challenge monitored with three oxygen-sensitive parameters", Applied Optics, **42**,2960-2967 (2003)

[13] Y. Gu, Y. Song, A. Constantinescu, H. Liu, R. P. Mason, " Vascular oxygen dynamics of breast tumors in response to physiological interventions monitored by Near Infrared Spectroscopy", to be submitted to Int. J. Radiat. Oncol. Biol. Phys.

[14] N. J. Baldwin, Y. Wang, T. C. Ng, "In situ ^{19}F MRS measurement of RIF-1 tumor blood volume: Corroboration by radioisotope-labeled [^{125}I]-albumin and correlation to tumor size", Magn. Reson. Imaging, **14**, 275-280(1996).

[15] H. P. Shukla, R. P. Mason, D. E. Woessner & P. P. Antich, "A comparison of three commercial perfluorocarbon emulsions as high field NMR probes of oxygen tension and temperature", J. Magn. Reson. B, **106**, 131-141 (1995).

Dynamic response of breast tumor oxygenation to hyperoxic respiratory challenge monitored with three oxygen-sensitive parameters

Yueqing Gu, Vincent A. Bourke, Jae G. Kim, Anca Constantinescu, Ralph P. Mason, and Hanli Liu

The simultaneous measurement of three oxygen-sensitive parameters [arterial hemoglobin oxygen saturation (SaO_2), tumor vascular-oxygenated hemoglobin concentration ([HbO_2]), and tumor oxygen tension (pO_2)] in response to hyperoxic respiratory challenge is demonstrated in rat breast tumors. The effects of two hyperoxic gases [oxygen and carbogen (5% CO_2 and 95% O_2)] were compared, by use of two groups of Fisher rats with subcutaneous 13762NF breast tumors implanted in pedicles on the foreback. Two different gas-inhalation sequences were compared, i.e., air–carbogen–air–oxygen–air and air–oxygen–air–carbogen–air. The results demonstrate that both of the inhaled, hyperoxic gases significantly improved the tumor oxygen status. All three parameters displayed similar dynamic response to hyperoxic gas interventions, but with different response times: the fastest for arterial SaO_2, followed by biphasic changes in tumor vascular [HbO_2], and then delayed responses for pO_2. Both of the gases induced similar changes in vascular oxygenation and regional tissue pO_2 in the rat tumors, and changes in [HbO_2] and mean pO_2 showed a linear correlation with large standard deviations, which presumably results from global versus local measurements. Indeed, the pO_2 data revealed heterogeneous regional response to hyperoxic interventions. Although preliminary near-infrared measurements had been demonstrated previously in this model, the addition of the pO_2 optical fiber probes provides a link between the noninvasive relative measurements of vascular phenomena based on endogenous reporter molecules, with the quantitative, albeit, invasive pO_2 determinations. © 2003 Optical Society of America

OCIS codes: 170.1470, 170.3660, 170.4580, 120.3890, 120.1880, 230.2090.

1. Introduction

It is widely recognized that hypoxic regions in solid tumors may limit the efficacy of nonsurgical therapy, including radiotherapy, photodynamic therapy, and chemotherapy.[1–4] Many adjuvant interventions have been tested, including simple strategies such as breathing hyperoxic gases.[5–7] However, a meta-analysis of some 10,000 patients showed only a modest benefit, and this benefit was restricted to specific tumor types.[8] It is thought that the failure of such interventions was largely due to the inability to identify those patients who would benefit. Indeed, there is growing emphasis on tailoring therapy to the individual characteristics of each patient's tumor. Furthermore, carbogen (5% CO_2 and 95% O_2) and oxygen have been used on experimental tumors in animals as well as on clinical trials in patients for many years.[9,10] But the therapeutic benefits of the two kinds of respiratory hyperoxic gases are diverse, depending on the tumor types and individuals.[11–13] Accordingly, accurate assessment of tumor oxygenation at various stages of tumor growth and in response to interventions may provide a better understanding of tumor development and may serve as a prognostic indicator for treatment outcome, potentially allowing therapy to be tailored to individual characteristics.

Various techniques have been developed to measure oxygen tension (pO_2) or vascular oxygenation of tumors.[14] Many methods are invasive, and those requiring biopsy preclude dynamic investigations. Optical techniques based on light absorption of endogenous chromophores, e.g., near-infrared (NIR)

Y. Gu, J. G. Kim, and H. Liu (Hanli@uta.edu) are with the Biomedical Engineering Program, The University of Texas at Arlington, Arlington, Texas 76019. V. A. Bourke, A. Constantinescu, and R. P. Mason are with the Department of Radiology, University of Texas Southwestern Medical Center, Dallas, Texas 75390.

Received 8 September 2002; revised manuscript received 15 January 2003.

0003-6935/03/162960-08$15.00/0

spectroscopy of oxygenated and deoxygenated hemoglobin, are entirely noninvasive and allow real-time monitoring of tumor vascular oxygenation.[15–17] However, NIR has limited spatial resolution, and it remains to be determined whether vascular oxygenation is related to therapeutic outcome. Hitherto, quantitative pO_2 has been shown to have prognostic value,[18–21] but pO_2 represents a balance between oxygen delivery and consumption. Thus, we seek to explore the interplay of vascular and tissue oxygenation. Electrodes have been used widely to study tumor oxygen dynamics with respect to interventions,[22–24] but they are generally limited to a single location and small probes can be fragile. We have ourselves recently shown a correlation between pO_2 and ΔHbO_2 in some tumors, but we noted distinct heterogeneity, and thus, the global NIR measurements were not always related to local pO_2.[25] Multiple fiber-optic probes may be inserted into a tumor,[26–28] and we have now investigated correlation between NIR measurements and multiple (three) simultaneous pO_2 measurements.

We now report simultaneous measurements of three oxygen-related parameters, i.e., arterial hemoglobin oxygen saturation, SaO_2; tumor oxygenated hemoglobin concentration, $[HbO_2]$; and tumor oxygen tension, pO_2, to assess dynamic responses of rat breast tumors to hyperoxic gases. Changes in tumor vascular $[HbO_2]$ were measured by NIR spectroscopy (NIRS) using a photon-migration, frequency-domain device; changes in regional pO_2 were monitored by a fluorescence-quenched, oxygen-sensing, fiber-optic system (FOXY); the arterial SaO_2 values were recorded with a fiber-based, pulse oximeter.

2. Materials and Methods

A. Near-Infrared Spectroscopy System for Measurement of Changes in $[HbO_2]$

NIR light (700 to 900 nm) has considerable tissue penetration depth (several centimeters) and permits *in vivo* sampling of large tissue volumes (e.g., human breast, brain, skeletal muscle, or tumors), since photon transport in tissue is dominated by scattering rather than by absorption. Absorption of NIR light by the oxygenated and the deoxygenated hemoglobin chromophores may be used to determine hemoglobin oxygenation and blood concentration changes. As described in detail previously,[16,25] a homodyne frequency-domain system (NIM, Philadelphia, Pennsylvania) was used to monitor the global changes in oxygenated and deoxygenated hemoglobin concentrations, $\Delta[HbO_2]$ and $\Delta[Hb]$, respectively, in rat breast tumors in response to variations in inhaled gas. Briefly, the light from two NIR laser diodes (758 nm and 785 nm) was coupled into a bifurcated fiber bundle and illuminated on the tumor, and the transmitted light was collected and propagated to a photomultiplier tube (Fig. 1). The fiber bundles were placed on the surface of the tumors in a transmittance mode parallel to the body of the rat. The fiber tips touched firmly on the skin (without compression) in the middle parts of the tumors, providing optimal geometry to interrogate deep tumor tissue.

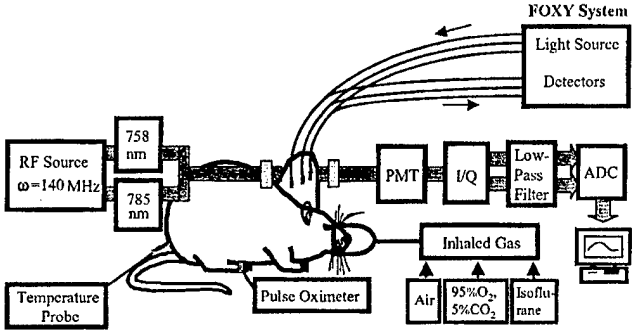

Fig. 1. Experimental setup for simultaneous oximetry. The 3-mm-diameter fiber bundles of the NIRS system deliver and detect the laser light through the tumor in transmittance geometry. PMT represents a photomultiplier tube. I/Q is an in-phase and quadrature phase demodulator for retrieving amplitude and phase information. The FOXY system comprises three fiber-optic oxygen-sensing probes that are inserted into different regions of the tumor. The pulse oximeter probe is placed on the hind foot of the rat.

Based on modified Beer–Lambert's law,[29] changes in oxygenated and deoxygenated hemoglobin concentrations, $\Delta[HbO_2]$ and $\Delta[Hb]$, due to respiratory intervention were derived from the measured amplitudes at the two wavelengths and calculated with the following equations[25]:

$$\Delta[HbO_2] = \frac{-10.63 \log\left(\frac{A_B}{A_T}\right)^{758} + 14.97 \log\left(\frac{A_B}{A_T}\right)^{785}}{d}, \quad (1)$$

$$\Delta[Hb] = \frac{8.95 \log\left(\frac{A_B}{A_T}\right)^{758} - 6.73 \log\left(\frac{A_B}{A_T}\right)^{785}}{d}, \quad (2)$$

where A_B and A_T are the baseline and transient amplitudes measured from the NIR system, respectively; d is the source–detector separation; the unit for both $\Delta[HbO_2]$ and $\Delta[Hb]$ is millimolar per differential path-length factor (DPF); and the DPF is for tumor tissues. As demonstrated in our previous study, normalization of $\Delta[HbO_2]$ and $\Delta[Hb]$ to their maximal values can eliminate the effects of d and DPF on the results.[25]

B. Fiber-Optic Oxygen-Sensing System for Measurement of Changes in pO_2

Regional pO_2 in tumors was monitored with a multichannel, fiber-optic, oxygen-sensing system (FOXY, Ocean Optics, Inc., Dunedin, Florida).[30] Three fluorescence-quenched, optical fiber probes (AL300, tip diameter 410 μm) were inserted into different regions of the tumors (Fig. 1). Probes were positioned so that at least one was in a poorly oxygenated region (low baseline pO_2) and at least one in a well-oxygenated region (high baseline pO_2). If necessary,

the probes were gently moved through the tumor until such diverse regions were located. In some cases, the mean pO_2 derived from the three individual measurements is presented. Although this is a commercial system, few details have been published previously,[31] and no applications to *in vivo* tumor oximetry have been published to our knowledge. Light from a pulsed blue LED (475 nm) was coupled into one branch of a bifurcated optical fiber bundle and propagated to the probe tip. The distal end of the probe is coated with a thin layer of a hydrophobic solgel material, where an oxygen-sensing ruthenium complex is effectively trapped. Illumination of the ruthenium complex causes fluorescence at ~600 nm. If the excited ruthenium complex encounters an oxygen molecule, the excess energy is transferred to the oxygen molecule in a nonradiative transition, decreasing or quenching the fluorescence signal. The degree of quenching correlates with the oxygen concentration, and hence, pO_2.

The fluorescence response of the ruthenium crystal complex is highly temperature dependent, so to accomplish probe calibration it was necessary to stream gases of known oxygen concentrations (100%, 20.9%, 10%, 2%, and 0%) through a cylindrical water jacket heated to 37 °C. Calibration curves were automatically calculated by means of the vendor-supplied software, with the second-order, polynomial calibration:

$$\frac{I_0}{I} = 1 + K_1[O] + K_2[O]^2 \qquad (3)$$

where, I_0 is the fluorescence intensity at zero oxygen concentration (nitrogen), I is the measured intensity of fluorescence at a pressure of oxygen, $[O]$ represents the oxygen concentration (related to pO_2), K_1 and K_2 are the first- and the second-order coefficients and are automatically supplied by the curve-fitting routine from the calibration measurements.

C. Pulse Oximeter for Measurement of Arterial S_aO_2

Arterial SaO_2 of the breast-tumor-bearing rats was also monitored with a fiber-optic pulse oximeter (Nonin Medical, Inc., Plymouth, Minnesota) placed on the hind foot of the rats. The system consisted of two optical fibers used for delivering and receiving the light. The tips were placed on either side of the foot in transmission mode.

D. Animal Model

Mammary adenocarcinomas 13762NF (originally obtained from the Division of Cancer Therapeutics, NIH, Bethesda, Maryland) were implanted in skin pedicles[32] on the foreback of adult female Fisher 344 rats (~150 g). Once the tumors reached 1–2 cm diameter, rats were anesthetized with 150-μl ketamine hydrochloride (100 mg/ml, i.p.) and maintained under general gaseous anesthesia with 1.3% isoflurane in air (1 dm^3/min). Body temperature was maintained at 37 °C by a warm water blanket. Tumors were shaved to improve optical contact for transmitting NIR light. The tumor diameters along the three major orthogonal axes (a, b, c) were measured with calipers and volume estimated with an ellipsoid approximation with the formula: $V = (\pi/6)(abc)$.

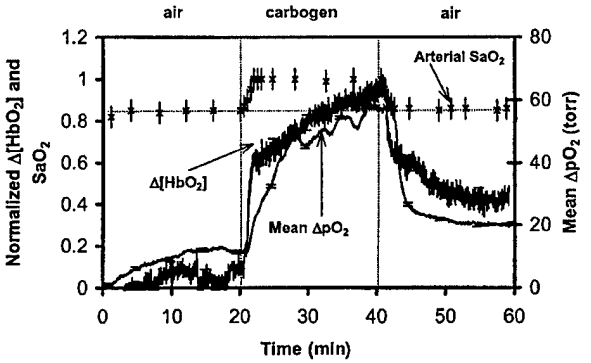

Fig. 2. Time profile of the three oxygen-sensitive parameters, i.e., the normalized changes of tumor $\Delta[HbO_2]$, the mean changes of tumor ΔpO_2, and the arterial SaO_2 with respect to carbogen breathing in a representative 13762NF rat breast tumor (No. 1, 3.2 cm^3).

Two groups of rats ($n = 7$ in each group) were used to compare the effects of carbogen and oxygen on vascular oxygenation of breast tumors. Group 1 experienced the gas-inhalation sequence of air–carbogen–air–oxygen–air. Group 2 was exposed to the reverse sequence of air–oxygen–air–carbogen–air. Each gas was maintained for 20 min. In addition, the FOXY pO_2 probes were applied to five rats from Group 1, and the dynamics of the three oxygen-related parameters were measured simultaneously.

3. Results

A. Dynamic Responses of Three Oxygen-Related Parameters to Carbogen Intervention

Typical time profiles of the normalized $\Delta[HbO_2]$, mean ΔpO_2, and SaO_2 in response to carbogen intervention are shown for a representative 13762NF breast tumor (No. 1, 3.2 cm^3) in Fig. 2. When the inspired gas was switched from air to carbogen, the SaO_2 readings increased rapidly and significantly from the baseline value of 85% to the maximum of 100% within 2.5 minutes ($p < 0.0001$). The normalized $\Delta[HbO_2]$ showed a sharp initial rise in the first minute ($p < 0.0001$) followed by a slower, gradual, but further significant increase over the next 19 min ($p < 0.001$). Mean ΔpO_2 increased rapidly by approximately 50 Torr within 8 min ($p < 0.0005$) and also continued a slower and gradual increase over the next 12 min ($p < 0.005$). Return to breathing air produced a significant decline for all three signals ($p < 0.0001$).

SaO_2 and pO_2 displayed a single-phase dynamic behavior in response to carbogen intervention, whereas $\Delta[HbO_2]$ showed an apparent biphasic response. These dynamics may be characterized by time constants of a single-exponential response. For the tumor in Fig. 3, SaO_2 had the fastest response, with a time constant of $\tau(SaO_2) = 1.1 \pm 0.2$ min ($R =$

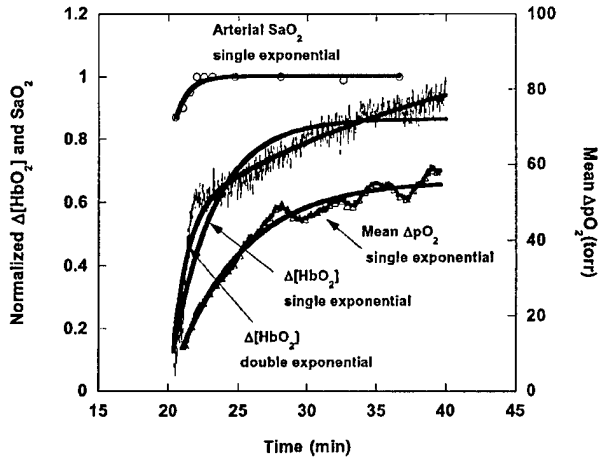

Fig. 3. Dynamic responses of the three oxygen-sensitive parameters to carbogen intervention in a rat breast tumor (No. 1, 3.2 cm^3). Single-exponential curve fitting yielded $SaO_2 = 0.204\{1 - \exp[-(t - 20.02)/1.1]\} + 0.85$ ($R = 0.93$), $\Delta[HbO_2] = 0.655\{1 - \exp[-(t - 20.36)/2.59]\} + 0.125$ ($R = 0.89$), and $\Delta pO_2 = 42.68\{1 - \exp[-(t - 21.01)/4.56]\} + 16.66$ ($R = 0.98$); biexponential fitting resulted in $\Delta[HbO_2] = 0.373\{1 - \exp[-(t - 20.36)/0.61]\} + 0.648\{1 - \exp[-(t - 20.36)/21]\}$ ($R = 0.97$).

0.93), followed by $[HbO_2]$ with $\tau(\Delta[HbO_2]) = 2.59 \pm 0.06$ min ($R = 0.89$), whereas ΔpO_2 yielded the slowest response $\tau(\Delta pO_2) = 4.56 \pm 0.06$ min ($R = 0.98$). Time constants for Group 1 are listed in Table 1. In every case $\tau(SaO_2) < \tau(\Delta[HbO_2]) < \tau(\Delta pO_2)$, based on the single-exponential fitting. No apparent relation between the time constant and the tumor volume was observed.

It is clear that the response of ΔHbO_2 is not well represented by a single exponential, and thus, a double-exponential expression with two time constants, τ_1 and τ_2, was also used (Fig. 3). Comparison between the biexponential fitting for $\Delta[HbO_2]$ and the single-exponential results for both SaO_2 and ΔpO_2 in the first five rat tumors (Table 1) shows that the time constants of SaO_2 ($\sim 1.2 \pm 0.4$ min) are similar to those of the first phase of $\Delta[HbO_2]$ ($\sim 0.5 \pm 0.2$ min), whereas the second phase is longer and highly variable ($\sim 14 \pm 11$ min). No significant correlations were found between any of the time constants in Table 1.

Time delay, t_d, between the time when the gas intervention was initiated and the time when the changes in signals were detected, reveals another difference among the three oxygen-sensitive parameters. For tumor 1 (Fig. 2), the SaO_2 signal was the first to respond to the intervention. Change in $\Delta[HbO_2]$ was observed 30 s later with $t_d = 30$ s, followed by changes in ΔpO_2 another 30 s later ($t_d = 60$ s). Similarly, when the gas was returned from carbogen to air, the SaO_2 signal decreased immediately, followed by declines in $\Delta[HbO_2]$ and in ΔpO_2 with t_d of 30 and 120 s later, respectively. As expected, changes in SaO_2 always preceded ΔHbO_2, and ΔpO_2 occurred last for all tumors.

B. Comparison of the Effects of Carbogen and Oxygen Intervention on Tumor Oxygenation

Switching from air breathing to carbogen or oxygen produced similar changes in ΔHbO_2 [Fig. 4(a)]. However, the time course was substantially different, requiring a biphasic exponential fit for carbogen, but a single exponential for oxygen [Fig. 4(b)]. For the seven tumors in Group 1, there was no significant difference ($p > 0.3$) in the maximum magnitude of $\Delta[HbO_2]$ caused by carbogen or oxygen interventions [Fig. 4(c)].

To examine the possible effect of preconditioning required that Group 2 experience a reversed gas intervention, with exposure to oxygen prior to carbogen [Fig. 5(a)]. In this case, the time constants of the normalized tumor vascular $\Delta[HbO_2]$ were now similar for both gas challenges: indeed, for six of seven tumors, carbogen no longer induced the biphasic behavior. Figure 5(b) shows that changes in $(\Delta HbO_2)_{max}$ were similar to those in Group 1, and again, the two gases did not produce significantly different response in $(\Delta HbO_2)_{max}$. This is emphasized for both Groups 1 and 2 by a strong linear correlation (slope $\cong 1.16$) between the $\Delta[HbO_2]_{max}$ values observed in response to each of the two con-

Table 1. Time Constants of SaO_2, $\Delta[HbO_2]$, and ΔpO_2 Response to Carbogen and Oxygen Intervention in the Breast Tumors[a]

Breast Tumors	Single-Exponential Fitting of SaO_2, $\Delta[HbO_2]$ and ΔpO_2 (Carbogen Intervention)						Double-Exponential Fitting for $\Delta[HbO_2]$ (Carbogen Intervention)			Single-Exponential Fitting of $\Delta[HbO_2]$ (O_2 Intervention)	
	SaO_2		$\Delta[HbO_2]$		ΔpO_2						
Volume (cm^3)	τ (min)	R	τ (min)	R	τ (min)	R	$\tau 1$ (min)	$\tau 2$ (min)	R	τ (min)	R
No. 1 (3.2)	1.1 ± 0.2	0.93	2.59 ± 0.06	0.89	4.56 ± 0.04	0.98	0.61 ± 0.03	21 ± 3	0.97	0.35 ± 0.01	0.92
No. 2 (3.0)	1.6 ± 0.2	0.98	3.40 ± 0.07	0.91	4.6 ± 0.1	0.82	0.62 ± 0.06	11 ± 1	0.96	0.51 ± 0.01	0.91
No. 3 (4.6)	1.2 ± 0.2	0.97	2.12 ± 0.06	0.76	2.26 ± 0.02	0.98	0.6 ± 0.1	37 ± 3	0.96	1.52 ± 0.02	0.89
No. 4 (2.6)	1.9 ± 0.3	0.98	2.68 ± 0.05	0.93	3.5 ± 0.1	0.86	0.12 ± 0.02	5.2 ± 0.1	0.98	1.71 ± 0.03	0.94
No. 5 (5.6)	0.8 ± 0.2	0.91	2.68 ± 0.05	0.74	4.51 ± 0.02	0.99	0.17 ± 0.03	12.5 ± 0.6	0.99	5.49 ± 0.03	0.98
No. 6 (1.9)	0.9 ± 0.2	0.81	1.62 ± 0.01	0.95	nd	/	0.63 ± 0.08	2.3 ± 0.1	0.96	5.16 ± 0.06	0.93
No. 7 (0.72)	1.0 ± 0.5	0.95	3.60 ± 0.03	0.93	nd	/	0.61 ± 0.02	10.5 ± 0.3	0.98	3.54 ± 0.03	0.95
Mean	1.2 ± 0.4		2.7 ± 0.6		4 ± 1		0.5 ± 0.2	14 ± 11		2.5 ± 2	

[a]Under the inhalation sequence of air–carbogen–air–oxygen–air.
[b]nd, not determined.

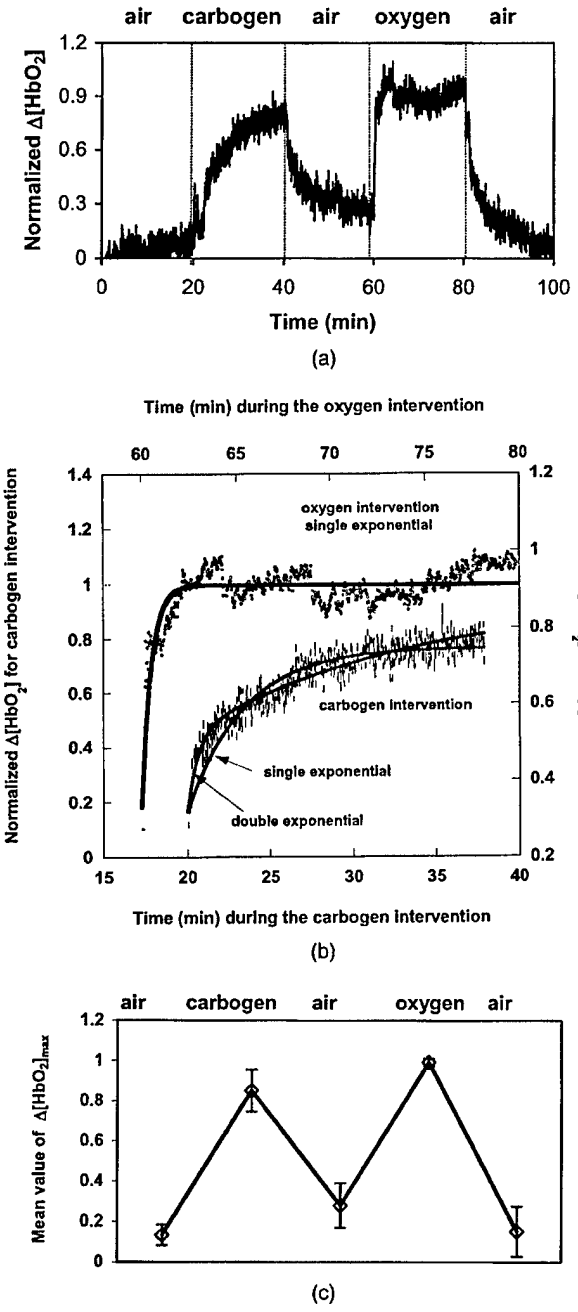

Fig. 4. (a) Time course of changes in tumor vascular $\Delta[HbO_2]$ for a representative 13762NF breast tumor from Group 1 (No. 2, 3.0 cm^3) with respect to altering inhaled gas. (b) Respective curve fits for the carbogen and oxygen interventions. (c) Average maximum values of normalized $\Delta[HbO_2]$ for the seven breast tumors in Group 1.

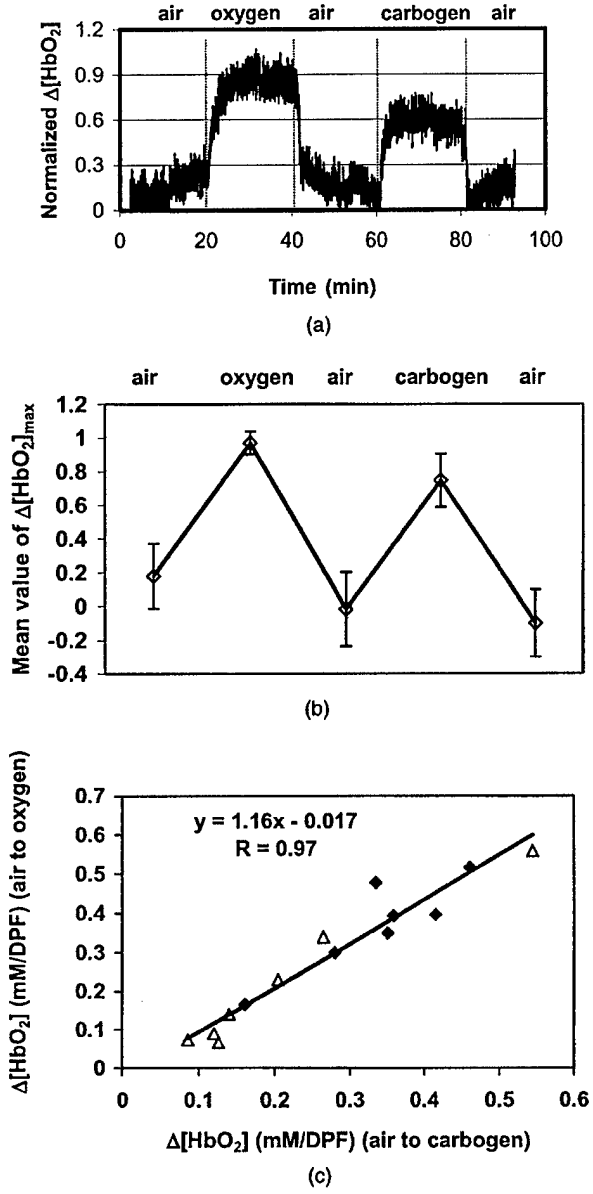

Fig. 5. (a) Dynamic changes in tumor vascular $\Delta[HbO_2]$ for a representative 13762NF breast tumor from Group 2 (No. 9, 2.6 cm^3) with gas-inhalation sequence reversed compared with Group 1. (b) Average maximum values of normalized $\Delta[HbO_2]$ for Group 2. Gas-inhalation sequence reversed compared with Group 1. (c) Correlation between maximum $\Delta[HbO_2]$ achieved with carbogen inhalation versus that with oxygen (R = 0.97): ◆, carbogen first; △, oxygen first.

secutive interventions [Fig. 5(c)]. In this case, nonnormalized data are shown for specific comparison of the absolute $\Delta[HbO_2]_{max}$ produced by oxygen and carbogen for each of the tumors.

C. Tumor pO_2

The FOXY pO_2 probes generally indicated distinct heterogeneity in pO_2. Moreover, response to the hyperoxic gas was diverse: those probes that indicated apparently well-oxygenated regions usually showed a large and rapid response, whereas those with lower baseline pO_2 often showed little change [Fig. 6(a)]. The pO_2 responses to the two interventions showed a highly consistent behavior at each individual location [Fig. 6(b)]. There was also a distinct correlation between the global NIR measurements and the mean ΔpO_2 (Fig. 7). Because of heterogeneity in regional pO_2, the standard deviations of the mean pO_2 values were large.

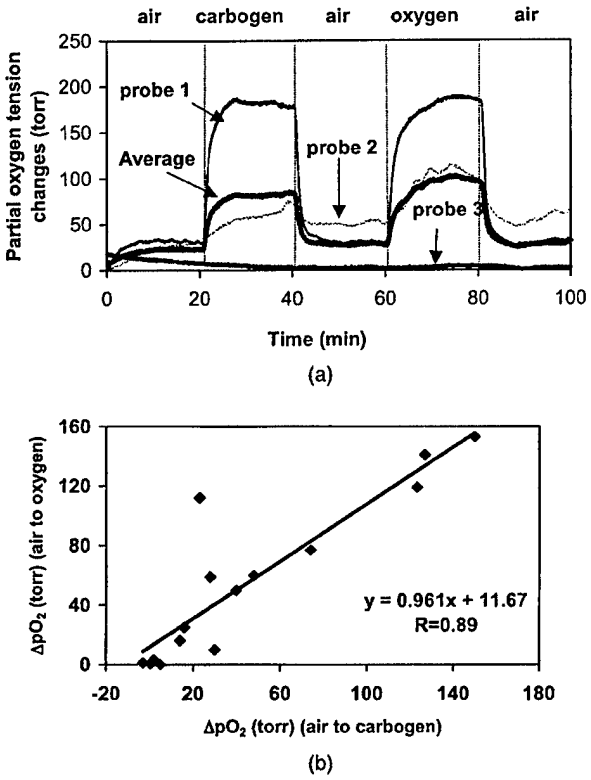

Fig. 6. (a) Time profiles of tumor ΔpO_2, measured with the three channels of the FOXY fiber-optic, oxygen-sensing system with respect to different gas inhalations for breast tumor No. 3 (4.6 cm^3). The mean signal for the three channels was calculated and is plotted by the thicker trace. (b) Correlation between ΔpO_2 at individual locations in the tumors in response to carbogen or oxygen for the five tumors in Group 1 ($R > 0.8$).

4. Discussion

In this study, we have simultaneously measured the arterial SaO_2, the global changes in the $\Delta[HbO_2]$ of tumor vasculature, and the regional changes in the ΔpO_2 of tumor tissue, in response to hyperoxic (i.e., carbogen and oxygen) gas interventions with a pulse oximeter, an NIRS system and a multichannel, fiber-optic, oxygen-sensing system, respectively. All three oxygen-sensitive indicators displayed similar dynamic tendency in response to carbogen intervention (Fig. 2).

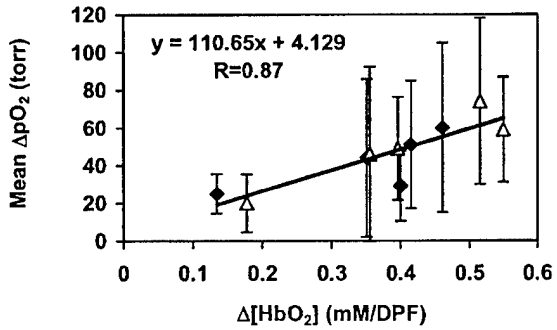

Fig. 7. Correlation between mean ΔpO_2 and $\Delta[HbO_2]$ for the five breast tumors ($R > 0.86$): ◆, transition from air to carbogen; △, transition from air to oxygen.

The simultaneous measurements demonstrate the compatibility of the NIRS system with the FOXY fiber-optic oxygen-sensing system, without interference. Both systems are relatively inexpensive and provide real-time measurements, but the multichannel FOXY fiber-optic system monitors ΔpO_2 in specific locations, whereas the NIRS system provides global measurements. Whether ΔHbO_2 determined with this methodology will be a clinically useful predictor for tumor response to oxygen-dependent interventions and therapies remains to be determined. However, it is established that measurements of pO_2 have prognostic value in the clinic[18,20] so that correlations between pO_2 and NIR measurements would be very important.

We have previously applied a polarographic oxygen electrode simultaneously with NIR.[25] However, that study provided only a single local pO_2 value, and in some cases correlations with global NIR measurements were very poor. The optical fiber system used here allows multiple locations to be interrogated simultaneously. The device can be expanded to many channels, but our system uses four channels. Unfortunately, probes are fragile, and the oxygen-sensitive coating on the tips is readily damaged. Thus, we only had three probes available for this study. Indeed, fiber-optic probe fragility is a well-recognized problem, and our previous experience with the more expensive OxyLite system was also restricted to three channels owing to probe damage.[26]

The FOXY system (~$13k) is much less expensive than the OxyLite (~$48k), and its mode of action is also simpler, detecting fluorescent signal intensity rather than fluorescence lifetime. It seems capable of measuring pO_2 across the whole range of atmospheric oxygen tensions (0–760 Torr), whereas the OxyLite is restricted and becomes very insensitive above approximately 100 Torr. However, our experience shows that although the FOXY system provides precise measurements of ΔpO_2, absolute values of pO_2 may not be reliable. We continue to perform validation experiments. By contrast, the OxyLite system seems to give very accurate pO_2 values.

Our experience shows that the FOXY probes are much easier to use than electrodes, particularly, in terms of calibration and stability. Since the probes are fragile, we insert them into tumors through a fine needle (25 gauge), which readily punctures the surrounding skin and penetrates tough fibrous tissues. The needle is then backed up from the tip to facilitate measurements. The probes often require a few minutes to settle at a stable baseline value, but then show good baseline stability and rapid response to interventions [Figs. 2 and 6(a)]. They are easily moved within the tumor to locate regions, presenting a particular pO_2 of interest, e.g. hypoxic or well oxygenated. In the search for appropriate locations, probes are moved forward to interrogate fresh tissues rather than in reverse, since blood may pool in the tracks owing to vascular damage. However, we observe

minimal bleeding on removal of the probes from the tumors.

We have found no interference between the NIR and FOXY instruments, although any tumor motion associated with moving the fiber probes can alter the optical contact of the NIR optrodes, and thus, alter apparent ΔHbO_2. Thus, baseline ΔHbO_2 is determined once the fiber probes are situated. New fiber-optic probes of the FOXY system have a thick coating of fluorescent gel and a black covering, but this wears with use and gradually allows reception of the NIR light. Since the LEDs of the two systems operate at very different wavelengths, viz. 475 versus 760 nm, there is no interference for detection. The detection of local NIR light by the FOXY probe opens the exciting possibility of detecting regional hemoglobin oxygen saturation. We believe the FOXY optical probes could be moved within the tumor to map the distribution and path of the transmitted NIR light, helping to explore and validate the optical characteristics of the tumor. This can simultaneously provide a correlation between local ΔHbO_2 and ΔpO_2.

In this study, we have examined a much larger group of rats than previously.[16,25] We have now shown rigorously that the two hyperoxic gases induce similar changes in vascular oxygenation (NIR) and regional tissue pO_2 (FOXY) in this type of rat breast tumor. These data are consistent with our previous observations using ^{19}F NMR imaging (FREDOM)[33] in this tumor type and also in rat prostate tumors.[34,35] If the two gases are indeed equivalent in terms of manipulation of tumor oxygenation, it could have great therapeutic benefit since the popular carbogen, which is in use in clinical trials,[36] can cause respiratory discomfort.

The current data show that ΔHbO_2 and ΔpO_2 are correlated (Fig. 7), and thus, such noninvasive observations could have value in the clinic. The major deficiency in our current NIR approach is lack of spatial discrimination, and thus efforts to implement NIR imaging will be of great value. It will also be interesting to correlate other measurements, such as blood-oxygen-level-dependent (BOLD) proton magnetic resonance imaging, which provide high spatial resolution, but which are sensitive to vascular flow and volume as well as oxygenation.[37]

The biphasic response of ΔHbO_2 to carbogen is intriguing, and we believe it represents the distinct vascular compartments of arterioles (high flow) and capillaries. However, the change to monophasic behavior, when carbogen is administered second, requires further exploration; in the future, we propose to test various concentrations of oxygen and carbon dioxide and air to separate the components of the response. The carbogen dioxide component of carbogen is known to be vasoactive; however, the specific effects may depend on tumor type, site of growth, and other factors.[9,38]

In terms of vascular oxygen delivery, the data in Table 1 reveal the progressive movement of oxygen: t_d (SaO_2) < t_d ($\Delta[HbO_2]$) < t_d (ΔpO_2). As expected, switching to hyperoxic gas caused the systemic arterial SaO_2 to increase, as a result of the immediate combination of deoxyhemoglobin with oxygen. The highly oxygenated blood circulated in the systemic vasculature of the rats (including the capillary bed of the tumor tissue), resulting in a delayed increase in $[HbO_2]$ in the tumor vasculature, and led to an unloading of oxygen to the tumor tissue. For the biexponential model of $\Delta[HbO_2]$, the fast component has a similar time constant to the SaO_2 measured with the pulse oximeter on the hind leg, strongly suggesting that it represents arteriolar oxygenation in the tumor. In this study, tumor volumes do not show any direct relation with time constants or changes of amplitude in response to hyperoxic gas interventions.

It is increasingly evident that oxygen and hypoxia play important roles in tumor development and response to therapy.[18] NIR offers an attractive noninvasive means of investigating tumor oxygenation, particularly in terms of dynamic response to interventions, but we had previously shown a potential mismatch between global ΔHbO_2 and local ΔpO_2.[25] The data presented here indicate a correlation between the global NIR measurements and mean pO_2 values with even as few as three representative locations per tumor. This does suggest that it will be important to develop regional NIR measurements and that even relatively crude mapping could reveal heterogeneity. In the meantime, we believe these studies provide further evidence for the value of NIRS to explore tumor physiology.

This study was supported in part by the Department of Defense Breast Cancer Research grants BC000833 (YG) and BC990287 (HL), and NIH RO1 CA79515 (RPM) and RO1 supplement CA79515-S (VB). We are grateful to Mengna Xia and Dawen Zhao for their assistance with data processing. We gratefully acknowledge Weina Cui for helpful discussions.

References

1. R. S. Bush, R. D. T. Jenkin, W. E. C. Allt, F. A. Beale, A. J. Dembo, and J. F. Pringle, "Definitive evidence for hypoxic cells influencing cure in cancer therapy," Br. J Cancer **37**(suppl 3), 302–306 (1978).
2. E. J. Hall, *Radiobiology for the Radiologist*, 4th ed. (Lippincott, Philadelphia, Pa., 1994).
3. M. Nordsmark and J. Overgaard, "A confirmatory prognostic study on oxygenation status and loco-regional control in advanced head and neck squamous cell carcinoma treated by radiation therapy," Radiother. Oncol. **57,** 39–43 (2000).
4. O. Thews, D. K. Kelleher, and P. Vaupel, "Erythropoietin restores the anemia-induced reduction in cyclophosphamide cytotoxicity in rat tumors," Cancer Res. **61,** 1358–1361 (2001).
5. J. H. A. M. Kaanders, L. A. M. Pop, H. A. M. Marres, R. W. M. van der Maazen, A. J. van der Kogel, and W. A. J. van Daal, "Radiotherapy with carbogen breathing and nicotinamide in head and neck cancer: feasibility and toxicity," Radiother. Oncol. **37,** 190–198 (1995).
6. M. I. Saunders, P. J. Hoskin, and K. Pigott, "Accelerated radiotherapy, carbogen and nicotinamide (ARCON) in locally advanced head and neck cancer: a feasibility study," Radiother. Oncol. **45,** 159–166 (1997).
7. J. A. Kruuv, W. R. Inch, and J. A. McCredie, "Blood flow and

oxygenation of tumors in mice. I. Effects of breathing gases containing carbon dioxide at atmospheric pressure," Cancer. **20,** 51–59 (1967).
8. J. Overgaard and M. R. Horsman, "Modification of hypoxia-induced radioresistance in tumors by the use of oxygen and sensitizers," Semin. Radiat. Oncol. **6,** 10–21 (1996).
9. P. Vaupel, D. K. Kelleher, and O. Thews, "Modulation of tumor oxygenation," Int. J. Radiat. Oncol. Bio. Phys. **42,** 843–848 (1998).
10. S. Dische, "What we learnt from hyperbaric oxygen?" Radiother. Oncol. **20**(Suppl.), 71–74 (1991).
11. S. Dische, M. I. Saunders, and R. Sealy, "Carcinoma of the cervix and the use of hyperbaric oxygen with radiotherapy: a report of a randomized controlled trial," Radiother. Oncol. **53,** 93–98 (1999).
12. V. M. Laurence, R. Ward, I. F. Dennis, and N. M. Bleehen, "Carbogen breathing with nicotinamide improves the oxygen status of tumors in patients," Br. J Cancer **72,** 198–205 (1995).
13. L. Martin, E. Lartigau, and P. Weeger, "Changes in the oxygenation of head and neck tumors during carbogen breathing," Radiother. Oncol. **27,** 123–130 (1993).
14. H. B. Stone, J. M. Brown, T. Phillips, and R. M. Sutherland, "Oxygen in human tumors: correlations between methods of measurement and response to therapy," Radiat. Res. **136,** 422–434 (1993).
15. E. L. Hull, D. L. Conover, and T. H. Foster, "Carbogen induced changes in rat mammary tumor oxygenation reported by near infrared spectroscopy," Br. J. Cancer **79,** 1709–1716 (1999).
16. H. Liu, Y. Song, K. L. Worden, X. Jiang, A. Constantinescu, and R. P. Mason, "Noninvasive investigation of blood oxygenation dynamics of tumors by near-infrared spectroscopy," Appl. Opt. **39,** 5231–5243 (2000).
17. R. G. Steen, K. Kitagishi, and K. Morgan, "*In vivo* measurement of tumor blood oxygenation by near-infrared spectroscopy: immediate effects of pentobarbital overdose or carmustine treatment," J. Neuro-Oncol. **22,** 209–220 (1994).
18. M. Höckel and P. Vaupel, "Tumor hypoxia: definitions and current clinical, biologic, and molecular aspects," J. Natl. Cancer Inst. **93,** 266–276 (2001).
19. L. Gray, A. Conger, M. Ebert, S. Hornsey, and O. Scott, "The concentration of oxygen dissolved in tissues at time of irradiation as a factor in radio-therapy," Br. J. Radiol. **26,** 638–648 (1953).
20. A. W. Fyles, M. Milosevic, R. Wong, M. C. Kavanagh, M. Pintile, A. Sun, W. Chapman, W. Levin, L. Manchul, T. J. Keane, and R. P. Hill, "Oxygenation predicts radiation response and survival in patients with cervix cancer," Radiother. Oncol. **48,** 149–156 (1998).
21. D. Zhao, A. Constantinescu, E. W. Hahn, and R. P. Mason, "Measurement of tumor oxygen dynamics predicts beneficial adjuvant intervention for radiotherapy in Dunning prostate R3327-HI tumors," Radiat. Res. (to be published) (2003).
22. C. Song, I. Lee, T. Hasegawa, J. Rhee, and S. Levitt, "Increase in pO_2 and radiosensitivity of tumors by Fluosol and carbogen," Cancer Res. **47,** 442–446 (1987).
23. D. Cater and I. Silver, "Quantitative measurements of oxygen tension in normal tissues and in the tumors of patients before and after radiotherapy," Acta Radiol. **53,** 233–256 (1960).
24. D. Zhao, A. Constantinescu, E. W. Hahn, and R. P. Mason, "Differential oxygen dynamics in two diverse Dunning prostate R3327 rat tumor sublines (MAT-Lu and HI) with respect to growth and respiratory challenge," Int. J. Radiat. Oncol. Biol. Phys. **53,** 744–756 (2002).
25. J. G. Kim, Y. Song, D. Zhao, A. Constantinescu, R. P. Mason, and H. Liu, "Interplay of tumor vascular oxygenation and pO_2 in tumors using NIRS, ^{19}F MR pO_2 mapping, and pO_2 needle electrode," J. Biomed. Optics **8,** 53–62 (2003).
26. D. Zhao, A. Constantinescu, E. W. Hahn, and R. P. Mason, "Tumor oxygen dynamics with respect to growth and respiratory challenge: investigation of the Dunning prostate R3327-HI tumor," Radiat. Res. **156,** 510–520 (2001).
27. J. Bussink, J. H. A. M. Kaanders, A. M. Strik, B. Vojnovic, and A. J. van der Kogel, "Optical sensor-based oxygen tension measurements correspond with hypoxia marker binding in three human tumor xenograft lines," Radiat. Res. **154,** 547–555 (2000).
28. J. R. Griffiths, "The OxyLite: a fibre-optic oxygen sensor," Br. J. Radiol. **72,** 627–630 (1999).
29. Y. Gu, Z. Qian, J. Chen, D. Blessington, N. Ramanujam, and B. Chance, "High resolution three dimensional scanning optical image system for intrinsic and extrinsic contrast agents in tissue," Rev. Sci. Instrum. **73,** 172–178 (2002).
30. Ocean Optics Inc., Dunedin, Fla., March 2003. http://www.oceanoptics.com/products/foxysystem.asp
31. C. B. Allen, B. K. Schneider, and C. J. White, "Limitations to oxygen diffusion in *in vitro* cell exposure systems in hyperoxia and hypoxia," Am. J. Physiol. Lung Cell Molec. Physiol. **281,** L1021–L1027 (2001).
32. E. W. Hahn, P. Peschke, R. P. Mason, E. E. Babcock, and P. P. Antich, "Isolated tumor growth in a surgically formed skin pedicle in the rat: a new tumor model for NMR studies," Magn. Reson. Imaging **11,** 1007–1017 (1993).
33. Y. Song, A. Constantinescu, and R. P. Mason, "Dynamic breast tumor oximetry: the development of prognostic radiology," Technol. Cancer Res. Treat. **1,** 1–8 (2002).
34. S. Hunjan, D. Zhao, A. Constantinescu, E. W. Hahn, P. P. Antich, and R. P. Mason, "Tumor oximetry: demonstration of an enhanced dynamic mapping procedure using Fluorine-19 echo planar magnetic resonance imaging in the Dunning prostate R3327-AT1 rat tumor," Int. J. Radiat. Oncol. Biol. Phys. **49,** 1097–1108 (2001).
35. D. Zhao, A. Constantinescu, L. Jiang, E. W. Hahn, and R. P. Mason, "Prognostic radiology: quantitative assessment of tumor oxygen dynamics by MRI," Am. J. Clin. Oncol. **24,** 462–466 (2001).
36. J. H. Kaanders, J. Bussink, and van der A. J. Kogel, "ARCON: a novel biology-based approach in radiotherapy," Lancet Oncol. **3,** 728–737 (2002).
37. F. A. Howe, S. P. Robinson, L. M. Rodrigues, and J. R. Griffiths, "Flow and oxygenation dependent (FLOOD) contrast MR imaging to monitor the response of rat tumors to carbogen breathing," Magn. Reson. Imaging. **17,** 1307–1318 (1999).
38. T. J. Dunn, R. D. Braun, W. E. Rhemus, G. L. Rosner, T. W. Secomb, G. M. Tozer, D. J. Chaplin, and M. W. Dewhirst, "The effects of hyperoxic and hypercarbic gases on tumour blood flow," Br. J. Cancer **80,** 117–126 (1999).

Vascular oxygen dynamics of breast tumors in response to physiological interventions monitored by Near Infrared Spectroscopy

Yueqing Gu, Ph. D.[+], Yulin Song, Ph. D.[+*], Anca Constantinescu, Ph. D. [*], Hanli Liu, Ph.D. and Ralph P. Mason, Ph. D. [*a],

Biomedical Engineering Graduate Program, The University of Texas at Arlington and

*Department of Radiology, The University of Texas Southwestern Medical Center, Dallas, Texas

[+] Contributed equally to this work

This work was supported in part by the Department of Defense Breast Cancer Research Initiative: pre-doctoral grant DAMD17-97-1-7261 (YS), post doctoral grant BC000833 (YG) and IDEA award BC990287 (HL), together with NIH RO1 CA79515 (EB002762) (RPM) and in conjunction with the Cancer Imaging Program P20 CA086354.

[a] Address correspondence to:
Ralph P. Mason, Ph.D., C. Chem.,
Department of Radiology,
U.T. Southwestern Medical Center,
5323 Harry Hines Blvd.,
Dallas, TX 75390-9058
Tel: (214) 648-8926; Fax: (214) 648-2991;
E. mail: Ralph.Mason@UTSouthwestern.edu

ABSTRACT

Purpose: The goal of this investigation was to demonstrate the feasibility of applying Near Infrared Spectroscopy (NIRS) to examine tumor vascular dynamics. Various interventions expected to modulate the concentration of oxygenated hemoglobin, $\Delta[HbO_2]$, and total hemoglobin, $\Delta[Hb]_{total}$, were evaluated in rat breast tumors.

Methods and Materials: Transmission mode NIRS was applied to 13762 breast adenocarcinomas, while the Fisher rats were exposed to respiratory challenge with the hyperoxic gases carbogen (5% CO_2 and 95% O_2), oxygen, a hypercarbic mixture of 5% CO_2 in air and with respect to infusion of the vasoactive agent hydralazine.

Results: Repeated carbogen breathing yielded increases in vascular oxygenation with highly reproducible modulation both in magnitude and response time. Carbogen and oxygen breathing each significantly elevated oxygenation of the tumor vasculature, however, the rate and pattern of response differed and depended on the sequence of gas breathing. Addition of CO_2 to air generated a small, but significant elevation of $\Delta[HbO_2]$. Hydralazine administration during carbogen or air breathing decreased both the vascular oxygenation and total vascular hemoglobin (vascular volume) significantly.

Conclusions: These results demonstrate NIRS as a non-invasive, real-time means for monitoring tumor vascular oxygen dynamics in response to acute interventions, indicating potential utility for evaluating novel therapies and possibly treatment planning.

Keywords: Near infrared spectroscopy, breast tumor, oxyhemoglobin, carbogen, hydralazine.

1. Introduction

There is increasing evidence that tumor oxygenation plays a critical role in disease progression and response to therapy. In particular, modulation of tumor oxygenation may improve therapeutic outcome, since hypoxic cells resist radiotherapy and certain drugs exhibit selective cytotoxicity. Several recent studies have shown poor prognosis for patients with relatively hypoxic tumors of the cervix and head and neck (1-4) and extensive hypoxia has been found in tumors of the prostate and breast (5, 6). While many attempts to improve therapeutic outcome by manipulation of tumor oxygenation have shown only modest success (7), recent work by Kaanders *et al.* (8) has shown dramatic improvement for patients with hypoxic head and neck tumors, when treated with the ARCON protocol. Thus, there is a developing interest in measuring tumor oxygenation, and many techniques have been developed for quantitative measurement of pO_2 (9, 10), *e.g.*, electrodes (11), optical probes (12-14), EPR (15-17), and ^{19}F MRI (18-21). The Eppendorf Histograph has provided extensive clinical data showing correlation between tumor oxygenation (either median pO_2 or hypoxic fraction) and therapeutic outcome and is considered by some to be a "gold standard". Other techniques detect hypoxia itself using labels such as pimonidazole or EF5 (8, 22) in biopsy specimens, though imaging approaches are being developed (23).

Near-infrared spectroscopy (NIRS) offers an alternative approach based on the differential light absorption of the strong chromophores oxy- and deoxy hemoglobin (Fig 1a). NIRS provides a non-invasive means to monitor global tumor vascular oxygenation in real time based on endogenous molecules. While many investigations have been conducted in the brain and breast in both laboratory and clinical settings over the last

decade, there have been relatively few reports of NIRS studies of solid tumors (12, 24-34). Most studies to date have used reflectance mode. By contrast, we have favored transmission mode, so as to interrogate deep tumor regions, and we have presented preliminary studies in rat breast and prostate tumors with respect to various interventions (12, 25, 26). In this study, we have extended our investigations to larger cohorts of animals and more diverse interventions to investigate vascular oxygenation. Specifically, altering inhaled gas from air to oxygen, carbogen (95% O_2 and 5% CO_2) and a hypercarbic air mixture (5% CO_2 in air), as well as administration of the vasoactive agent hydralazine (HDZ).

2. Methods and Materials

2.1 NIRS for measurement of changes in $[HbO_2]$ and $[Hb]_{total}$

The homodyne frequency-domain NIRS system (NIM, Philadelphia, PA) used in this study has been described in detail previously (25). Briefly, as shown in Fig. 1(b), the amplitude-modulated light (140 MHz) from two NIR laser diodes at 758 nm and 785 nm was coupled into a bifurcated fiber bundle and illuminated on one side of the tumor. The light diffusing through the tumor was collected by a second fiber bundle and propagated to a photomultiplier tube (PMT). The signal from the PMT was demodulated through an In-phase and Quadrature-phase circuit, and the amplitude variations recorded. Absorption of the NIR light by the two major absorbers within the tumor tissue, oxygenated and deoxygenated hemoglobin, can be quantified by modifying Beer-Lambert's law (25). Changes in oxygenated, deoxygenated, and total hemoglobin

concentrations, *i.e.*, $\Delta[HbO_2]$, $\Delta[Hb]$ and $\Delta[Hb]_{total}$ are calculated using equations, which have been derived previously (12, 26):

$$\Delta[HbO_2] = \frac{-10.63 \cdot \log(\frac{A_B}{A_T})^{758} + 14.97 \cdot \log(\frac{A_B}{A_T})^{785}}{d}, \quad (1)$$

$$\Delta[Hb] = \frac{8.95 \cdot \log(\frac{A_B}{A_T})^{758} - 6.73 \cdot \log(\frac{A_B}{A_T})^{785}}{d}, \quad (2)$$

$$\Delta[Hb]_{total} = \Delta[HbO_2] + \Delta[Hb], \quad (3)$$

where A_B and A_T are the baseline and transient amplitudes measured from the NIR system, respectively, and "d" is the source-detector separation, subject to the differential path-length factor (DPF) for tumor tissues. Thus, $\Delta[HbO_2]$, $\Delta[Hb]$ and $\Delta[Hb]_{total}$ all have relative units of mM/DPF. The four coefficients in the equations were derived using the extinction coefficients of Hb and HbO_2 at corresponding wavelengths and have been corrected for the pathlength differences at the two wavelengths (26).

2.2 Animal model and protocols

The Institutional Animal Care and Use Committee approved these investigations. Rat mammary adenocarcinomas 13762NF (35) (originally obtained from DCT, NCI) were implanted in skin pedicles (36) on the foreback of adult female Fisher 344 rats (~150 g). Once the tumors reached 1~3 cm diameter, rats were anesthetized with 150-

μl ketamine hydrochloride (100 mg/ml, i.p.) and maintained under general gaseous anesthesia with 1.3% isoflurane in air (1 dm^3/min). For gas interventions, the anesthetic and gas flow were maintained at a constant level. Tumors were shaved to improve optical contact for NIR light transmission, and the body temperature was maintained at 37 ^{0}C using a warm water blanket. Tumor volume was estimated using an ellipsoid approximation ($V=(\pi/6).a.b.c$) from the three orthogonal diameters (a,b,c). In some cases a pulse oximeter (Nonin Medical Inc., Plymouth, MN) was applied to the hind foot to assess dynamic response of arterial oxygenation.

In this study, four groups of rats were used to investigate the dynamic response of breast tumor oxygenation to interventions. Group 1 (n=8) experienced repeated carbogen breathing using the sequence air-carbogen-air-carbogen-air to demonstrate reproducible effects of carbogen on tumor oxygenation. Group 2 (n=7) breathed the sequence air-carbogen–air–oxygen–air, while Group 3 (n=7) experienced the reverse sequence (air-oxygen-air-carbogen-air), so as to compare the two hyperoxic gas interventions and allow for any preconditioning. A subgroup (3A) also received an i.v. infusion of hydralazine (HDZ; 5 mg/kg in 0.5 ml saline, Sigma) as a bolus by hand (< 1 min) in the tail vein during the carbogen breathing (air-oxygen-air-carbogen-carbogen+HDZ–air; n= 5). Group 4 (n=5) experienced air-hypercarbic air (5% CO_2 in air)–carbogen–air–oxygen–air-air+HDZ, to investigate the effect of CO_2 on the tumor vascular bed. Each gas was applied for 20-24 minutes in all the breathing sequences.

3. Results

Figure 2a shows the typical time course for response of $\Delta[HbO_2]$ to successive carbogen interventions for a representative Group 1 tumor (No. 2, 9.9 cm^3). When the inhaled gas was switched from air to carbogen, $\Delta[HbO_2]$ increased rapidly and significantly ($p < 0.0001$) from the baseline to about 0.87 ± 0.03 within the first two minutes, followed by a slower, but further significant increase ($p<0.001$) over the next 21 minutes. Returning to air breathing produced a significant drop ($p < 0.0001$) of $\Delta[HbO_2]$ with asymptotic tendency towards the baseline value. A very similar temporal response was observed during the second cycle of carbogen intervention. The magnitude of response was highly consistent, as shown for the eight individual tumors in Fig. 2b (R^2 >0.92). In addition to magnitude of response, the dynamic behavior of $\Delta[HbO_2]$ with respect to carbogen intervention may be characterized by time constants for exponential curves (25). We have previously found that a bi-exponential fit is required to represent the biphasic nature of the response to carbogen breathing, and fitted curves are overlaid on Fig. 2a. We believe the fast component represents rapid arteriolar inflow with a typical time constant < 1 minute, whereas the 2^{nd} component is more sluggish. The ratio $\tau 1/\tau 2$ reveals the relative efficiency of these components, which was highly reproducible for the successive interventions (Fig. 2c).

To assess the relative ability of oxygen versus carbogen to modulate tumor vascular oxygenation, response to the two gases was compared. Separate groups of rats received the gases in reversed sequence in order to reveal any preconditioning effects. Figure 3 shows the time course of $\Delta[HbO_2]$ for a representative 13762NF breast tumor (3.2 cm^3) in Group 2. The carbogen intervention produced a similar biphasic

response of $\Delta[HbO_2]$ to that seen for Group 1. Following the initial exposure to carbogen and 20 minutes of air breathing for re-equilibration, the rat was exposed to oxygen. As with carbogen, there was a rapid increase in $\Delta[HbO_2]$ within the first 2 minutes, but this was followed by a plateau and curve fitting required a single exponential only. The maximal response of $\Delta[HbO_2]$ to carbogen and oxygen interventions was similar, as shown in Fig. 3b. While each gas produced a significant elevation in $\Delta[HbO_2]$, there was no significant difference in magnitude for these two hyperoxic gas interventions ($p>0.3$). However, we note that 20 mins was sometimes insufficient time for $\Delta[HbO_2]$ to return to baseline after carbogen breathing. Thus, the apparent increase is based on an elevated starting point. To address this potential anomaly, we considered both the ascending response with each hyperoxic gas and the ascending response to carbogen versus the decrease following oxygen inhalation, which occurred more rapidly (Fig. 3a). Indeed, both the increase and the decline in $\Delta[HbO_2]$ were significantly faster with respect to oxygen breathing than carbogen (Fig. 3c, d).

In order to examine the possible effect of preconditioning, tumors in Group 3 experienced the "reversed" gas intervention, with exposure to oxygen prior to carbogen (Fig. 4a). As for Group 2, the maximal changes of $\Delta[HbO_2]$ due to oxygen or carbogen intervention for each of these 7 tumors were found to be similar (Fig. 4b). However, both interventions now produced a monophasic response: in 6 of the 7 tumors the biphasic response to carbogen was no longer seen.

To further explore the vasoactive contribution of the CO_2 component, rats in Group 4 inhaled a hypercarbic air mixture (air + 5% CO_2), followed by carbogen (95% O_2 +5% CO_2). Fig. 5a shows the time course of $\Delta[HbO_2]$ for a representative tumor (1.9

cm^3). When CO_2 was added to the inhaled air $\Delta[HbO_2]$ increased immediately, and significantly, to a plateau 0.15 ± 0.01 (normalized to the maximum value achieved with hyperoxic gas; $p<0.05$). Response to carbogen was as before. Typically, addition of the CO_2 component to air caused $\Delta[HbO_2]$ to increase by about 10-20% of that due to carbogen (Fig. 5b).

Several rats were also infused with HDZ during carbogen (subgroup 3A) or air breathing (Group 4), and the response of $\Delta[HbO_2]$ is shown for representative tumors in Figs. 4a and 5a. For Group 3a, the mean decrease in $\Delta[HbO_2]$ was 0.8 ± 0.2 for the transition oxygen to air, 1.2 ± 0.4 following HDZ administration during carbogen breathing, and a further 0.5 ± 0.3 for the final switch back to air. The decrease in oxygenation due to hydralazine was generally greater than the change accompanying oxygen to air breathing. However, the change attributable to HDZ was not significantly different during carbogen (Group 3a) or air (Group 4) breathing.

In addition to $\Delta[HbO_2]$, dual wavelength NIRS can also show changes in total hemoglobin ($\Delta[Hb]_{total}$), as shown by equation 3. Fig. 2a indicates that $\Delta[Hb]_{total}$ increased in response to breathing carbogen with a response about 20% of that for $\Delta[HbO_2]$. This was typical of many tumors, though some showed minimal response and often there was a continual drift throughout the variation in inhaled gases (Figs. 4a and 5a). Return to air breathing rarely reversed the $\Delta[Hb]_{total}$ and minimal change accompanied initial oxygen or secondary carbogen challenges (Fig. 2a, 4a, 5a). In some cases, $\Delta[Hb]_{total}$ increased with addition of CO_2 to air, but the pattern was highly variable. Infusion of HDZ always caused a significant decline in $\Delta[Hb]_{total}$, and during air

breathing the magnitude of the changes approached or exceeded the change in $\Delta[HbO_2]$.

4. Discussion

These studies reveal the vascular response to breathing hyperoxic and hypercarbic gases and the vasoactive pharmacological agent hydralazine. NIRS is non-invasive and provides a real time assessment of changes in tumor vascular hemoglobin saturation. These investigations provide a considerable extension of our previous NIR studies of tumors (12, 25, 26), in terms of numbers of animals, range of interventions, and extent of analysis. Most importantly, the results provide further demonstration of the ease and utility of NIRS studies of tumors.

As we have previously observed in various rat tumors (12, 25), switching the inhaled gas from air to carbogen produced a rapid biphasic elevation in hemoglobin oxygenation. The rapid component has a time constant in the range of seconds to a minute, and approaches that observed for arterial oxygen saturation detected in the hind foot with a pulse oximeter (Fig. 3a). The slow component (10 to 50 times slower) continues for many minutes, and generally represents 10-20% of the total change. Oxygenation was reversible upon returning to air inhalation. The decrease in $\Delta[HbO_2]$ was also biphasic, and elevated oxyhemoglobin was still present after ten to twenty minutes in many cases (Fig. 2a, 3a). The response was found to be highly consistent for repeat carbogen interventions (Fig. 2), as emphasized both in terms of magnitude (Fig. 2b) and rate (Fig. 2c). The high reproducibility of results suggests that repeat

interventions could be a valuable method for exploring the efficacy of interventions designed to modulate tumor vascular oxygenation (*e.g.*, vascular targeting agents).

Response to oxygen was much more rapid and fit well to a mono exponential curve. For almost every tumor, the time to reach 80% of maximum elevation in $\Delta[HbO_2]$ was longer for carbogen and for the group of seven tumors the difference was significant. Likewise, the decline in $\Delta[HbO_2]$ was more rapid following exposure to oxygen (Fig. 3d). Further examination of Fig. 3a indicates that the maximum $\Delta[HbO_2]$ reached with either hyperoxic gas was similar, but required longer with carbogen. Given that tumors had often not returned to baseline between hyperoxic gases, there could be a question of pre-conditioning or residual oxygenation. The decline in $\Delta[HbO_2]$ following oxygen breathing was faster than following carbogen, prompting a comparison of the increase on the rising part of carbogen (Fig. 3b) with the decrease following oxygen. Both analyses showed a strong correlation demonstrating that the ultimate increase in $\Delta[HbO_2]$ is similar for either hyperoxic gas.

Intriguingly, the biphasic response (slow component) for carbogen was usually eliminated, when the order of breathing hyperoxic gases was reversed (Fig. 4), yet the ultimate response was equivalent (Fig. 4b), whichever gas was breathed first. These data may be important in the context of the existing literature. Many investigators have compared the relative merits of oxygen or carbogen for improving tumor oxygenation. Overall carbogen is favored, and is being applied in clinical trials such as ARCON (3, 37). Our own previous investigations in the subcutaneous (pedicle) syngeneic breast tumor model showed that each gas appeared equally effective at improving tumor oxygenation (38). In practice oxygen might be favored since the response is more rapid,

suggesting that an effective pre-irradiation breathing time could be shorter. Given the reported respiratory distress induced by 5%CO_2, oxygen appears advantageous. However, as a corollary, the elevated oxygenation is more persistent following carbogen breathing, as also reported previously by Thews *et al.* (39). This could be important in circumstances where hyperoxic gas may be administered prior to, but not during irradiation. Indeed, others found evidence for persistence of improved oxygenation following exposure to hyperbaric oxygen (40, 41).

While improvement of tumor oxygenation has been a primary goal of much research and many clinical trials, an alternative paradigm is induction of hypoxia to enhance the efficacy of hypoxia selective cytotoxins, *e.g.*, tirapazamine (42). Our results show that while either gas is being breathed (air or carbogen) IV infusion of HDZ caused a rapid decline in $\Delta[HbO_2]$ to a level below baseline (Figs. 4a , 5a). The overall change in $\Delta[HbO_2]$ due to HDZ infusion was similar, whether the rats were breathing air or carbogen. The decline in $\Delta[HbO_2]$ could be caused by decreased hemoglobin oxygen saturation or reduced blood volume (*viz.* hematocrit). NIRS can provide measurements of both $\Delta[Hb]_{total}$ and $\Delta[HbO_2]$, simultaneously, as we have demonstrated in preliminary data in the past (25). Our current data indicate substantial changes in $\Delta[Hb]_{total}$ revealing reduced vascular volume in response to HDZ infusion coinciding with previous reports for implanted tumors (43-45).

Insight into tumor vascular volume is also pertinent to the hyperoxic gases, where there has been much debate concerning the relative vasoconstriction versus vasodilatory effects of CO_2 (46). Here, the addition of CO_2 to air caused a significant increase in $\Delta[HbO_2]$, but results for $\Delta[Hb]_{total}$ were less distinct. Likewise, the hyperoxic

gases were accompanied by a variable response in $\Delta[Hb]_{total}$. Our previous work in phantoms has rigorously validated the stability of the instrument and veracity of the algorithms used here (26), leading us to believe that our observations represent physiological phenomena. The results for $\Delta[HbO_2]$ with the hyperoxic gases are both consistent and intuitive. The results for $\Delta[Hb]_{total}$ are as expected for HDZ. The observations for response of $\Delta[Hb]_{total}$ to gas challenge indicate highly variable behavior. However, it must be noted that changes in $\Delta[Hb]_{total}$ are relatively smaller than $\Delta[HbO_2]$, so that errors in calculation become more significant.

Others have suggested that the carbon dioxide component of carbogen is critical to improving tumor oxygenation. Some tumors appear to respond only in the presence of CO_2 (33), which has variously been described as a vasoconstrictor or vasodilator (46). BOLD (or FLOOD - Flow and Oxygen Dependant contrast) MRI of G3H prolactinomas, a highly vascularized and perfused tumor type, showed some response to the addition CO_2 to air and much greater response to carbogen (47). However, oxygen produced a smaller effect than either hypercarbic gas. Here, carbogen and oxygen both induced significant increases in vascular hemoglobin oxygenation, which were essentially equal, though changes accompanying carbogen were slower. To probe the importance of the CO_2 component further, we tested the addition of 5% CO_2 to air. In all five tumors of Group 4, the addition of 5% CO_2 produced a rapid increase in $\Delta[HbO_2]$ with a stable plateau. Further switch to carbogen produced the usual response, which was five to six times greater than that due to the addition of CO_2 to air alone (Fig. 5b). The importance of the CO_2 component remains intriguing, since it generates rapid

response, when added to air, but appears to be responsible for the biphasic response of carbogen.

NIRS provides a global assessment, in contrast to BOLD MRI, which can provide high resolution images (20, 47). Imaging can show heterogeneity in temporal and spatial response, but results are often summarized using data reduction to show mean values only. As such, an *a priori* global measurement can provide similar insight into dynamic tumor physiology or drug pharmacodynamics, while being cheaper and easier to implement. Our approach to NIRS uses transmission mode, which we believe probes large and deep portions of the tumor, including the periphery on each side, as well as the center. This is in contrast to the methodology used by most other investigators, who apply reflectance mode (24, 28-30), which predominately indicates the behavior of the peripheral vasculature. Indeed, results from Hull *et al.* (24) are consistent with the fast component that we attribute to the well-perfused regions of our tumors.

Likely, the response to interventions depends on tumor type, site of implantation, and anesthetic. To place our current work in context, the 13762NF tumor type was originally developed by Bogden *et al.* (35) and has been used in investigations of tumor oxygenation in the past. In particular, Teicher *et al.* (48, 49) examined the effects of various cytotoxic drugs and blood substitutes on pO_2 using the Eppendorf Histograph. When tumors were implanted subcutaneously in the hind limb of Fisher rats there was extensive base line hypoxia with HF_5 greater than 60% (48).

We have previously investigated dynamic oxygenation in the 13762 NF adenocarcinoma using *FREDOM* (Fluorocarbon Relaxometry using Echo planar imaging for Dynamic Oxygen Mapping) (38). It should be noted that this particular tumor

develops extensive central necrosis and exhibits great heterogeneity in terms of tissue appearance and tumor oxygenation. The baseline hypoxic faction, in our hands, ranged from five to sixty percent with increasing hypoxic fraction and decreasing mean pO_2 as the tumors grew. Interestingly, the response to oxygen or carbogen was very similar, and on a voxel by voxel basis, the maximum pO_2 achieved was proportional to the initial baseline pO_2. It was also noteworthy that after forty minutes exposure to oxygen or carbogen, the mean tumor pO_2 continued to rise and had not reached a plateau. Not surprisingly, this indicates that the diffusion of oxygen into the tumor tissue is considerably slower than changes in vascular oxygenation, and continues beyond the time when the vascular oxygenation has reached a plateau. Investigations with oxygen electrodes (26) or FOXY^{TM} fiber optic probes (12) in these breast tumors showed heterogeneity within the tumors with baseline pO_2 ranging from hypoxia to greater than 50 torr. These other techniques also indicated heterogeneity in response. Generally, those regions that had an initially low pO_2 showed minimal response to oxygenation, while those with higher pO_2 showed a rapid response. Thus, while we believe NIRS can provide important insight into the pharmacodynamics of interventions on tumors, it must be noted that responsive regions may mask the tumor heterogeneity, and in particular, fail to show those regions that do not respond (26). This emphasizes the need for NIR imaging, and indeed, we have obtained preliminary data in this tumor type using a single transmitter and three receivers placed at various regions across the tumor, indicating that while each region of the tumor responded to hyperoxic gas, the extent and rate were different, showing the heterogeneity of tumor vasculature (50).

In conclusion, we believe that NIRS presents a new opportunity to examine tumor vasculature rapidly, non-invasively, and cheaply. Ease of implementation will allow rapid application to accessible tumors in patients. The inherent compatibility of fiber optics technology and light with other modalities, such as electrodes (26) and MRI (28), will facilitate multiparametric multimodality investigations in the future.

ACKNOWLEDGEMENT

We are grateful to Jae G. Kim, Vincent Bourke, and Mengna Xia for assistance.

Figure Legends

Figure 1

a) Relative absorption characteristics for oxy and deoxy-hemoglobin (based on (51))

b) Schematic experimental setup for the NIR spectroscopy system. NIR light is delivered and detected using two 3 mm-diameter fiber bundles placed in transmittance geometry around the tumor. PMT represents a photomultiplier tube. I/Q is an in-phase and quadrature phase demodulator for retrieving amplitude and phase information.

Figure 2

a) Time course of tumor vascular $\Delta[HbO_2]$ and $\Delta[Hb]_{total}$ with respect to altering inhaled gas in the sequence carbogen-air-carbogen-air for a representative 13762NF breast tumor in Group 1. Bi-exponential curve fitting to the dynamic responses of $\Delta[HbO_2]$ gave time constants τ_1=0.854 ±0.008 min and τ_2=7.56 ±0.09 min for the first intervention, and τ_1 = 0.653 ±0.004 min and τ_2 = 6.01 ±0.08 min for the second intervention with R^2>0.94 and χ^2<1.2 in both cases.

b) Comparison of $\Delta[HbO_2]$ produced by carbogen breathing for each tumor in Group 1 in the two cycles (R^2>0.92).

c) Comparison of the ratios of the time constants, τ_1 and τ_2, for the two interventions. There was strong linear correlation (R^2>0.9).

Figure 3

a. Time course of tumor vascular $\Delta[HbO_2]$ for a representative 13762NF breast tumor in Group 2. Curve fitting required a bi-exponential application for the carbogen intervention, but mono exponential for oxygen. Two-exponential fitting for the carbogen intervention yielded: $0.318\{1-\exp[-(t-19.656)/0.59]\}+0.394\{1-\exp[-(t-19.656)/21]\}$ with $R^2>0.96$, and mono exponential fitting for the oxygen intervention yielded: $0.484\{1-\exp[-(t-59.893)/0.397]\} +0.138$ with $R^2>0.8$. Variation in arterial oxygen saturation is also shown.

b. Comparison of maximal changes of $\Delta[HbO_2]$, caused by carbogen and oxygen interventions for tumors in Group 2. □ Comparison of the rising parts for each intervention; □ Comparison of the rising part for carbogen versus the falling part for oxygen. In both cases $R^2>0.8$.

c. Comparison of response times to each gas intervention. Here, the time to 80% maximum response to each intervention is compared for carbogen versus oxygen: Δ rising parts (onset of hyperoxia), □ falling parts (return to normoxic gas breathing). The line of unity shows that the time for carbogen was almost always longer than for oxygen, but the correlation between the times was very weak for either rising or falling components ($R^2<0.25$).

d. The average time for the 7 rats in Group 2 for signals to increase or decrease to 80% of the maximal $\Delta[HbO_2]$ in the rising part or falling part for carbogen (open bars) and oxygen interventions (shaded bars), respectively.

Figure 4

a. Time course of tumor vascular $\Delta[HbO_2]$ and $\Delta[Hb]_{total}$ for a representative tumor in Group 3a.

b. Correlation between maximum $\Delta[HbO_2]$ achieved with carbogen inhalation versus that with oxygen (R^2 >0.94): carbogen prior to oxygen (Group 2), ▲ oxygen prior to carbogen (Group 3).

Figure 5

a Time course of tumor vascular $\Delta[HbO_2]$ and $\Delta[Hb]_{total}$ for a representative tumor in Group 4.

b Comparison of maximal changes of tumor vascular oxygen hemoglobin concentration, $\Delta[HbO_2]$, caused by hypercarbic gas. Open bars from air to air+CO_2, hatched bars from air+CO_2, to oxygen + CO_2 (carbogen).

References

1. Fyles AW, Milosevic M, Wong R, *et al.* Oxygenation predicts radiation response and survival in patients with cervix cancer. *Radiother. Oncol.* 1998;48:149-56.
2. Brizel DM, Sibly GS, Prosmitz LR, *et al.* Tumor hypoxia adversely affects the prognosis of carcinoma of the head and neck. *Int. J. Radiat. Oncol. Biol. Phys.* 1997;38:285-289.
3. Kaanders JAHM, Pop LAM, Marres HAM, et al. Experience in 215 patients with advanced head and neck cancer. *Int. J. Radiat. Oncol. Biol. Phys.* 2002;52:769-778.
4. Nordsmark M, Overgaard M, Overgaard J. Pretreatment oxygenation predicts radiation response in advanced squamous cell carcinoma of head and neck. *Radiother. Oncol.* 1996;41:31-39.
5. Hohenberger P, Felger C, Haensch W, *et al.* Tumor oxygenation correlates with molecular growth determinants in breast cancer. *Breast Cancer Res. Treatment* 1998;48:97-106.
6. Movsas B, Chapman JD, Horwitz EM, *et al.* Hypoxic regions exist in human prostate carcinoma. *Urology* 1999;53:11-18.
7. Overgaard J, Horsman MR. Modification of hypoxia-induced radioresistance in tumors by the use of oxygen and sensitizers. *Semin. Radiat. Oncol.* 1996;6:10-21.

8. Kaanders JHAM, Wijffels KIEM, Marres HAM, *et al.* Pimonidazole binding and tumor vascularity predict for treatment outcome in head and neck cancer. *Cancer Res* 2002;62:7066-7074.

9. Stone HB, Brown JM, Phillips T, *et al.* Oxygen in human tumors: correlations between methods of measurement and response to therapy. *Radiat. Res.* 1993;136:422-434.

10. Mason RP, Ran S, Thorpe PE. Quantitative assessment of tumor oxygen dynamics: Molecular Imaging for Prognostic Radiology. *J. Cell. Biochem.* 2002;87S:45-53.

11. Höckel M, Schlenger K, Knoop C, *et al.* Oxygenation of carcinomas of the uterine cervix: evaluation by computerized O_2 tension measurements. *Cancer Res.* 1991;51:6098-6102.

12. Gu Y, Bourke V, Kim JG, *et al.* Dynamic Response of Breast Tumor Oxygenation to Hyperoxic Respiratory Challenge Monitored with Three Oxygen-Sensitive Parameters. *Applied Optics* 2003;42:1-8.

13. Braun RD, Lanzen JL, Snyder SA, *et al.* Comparison of tumor and normal tissue oxygen tension measurements using OxyLite or microelectrodes in rodents. *AJP - Heart & Circulatory Physiology* 2001;280:H2533-44.

14. Wilson DF, Vinogradov SA, Dugan BW, *et al.* Measurement of tumor oxygenation using new frequency domain phosphorometers. *Comp. Biochem. Physiol. Part A, Molecul. Integrat. Physiol.* 2002;132:153-9.

15. O'Hara JA, Blumenthal RD, Grinberg OY, *et al.* Response to radioimmunotherapy correlates with tumor pO2 measured by EPR oximetry in human tumor xenografts. *Radiat. Res.* 2001;155:466-73.

16. Elas M, Williams BB, Parasca A, *et al.* Quantitative tumor oxymetric images from 4D electron paramagnetic resonance imaging (EPRI): Methodology and comparison with blood oxygen level-dependent (BOLD) MRI. *Magn. Reson. Med.* 2003;49:682-91.

17. Krishna MC, English S, Yamada K, *et al.* Overhauser enhanced magnetic resonance imaging for tumor oximetry: coregistration of tumor anatomy and tissue oxygen concentration. *PNAS (USA)* 2002;99:2216-21.

18. Zhao D, Constantinescu A, Jiang L, *et al.* Prognostic Radiology: quantitative assessment of tumor oxygen dynamics by MRI. *Am. J. Clin. Oncol* 2001;24:462-466.

19. Zhao D, Constantinescu A, Chang C-H, *et al.* Measurement of tumor oxygen dynamics predicts beneficial adjuvant intervention for radiotherapy in Dunning prostate R3327-HI tumors. *Radiat. Res.* 2003;159:621-631.

20. Fan X, River JN, Zamora M, *et al.* Effect of carbogen on tumor oxygenation: combined fluorine-19 and proton MRI measurements. *Int. J. Radiat. Oncol. Biol. Phys.* 2002;54:1202-9.

21. Wang Z, Su M-Y, Nalcioglu O. Applications of Dynamic Contrast Enhanced MRI in Oncology: Measurement of Tumor Oxygen Tension. *Technol. Cancer Res. Treat.* 2002;1:29-38.

22. Evans SM, Hahn S, Pook DR, *et al.* Detection of hypoxia in human squamous cell carcinoma by EF5 binding. *Cancer Res.* 2000;60:2018-2024.

23. Dehdashti F, Grigsby PW, Mintun MA, *et al.* Assessing tumor hypoxia in cervical cancer by positron emission tomography with 60Cu-ATSM: relationship to therapeutic response-a preliminary report. *Int. J. Radia. Oncol. Biol., Phys.* 2003;55:1233-8.

24. Hull EL, Conover DL, Foster TH. Carbogen-induced changes in rat mammary tumour oxygenation reported by near infrared spectroscopy. *Br. J. Cancer* 1999;79:1709-1716.

25. Liu H, Song Y, Worden KL, *et al.* Noninvasive Investigation of Blood Oxygenation Dynamics of Tumors by Near-Infrared Spectroscopy. *Appl. Optic* 2000;39:5231-43.

26. Kim JG, Zhao D, Constantinescu A, *et al.* Interplay of Tumor Vascular Oxygenation and Tumor pO_2 Observed Using NIRS, Oxygen Needle Electrode, and ^{19}F MR pO_2 Mapping. *J. Biomed. Optics* 2003;8:53-62.

27. Sostman HD, Rockwell S, Sylva AL, *et al.* Evaluation of BA 1112 rhabdomyosarcoma oxygenation with microelectrodes, optical spectrometry, radiosensitivity, and MRS. *Magn. Reson. Med* 1991;20:253-267.

28. Gulsen G, Yu H, Wang J, *et al.* Congruent MRI and near-infrared spectroscopy for functional and structural imaging of tumors. *Technol. Cancer Res. Treat.* 2002; 1:497-505.

29. Kragh M, Quistorff B, Kristjansen PE. Quantitative estimates of angiogenic and anti-angiogenic activity by laser Doppler flowmetry (LDF) and near infra-red spectroscopy (NIRS). *Eur. J. Cancer* 2001;37:924-9.

30. Steinberg F, Rohrborn HJ, Scheufler KM, *et al.* NIR reflection spectroscopy based oxygen measurements and therapy monitoring in brain tissue and intracranial neoplasms. Correlation to MRI and angiography. *Adv. Exp. Med. Biol.* 1997;428:553-60.

31. Heffer EL, Fantini S. Quantitative oximetry of breast tumors: a near-infrared method that identifies two optimal wavelengths for each tumor. *Applied Optics* 2002;41:3827-39.

32. McBride TO, Pogue BW, Poplack S, *et al.* Multispectral near-infrared tomography: a case study in compensating for water and lipid content in hemoglobin imaging of the breast. *J. Biomed. Optics* 2002;7:72-9.

33. van der Sanden BJP, Heerschap A, Hoofd L, *et al.* Effect of carbogen breathing on the physiological profile of human glioma xenografts. *Magn. Reson. Med.* 1999;*42*:490-9.

34. Steen RG, Kitagishi K, Morgan K. In vivo measurement of tumor blood oxygenation by near-infrared spectroscopy: immediate effects of pentobarbital overdose or carmustine treatment. *J. Neuro-Oncol.* 1994;22:209-20.

35. Bogden AE, Kelton DE, Cobb WR, *et al.* Effect of serial passage in nude athymic mice on the growth characteristics and chemotherapy responsiveness of 13762 and R3230AC mammary tumor xenografts. *Cancer Res.* 1978;38:59-63.

36. Hahn EW, Peschke P, Mason RP, *et al.* Isolated tumor growth in a surgically formed skin pedicle in the rat: A new tumor model for NMR studies. *Magn. Reson. Imaging* 1993;11:1007-1017.

37. Denekamp J, Fowler JF. ARCON-current status: summary of a workshop on preclinical and clinical studies. *Acta Oncol.* 1997;36:517-525.

38. Song Y, Constantinescu A, Mason RP. Dynamic Breast tumor oximetry: the development of Prognostic Radiology. *Technol. Cancer Res. Treat.* 2002;1:471-478.

39. Thews O, Kelleher DK, Vaupel P. Tumor oxygenation under normobaric and hyperbaric hyperoxia: impact of various inspiratory CO2 concentration. *Adv. Exp. Med. Biol.* 1997;428:79-87.

40. Kunugita N, Kohshi K, Kinoshita Y, *et al.* Radiotherapy after hyperbaric oxygenation improves radioresponse in experimental tumor models. *Cancer Letters* 2001;164:149-54.

41. Becker A, Kuhnt T, Liedtke H, *et al.* Oxygenation measurements in head and neck cancers during hyperbaric oxygenation. *Strahlenther. Onkol.* 2002;178:105-8.

42. Brown JM. Exploiting the hypoxic cancer cell: mechanisms and therapeutic strategies. *Molecular Medicine Today* 2000;6:157-162.

43. Fenton BM. Influence of hydralazine administration on oxygenation in spontaneous and transplanted tumor models. *Int. J. Radiat. Oncol. Biol. Phys.* 2001;49:799-808.

44. Horsman MR, Nordsmark M, Hoyer M, *et al.* Direct evidence that hydralazine can induce hypoxia in both transplanted and spontaneous murine tumours. *Br. J. Cancer* 1995;72:1474-8.

45. Wood PJ, Stratford IJ, Sansom JM, *et al.* The response of spontaneous and transplantable murine tumors to vasoactive agents measured by ^{31}P magnetic resonance spectroscopy. *Int J. Radiat. Oncol. Biol. Phys.* 1992;22:473-6.

46. Dunn TJ, Braun RD, Rhemus WE, *et al.* The effects of hyperoxic and hypercarbic gases on tumour blood flow. *Br. J. Cancer* 1999;80:117-26.

47. Robinson SP, Collingridge DR, Howe FA, *et al.* Tumor response to hypercapnia and hyperoxia monitored by FLOOD magnetic resonance imaging. *NMR Biomed* 1999;12:98-106.

48. Dupuis NP, Kusumoto T, Robinson MF, *et al.* Restoration of tumor oxygenation after cytotoxic therapy by a perflubron emulsion/carbogen breathing. *Art. Cells. Blood Subs. Immob. Biotech.* 1995;23:423-429.

49. Teicher BA, Ara G, Herbst R, *et al.* PEG-hemoglobin: effects on tumor oxygenation and response to chemotherapy. *In Vivo* 1997;11:301-11.

50. Kim JG, Gu Y, Constantinescu A, *et al.* Non-Uniform Tumor Vascular Oxygen Dynamics Monitored By Three-Channel Near-Infrared Spectroscopy. *Proc. SPIE-Int. Soc. Opt. Eng* 2003;4955:388-396.

51. http://omlc.ogi.edu/spectra/hemoglobin/index.html

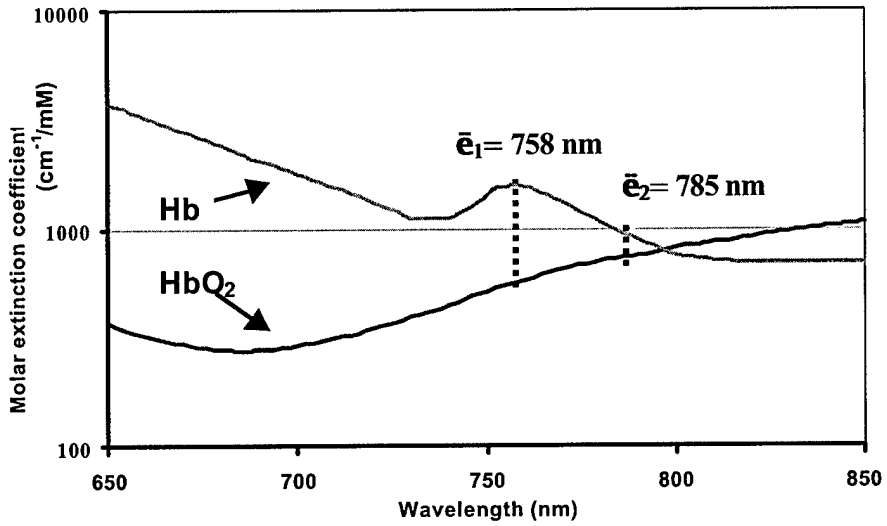

Figure 1a

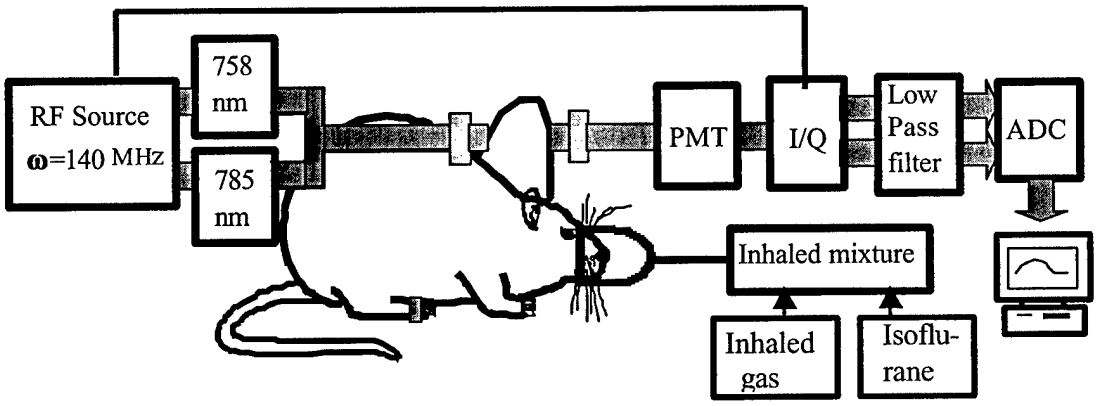

Figure 1b

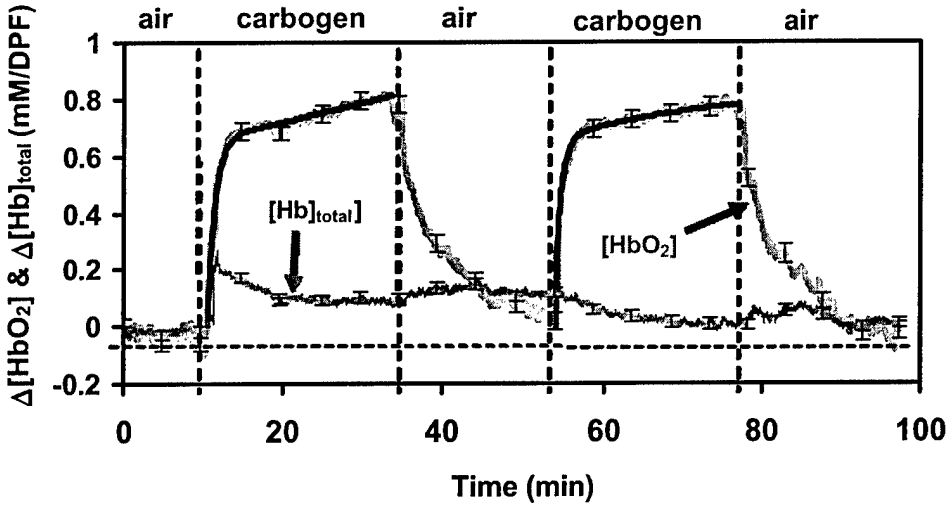

Figure 2a

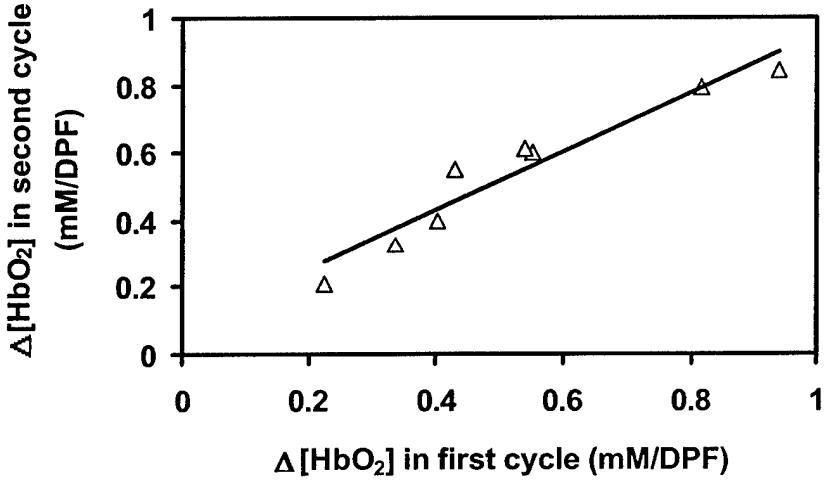

Figure 2b

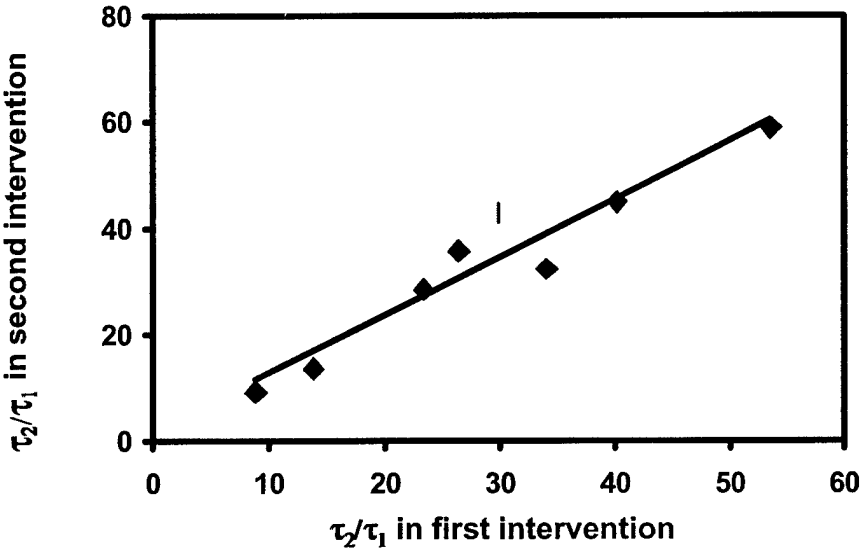
80
60
40
20
0
0
10
20
30
40
50
60
τ_2/τ_1 in second intervention
τ_2/τ_1 in first intervention

Figure 2c

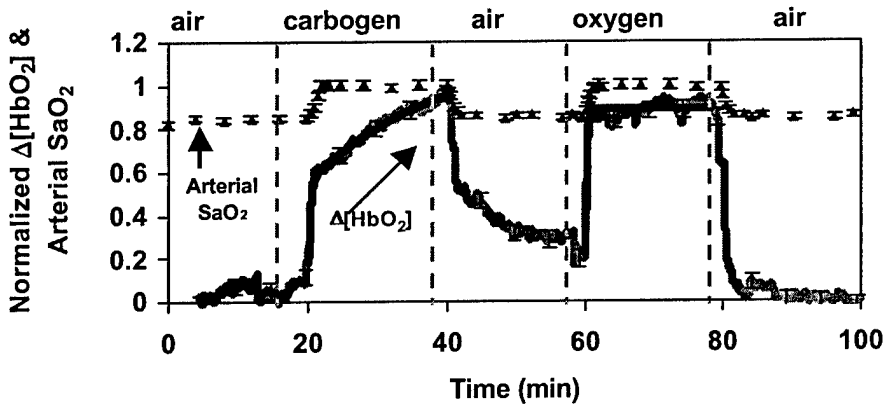

Figure 3a

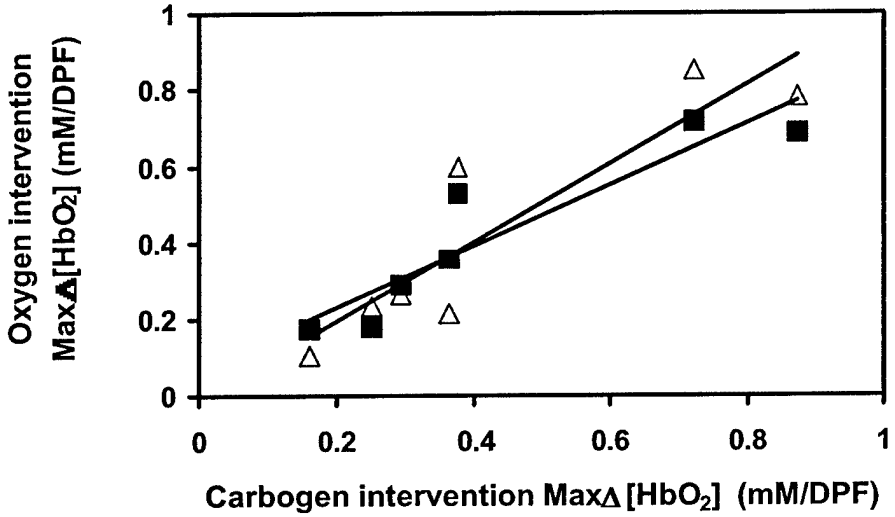

Figure 3b

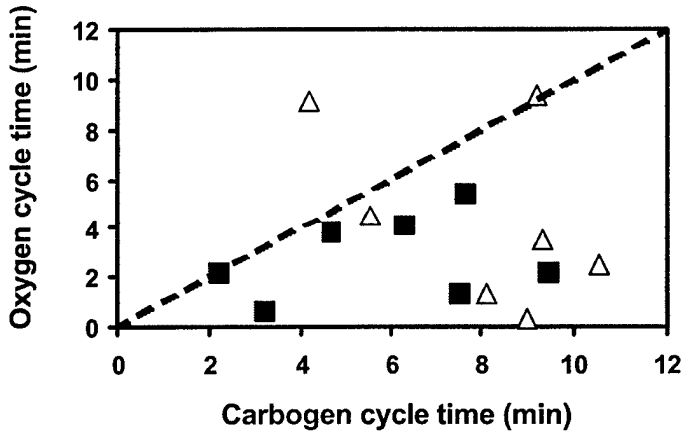

Figure 3c

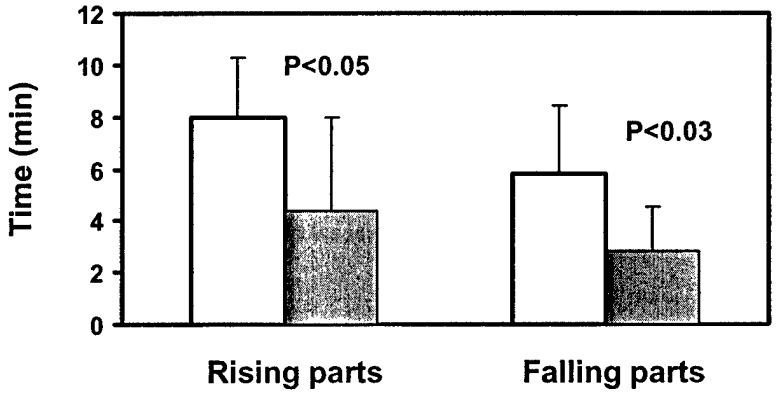

Figure 3d

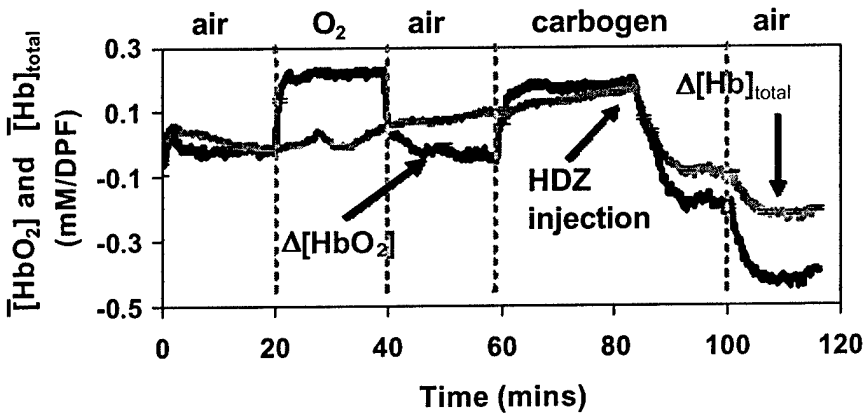

Figure 4a

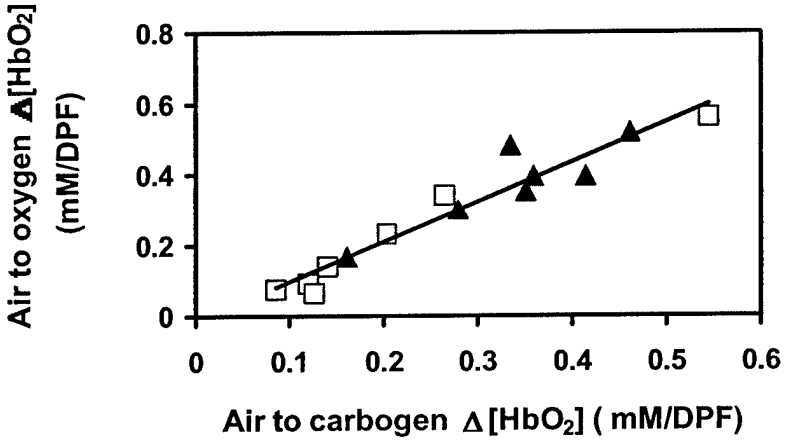

Figure 4b

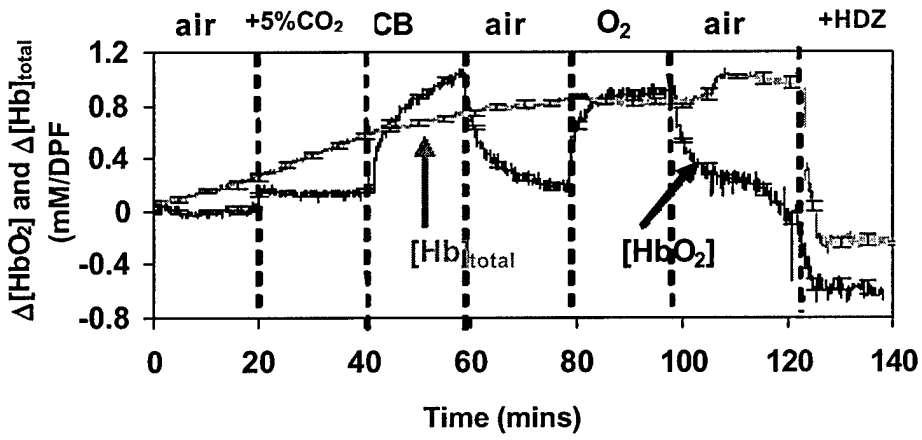

Figure 5a

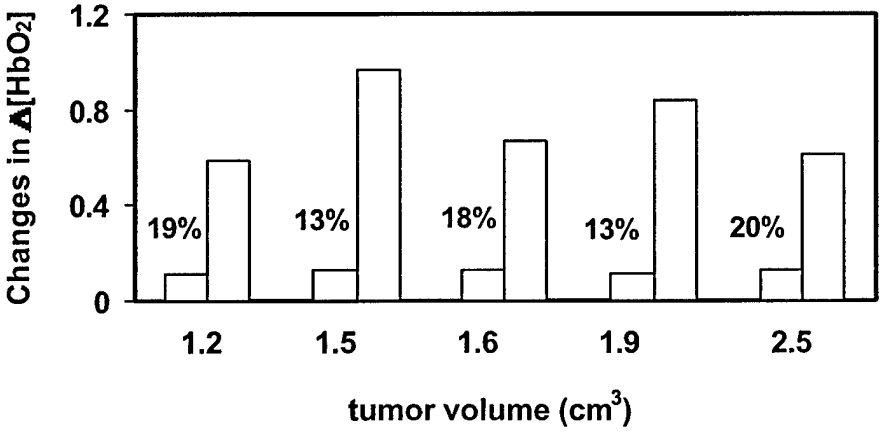

Figure 5b

Tumor Vascular Volume and Oxygenation in Response to Therapeutic Interventions Assessed by Near Infrared Spectroscopy and ^{19}F MRS of PFOB

Yueqing Gu, Hanli Liu

Joint Program in Biomedical Engineering, University of Texas at Arlington, Arlington, TX 76019

Yulin Song, Weina Cui, Anca Constantinescu, Ralph P. Mason

Department of Radiology, University of Texas Southwestern Medical Center at Dallas, TX 75390

ABSTRACT

The changes of total hemoglobin concentration, $\Delta[Hb]_{total}$, and blood volume, $\Delta V_{T\text{-}blood}$ in solid mammary tumors and prostate tumors were monitored during hyperoxic gas intervention by using near-infrared spectroscopy (NIRS) and ^{19}F MRS of PFOB, respectively. The linear correlation between $\Delta[Hb]_{total}$ and $\Delta V_{T\text{-}blood}$ demonstrated the ability of NIRS as an accurate, non-invasive, real time, monitoring tool for tumor hemoglobin concentration measurement. Furthermore, the changes of tumor oxygenated hemoglobin concentration, $\Delta[HbO_2]$, and $\Delta[Hb]_{total}$ were monitored by NIRS during different interventions in both 39 breast tumors and 21 prostate tumors. Results showed that hyperoxic gases, i.e., carbogen (5% CO_2 and 95% O_2) and oxygen, can significantly elevate $\Delta[HbO_2]$ in all of the 39 breast tumors and only in 10 of the 21 prostate tumors. With the same interventions, 15 of the 39 breast tumors have good responses in $\Delta[Hb]_{total.}$, and so does only 1 of the 21 prostate tumors. In contrast, hydralazine, a vasoactive agent, has the ability to significantly reduce $\Delta[HbO_2]$ and $\Delta[Hb]_{total}$ in both the breast tumors and prostate tumors. These results demonstrate that the NIRS may become a potential monitoring tool to for tumor treatment prognosis and optimization in cancer therapy.

Key words: hemoglobin concentration, blood volume, breast tumor, prostate tumor, hyperoxic gas, hydralazine

1. Introduction

Hemodynamic parameters, such as blood volume, blood oxygenation and total hemoglobin concentration ($[Hb]_{total}$), etc, possess essential information for the management of the critical illness. Effective monitoring of these parameters permit analysis of key circulatory functions and the anticipation of deterioration so that pro-active treatments can be initiated[1,2,3]. In particular, tumor vascular hemodynamic parameters affect not only tumor growth and survival, but also efficacy of cancer treatments[4]. It has been widely realized that tumor hypoxica may limit the efficacy of non-surgical treatments[5,6,7,8]. Tumor vascular hemoglobin concentration has also been shown to have strong correlation with tumor local control probability[9,10,11]; a 2~4 fold contrast of total hemoglobin between normal and tumor tissue was also reported[12]. Moreover, the dynamic response of tumor hemodynamic parameters, such as tumor Hb concentration, with respect to external interventions may correlate with the type and extent of vascular diseases[13]. Accordingly, accurate assessment of tumor vascular oxygenation and Hb concentration at various stages of tumor growth and in response to interventions may provide a better understanding of tumor development and may serve as a prognostic indicator for treatment outcome, potentially allowing therapy to be tailored to individual characteristics[14,15,16].

Given the importance of tumor oxygenation and hemoglobin concentration, many techniques have been developed, such as electrodes,[17,18] EPR,[19,20] and MRI[21,22,23], for quantitative measurement of tumor oxygen tension (pO_2)[24,25] and blood volume[26,27]. Other techniques for tumor pO_2 and blood volume measurements are involved using radioactively labeled tracers and often require the excision of the tumor[28,29,30,31]. These instrumental modalities are invasive or high cost. Thus, a non-invasive, cost-effective, and easy-to-operate system is highly desirable in both research settings and clinical practice.

Near infrared spectroscopy (NIRS), with good temporal resolution and lower cost, provides such a noninvasive, non-ionizing, real time means to monitor the total hemoglobin concentration and oxygen saturation of tissue vasculature[32,33]. Previously, we have demonstrated the practicability and accuracy of NIRS for the measurement of tumor vascular oxygenation changes (HbO_2), under various therapeutic interventions, by comparative measurements with a pulse oximeter[34], needle electrode, MRI[35] and multi-channel FOXY™ oxygen sensor[36]. However, unlike the often observed, highly repeatable, tumor HbO_2 changes caused by hyperoxic gas inhalations, the previous results of tumor vascular hemoglobin concentrations, $[Hb]_{total}$, measured by NIRS were often largely variable from tumor to tumor, without consistent patterns[37]. Because of the inconclusive observations in $\Delta[Hb]_{total}$, we have wondered whether the methodology of NIRS is reliable for quantification of tumor total hemoglobin concentration. Thus, we have conducted this study to validate the NIRS as an accurate means to be able to quantify changes in tumor vascular blood volume through another independent method.

Specifically, in this paper, we will firstly evaluate the accuracy of NIRS for the measurement of changes in vascular total hemoglobin concentration, $\Delta[Hb]_{total}$, in breast and prostate tumors by using ^{19}F MRS of Perfluorooctylbromide (PFOB). The latter method has been shown to have the ability in assessing tumor blood volume[38](*** can you use some original references?) and will be used to correlate with tumor $\Delta[Hb]_{total}$. After obtaining the complementary results between the two methodologies, we will further utilize NIRS to investigate the dynamic changes in $[Hb]_{total}$ and $[HbO_2]$ with larger groups of breast and prostate tumors, under such interventions as hyperoxic gas (carbogen or oxygen) inhalation or vascoactive agent administration (hydralazine). In this way, tumor vascular volume, $[Hb]_{total}$, and oxygenation, $[HbO_2]$ in response to different interventions from both breast and prostate tumors

will be qualitatively investigated, demonstrating that NIRS can be a valuable tool for tumor hymodynamic measurement.

2. Materials and Methods

2.1 Near Infrared Spectroscopy for the Measurement of $\Delta[Hb]_{total}$ and $\Delta[HbO_2]$

A homodyne, frequency-domain, NIRS system (NIM, Philadelphia, PA) used in this study has been described in detail previously[34,35,36]. Briefly, the amplitude-modulated light at 140 MHz from two NIR laser diodes at 758 nm and 785 nm was projected on one side of the tumor through a delivery fiber bundle. The diffused light through tumor tissue was collected and propagated to a photomultiplier tube (PMT) by a second fiber bundle. The signal from the PMT was demodulated through an In-phase and Quadrature-phase circuit, and the amplitude and phase were recorded. Based on modified Beer-Lambert's law[34, 39], the changes in oxygenated, deoxygenated, and total hemoglobin concentrations, i.e., $\Delta[HbO_2]$, $\Delta[Hb]$ and $\Delta[Hb]_{total}$, respectively, due to respiratory intervention are calculated using the following equations, which have been derived previously[35]:

$$\Delta[HbO_2] = \frac{-10.63 \cdot \log(\frac{A_B}{A_T})^{758} + 14.97 \cdot \log(\frac{A_B}{A_T})^{785}}{d}, \quad (1)$$

$$\Delta[Hb] = \frac{8.95 \cdot \log(\frac{A_B}{A_T})^{758} - 6.73 \cdot \log(\frac{A_B}{A_T})^{785}}{d}, \quad (2)$$

$$\Delta[Hb]_{total} = \Delta[HbO_2] + \Delta[Hb]. \quad (3)$$

where A_B and A_T are the baseline and transient amplitudes measured from the NIRS system, respectively, "d" is the source-detector separation, and the unit for all $\Delta[HbO_2]$, $\Delta[Hb]$ and $\Delta[Hb]_{total}$ is mM/DPF, where DPF is the differential path-length factor for tumor tissues.

2.2 ^{19}F MRS of PFOB for the Measurement of Tumor Blood Volume

An Omega CSI 4.7-Telsa, superconducting magnet system (Acustar^{TM}, Bruker Instrument, Inc., Fremont, CA) was used for the measurement of tumor blood volume. The artificial blood substitutes[40], Perfluorooctylbromide (PFOB) ($C_8F_{17}Br$) emulsions (Alliance pharmaceutical Corp., San Diego,CA) with inert characteristic in chemical and biochemical reactions (***), was intravenously infused into the rat blood stream as a blood volume indicator for ^{19}F magnetic resonance spectroscopy (MRS) measurements. Either breast or prostate tumors were placed within a frequency-tunable ($^{1}H/^{19}F$), single-turn, solenoid coil, accompanying with a sealed capillary containing sodium trifluoroacetate (TFA) used as an external standard for quantifying tumor blood volume. The rats were positioned in the magnet with the tumors at the isocenter of the magnet. The 90^0 pulse width (pw) was determined from a 180^0 null of the whole tumor. Shimming was performed on the tumor tissue water proton FID (200.1 MHz at 4.7 ***) to a typical line width of 60 Hz. The rats were exposed to hyperoxic respiratory, and spectra were acquired with a long repetition time (TR = 30 s) to ensure that changes in T1 due to variable oxygenation would not interfere with volume measurements[41]. Figures 1(a) and 1(b) show the molecular structure and a typical ^{19}F NMR (Nuclear*** Magnetic Resonance) spectrum of PFOB emulsion.

Given a set of NMR spectra acquired with chosen system parameters, it has been shown (***? Or it is expected) that the integration of ^{19}F signal from a tumor was linearly proportional to the total number of ^{19}F nuclear spins of PFOB in the tumor, which, in turn, was linearly proportional to the total blood volume in the tumor, assuming that the PFOB emulsion had

reached an equilibrium state with the blood throughout the tumor. Thus, the areas under spectral peaks of PFOB were integrated in the data post-processing.

After the tumor measurement, rats were removed from the RF coil, with the reference TFA capillary still left in the original position. Amount of 0.5 ml blood sample was then drawn by tail vein from the rats and was placed into the RF coil without disturbing the reference TFA capillary. While keeping the same system acquisition parameters, another set of ^{19}F spectrum from the rat blood sample was acquired, and the corresponding integration of ^{19}F signals were calculated. It follows that the blood volume in tumor vasculature can be calculated based on the following equation:

$$V_{T\_blood} = V_{S\_blood} \cdot \left(\frac{I_{T\_blood}}{I_{S\_blood}}\right) \cdot \left(\frac{I_{S\_TFA}}{I_{T\_TFA}}\right), \qquad (4)$$

where V_{T_blood} and V_{S_blood} were the tumor vascular blood volume and blood sample volume (ml), respectively, and I_{T_blood} and I_{S_blood} were the integrated NMR signals from the ^{19}F peaks of PFOB in the rat tumor and in the blood sample, respectively. I_{blood_TFA} and I_{Tumor_TFA} were the respective integrations of ^{19}F NMR signals from the TFA capillary, which was used as a calibration standard to accompany with the blood sample and the tumor measurement.

2.3 Protocol in phantom experiments

Phantom studies were conducted in both NIRS and ^{19}F MRS of PFOB to evaluate the accuracy of measurement in $\Delta[HbO_2]$, $\Delta[Hb]_{total}$ and blood volume. For the evaluation of NIRS, 100 ml of 20% intralipid (Fresenius Kabi Clayton, L.P., NC) was mixed in 1900 ml saline to get 2 L of 1% intralipid solution with a reduced optical scattering coefficient (μ_s') of ~10 cm^{-1}. 2 packets of phosphate buffered saline powder (Sigma, St. Louis, MO) were added in the solution to obtain a pH value of 7.4. Amount of 14 g of yeast powder was dissolved in the phantom solution to consume oxygen. The source and detector of the NIRS, with a separation of 4 cm,

were placed on the surface of a glass container filled with the phantom liquid for the measurement. After the baseline recorded, 6 ml of rat blood was added into the solution twice to cause the change in $[Hb]_{total.}$ Oxygen gas was then bubbled into the phantom solution to oxygenate the hemoglobin in solution and result in change in $[HbO_2]$.

For assessing the measurement of blood volume by ^{19}F MRS, 2 ml PFOB emulsion, 3 ml 1% intralipid and 10 ml rat blood were mixed together to obtain a 15-ml original phantom solution stored in a container. Then 3 ml of the solution was taken out for ^{19}F MRS measurement, and another 3 ml of 1% intralipid was added to the container for dilution of PFOB and blood. Following this procedure, the solution was diluted multiple times at different concentrations. Meanwhile, 30 mg of TFA were diluted in 2-ml sterile water and kept inside the RF coil as an external calibration label for each measurement.

2.4 Animal model and protocols

Mammary adenocarcinomas 13762NF and Dunning prostate asenocarcinomas R3327-AT1 were implanted in skin pedicles on the forebacks of female Fisher 344 rats (~150g) and adult male Copenhagen rats (~250g), respectively. Once the tumors reached 1~2 cm diameter, rats were anesthetized with ketamine hydrochloride (100 mg/ml,i.p.) and maintained under general gaseous anesthesia with 1.3% isoflurane in air(1 dm^3/min). Tumors were shaved to improve optical contact for NIR light transmission. And tumor physical volume was estimated using an ellipsoid approximation ($V=(\pi/6).a.b.c$) from the three orthogonal diameters (a,b,c).

In this study, 39 breast tumor bearing Fisher rats and 21 prostate tumor bearing Copenhagen rats experienced alternative carbogen (5% CO_2 and 95% O_2) and oxygen interventions, i.e., air-carbogen–air, air-oxygen-air-carbogen-air, or the reversed gas breathing sequence. Changes in $[HbO_2]$ and $[Hb]_{total}$ with respect to hyperoxic gas interventions were monitored by NIRS. If the

hyperoxic gases regulated $\Delta[Hb]_{total}$ significantly, the same rat was re-anesthetized in the next day and i.v. infused with 2 ml of PFOB emulsion. The ^{19}F MRS measurement for tumor blood volume was performed 30 min later to give sufficient time for the PFOB emulsion to reach an equilibrium state within the blood stream. The protocol of the inhaled gas was the same as that used in the NIRS measurements. Also, Hydralazine (HDZ; 5 mg/kg in 0.5 ml saline, Sigma) was infused i.v. into 19 of the 39 Fisher rats and 6 of the 21 Copenhagen rats after carbogen intervention to examine the changes of tumor hemodynamic behaviors.

3. Results

3.1 Phantom experiments

Figure 2 (a) shows temporal profiles of $\Delta[HbO_2]$, $\Delta[Hb]$ and $\Delta[Hb]_{total}$ during a complete phantom experiment. After the baseline reading, 3 ml of rat blood was added to the phantom solution (pH=7.4, μ_s'=10 cm^{-1}), producing a rapid and significant increase in both $\Delta[HbO_2]$ ($p<0.0001$) and $\Delta[Hb]_{total}$ ($p<0.0001$). The yeast in the solution consumed oxygen quickly, leading to unload of oxygen from HbO_2, and thus, resulting in a decrease in $[HbO_2]$ down to the baseline and $\Delta[Hb]$ up to 0.21±0.01 mM/DPF. When O_2 was bubbled into the solution, $\Delta[HbO_2]$ increased and reached a plateau at the maximum, while $\Delta[Hb]$ decreased down to the baseline. After the hemoglobin in the solution was completely oxygenated, the O_2 bubbling was stopped, and another deoxygenation process started again due to the O_2 consumption of yeast. As expected, this process resulted in an elevation of [Hb] and a decrease in $[HbO_2]$. Furthermore, it is clearly shown that $\Delta[Hb]_{total}$ kept constant during the entire period of oxygenation-deoxygenation cycle. Similar results are observed in the second cycle of the experiment where

another 3 ml of rat blood was added into the solution. This phantom experiment demonstrates the accuracy and reliability of the NIRS measurement on changes in both $[Hb]_{total}$ and $[HbO_2]$..

Figure 2 (b) plots *** (intensity or integrated signal?). This figure reveals a strong linear correlation (R^2=0.97) between the blood volume and the intensity of PFOB measured by ^{19}F MRS in the phantom sample, demonstrating the principle and correctness of MRS measurement.

3.2 Consistency of $\Delta[Hb]_{total}$ obtained by NIRS and tumor blood volume by ^{19}F NMR of PFOB

3.2.1 Breast tumor measurements

Fig. 3(a) shows the time course profiles of $\Delta[Hb]_{total}$ and $\Delta[HbO_2]$ monitored by NIRS in response to hyperoxic gas interventions, i.e., air-carbogen-air-oxygen-air, for a representative breast tumor (2.6 cm^3). When the inhaled gas was switched from air to carbogen, $\Delta[Hb]_{total}$ increased significantly ($p < 0.0001$) from baseline 0.002±0.006 to the maximum of 0.079± 0.004 (mM/DPF) over the period of carbogen intervention. After the gas was switched back to air, a significant drop ($p < 0.0001$) of $\Delta[Hb]_{total}$ occurred, and followed by a plateau at 0.036± 0.004 (mM/DPF). A similar temporal response pattern was repeated in the oxygen intervention cycle. The maximal magnitude change in $[Hb]_{total}$ due to oxygen intervention is about 0.077± 0.004 mM/DPF. Compared to $\Delta[Hb]_{total}$, $\Delta[HbO_2]$ had a similar temporal profile with larger magnitude increases, which has been reported extensively in our previous publications[34,35,36,42].

For comparison, the same rat was experienced the same gas intervention sequence, i.e., air-carbogen-air-oxygen-air, during the ^{19}F MRS measurement in the next day. Figure 3(b) shows the tumor blood volume, $V_{T\text{-}blood}$, with respect to the gas interventions measured by ^{19}F MRS of PFOB for the same breast tumor (2.6 cm^3). This figure shows that $V_{T\text{-}blood}$ increased significantly ($p<0.0001$) from baseline 0.808± 0.009 cm^3 to the maximum of about 0.896± 0.009

cm^3 during carbogen intervention, followed by a quick return as air breathing was switched on. A similar profile was continued in the oxygen intervention cycle. Further comparison between Figures 3(a) and 3(b) exhibits the overall consistent trend between $V_{T\text{-}blood}$ and $\Delta[Hb]_{total}$. .

To further investigate the relationship between $V_{T\text{-}blood}$ and $\Delta[Hb]_{total}$, several experiments were repeated from this tumor using the same protocols. (*** How did you get four points in Fig. 3c? You need to mention it.) Figure 3(c) reveals a strong linear relationship (R^2 =0.95) between maximal changes in $[Hb]_{total}$ and $V_{T\text{-}blood}$ for each gas inhalation from this breast tumor (2.6 cm^3). Then, 9 out of the 39 Fisher rats, with good response of $\Delta[Hb]_{total}$ to gas interventions (either carbogen or oxygen),, were performed with the MRS measurement next day after the NIRS monitoring. Figure 4(a) illustrates the results, demonstrating a linear correlation (R^2 =0.66) between tumor vascular $\Delta[Hb]_{total}$ obtained from NIRS and $\Delta V_{T\text{-}blood}$ from MRS. Moreover, since the ^{19}F MRS of PFOB permits quantification of the baseline tumor blood volumes, $V_{T\text{-}blood}$, we have also obtained a linear correlation (R^2 =0.75) between the $V_{T\text{-}blood}$ and physical tumor volumes , as shown in Fig.4(b), for the 9 respective breast tumors.

3.2.2 Prostate tumor measurements

The results obtained from prostate tumors were often different from those taken from the breast tumors. Figure 5(a) displays the time course profiles of $\Delta[Hb]_{total}$ and $\Delta[HbO_2]$ with respect to the repeated carbogen intervention (air-carbogen-air-carbogen-air) for a representative prostate tumor (8.9 cm^3). Carbogen interventions in both of the cycles didn't produce significant changes in $\Delta[Hb]_{total}$, but $\Delta[HbO_2]$ showed good response in the second carbogen intervention. To verify $\Delta[Hb]_{total}$ obtained from NIRS, the same rat was performed with the MRS experiment for blood volume measurement in the following day. Figure 5(b) shows the tumor blood volume measured by ^{19}F MRS of PFOB with respect to different gas inhalations for the same prostate

tumor (8.9 cm^3). It illustrates that little change in tumor blood volume was observed during the carbogen interventions,being consistent with the result taken from NIRS for $\Delta[Hb]_{total}$.Three more (or two more***?) prostate tumor bearing Copenhagen rats were studied using both NIRS and ^{19}F MRS, where no changes have been observed in either $\Delta[Hb]_{total}$ or $V_{T\text{-}blood}$ during the hyperoxic gas interventions. In addition, all 21 Copenhagen rats were measured for both $\Delta[Hb]_{total}$ and $\Delta[HbO_2]$ in response to the respiratory interventions with the NIRS. Almost all did not show any changes in $\Delta[Hb]_{total}$, while nearly 50% of the rats exhibited tumor oxygenation increases in $\Delta[HbO_2]$, as listed in Table 1.

3.3 Effects of hydralazine on $\Delta[Hb]_{total}$ and $\Delta[HbO_2]$ for both breast tumor and prostate tumor

Besides hyperoxic gas interventions, a vasoactive agent, hydralazine (HDZ), was used to examine the changes in tumor vascular volume and oxygenation. Figure 6(a) is the time profile of $\Delta[Hb]_{total}$ and $\Delta[HbO_2]$ in response to different interventions, i.e., air-oxygen-air-carbogen-carbogen+HDZ-air, for a representative breast tumor (5.1 cm^3). In common with our earlier observations for breast tumors, both oxygen and carbogen breathing produced significant ($p<0.0001$) elevations in $\Delta[HbO_2]$, but no significant rapid change in $\Delta[Hb]_{total}$ was displayed due to the gas interventions. It is clear that administration of hydralazine into the rat blood stream after hyperoxic gas interventions caused a significant decrease in both $\Delta[Hb]_{Total}$ and $\Delta[HbO_2]$ ($p<0.0001$). A similar example is shown in Figure 6(b) for a prostate tumor: the administration of hydralazine resulted in a significant decrease in both $\Delta[Hb]_{total}$ and $\Delta[HbO_2]$ ($p<0.0001$), although neither oxygen nor carbogen inhalation gave rise to any significant change in either $\Delta[Hb]_{total}$ or $\Delta[HbO_2]$ in this representative prostate tumor.

3.4 Statistic results among breast and prostate tumors.

As described in section 2.4, 39 breast tumor bearing Fisher rats and 21 prostate tumor bearing Copenhagen rats experienced different hyperoxic gas interventions, where both $\Delta[Hb]_{total}$ and $\Delta[HbO_2]$ were monitored by NIRS. As listed in Table 1, the results show that all of the 39 Fisher rat breast tumors have significant increases in $\Delta[HbO_2]$ in response to hyperoxic gas interventions , but only 10 out of the 21 Copenhagen rat prostate tumors have good responses in $\Delta[HbO_2]$. Furthermore, , 15 out of the 39 breast tumors have large changes in $\Delta[Hb]_{total}$, but only 1 of 21 prostate tumors has responsible changes in $\Delta[Hb]_{total}$. Among the 15 breast tumors which showed good responses in $\Delta[Hb]_{total,}$ 9 of them were performed with the ^{19}F MRS measurements in the next day after the NIR readings. The data obtained from NIRS and from MRS agree well with one another (Figure 4(a)). In addition, hydralazine was i.v. administrated into 19 breast tumors and 6 prostate tumors after hyperoxic gas interventions. Both $\Delta[HbO_2]$ and tumor physical volume displayed significant decreases in both breast tumors and prostate tumors, as summarized in Table I.

To investigate the possible relationship between the tumor physical volume and tumor responses to hyperoxic gas interventions, we utilize a semi-quantitative or digitized analysis method. Basically, we assign value "1" to represent a significant response, "0" to no response at all, and "0.5" to a somewhat response without significant changes, during the entire hyperoxic interventions. In this way, we can obtain semi-quantitative dependence of tumor response to the gas interventions on tumor physical volume. Figures 7(a) and 7(b) illustrate such digitized plots for $\Delta[Hb]_{total}$ response from the 39 breast tumors and for $\Delta[HbO_2]$ response from the 19 (***why not 21) prostate tumors, respectively. These two figures clearly suggest that smaller tumors have better responses to hyperoxic gas interventions.

4. Discussion

In this study, the feasibility and accuracy of NIRS for the measurements $\Delta[Hb]_{Total}$ were rigorously evaluated by comparing with the blood volume measurement using ^{19}F MRS, as shown in Figures 3(c) and 4(a). These experimental results demonstrate that tumor vascular $\Delta[Hb]_{total}$ determined by NIRS and tumor blood volume $V_{T\text{-}blood}$ obtained from ^{19}F MRS are linearly correlated with one another under hyperoxic gas interventions. . Since ^{19}F MRS of PFOB is considered as a well-established method for blood volume measurement'[38] (some original papers?), the comparative study between the NIRS and ^{19}F MRS presented in this paper validates the correctness and reliability of NIRS for determination of tumor vascular total hemoglobin concentration. Furthermore, while ^{19}F MRS of PFOB can be applied to deep tumors with special pulse sequences, NIRS can be used to monitor the acute response of tumors to different therapeutic interventions. The longitudinal (***?) measurements of tumor blood volume by MRS and hemoglobin concentration by NIRS could reveal insight into tumor development and perhaps provide a prognostic indicator for tumor therapy (*** Is it necessary for the last sentence?).

After having validated the NIRS for correct measurement of $\Delta[Hb]_{total}$, we investigated the changes in tumor vascular oxygenation and total hemoglobin concentration, i.e., $\Delta[HbO_2]$, $\Delta[Hb]_{total}$, on 39 breast tumors and 21 prostate tumors with different interventions. Statistical data in Table I show that 100% (39/39) of the breast tumors and only 48% (10/21) of the prostate tumors have significant elevations in $\Delta[HbO_2]$ with respect to hyperoxic gas intervention. For $\Delta[Hb]_{total}$, 38% (15/39) of the breast tumors and only 4.7 % (1/21) of the prostate tumors have good responses to hyperoxic gas breathing. The statistic results demonstrate that breast tumors

have better responses to hyperoxic gas intervention than prostate tumors, and tumor $\Delta[HbO_2]$ is more sensitive to hyperoxic gas interventions than tumor $\Delta[Hb]_{total}$. The different response behaviors observed here could be used to assist or guide the options/selections of non-surgical treatments when dealing with different tumor lines.

Although the improvement of tumor oxygenation has been a primary goal of much research and many clinical trials, induction of tumor hypoxia to enhance the efficacy of hypoxia selective cytotoxins, e.g., tirapazamine, provides an alternative way for cancer treatment. When hydralazine, a vasoactive agent, was administrated into rat blood stream, both $\Delta[HbO_2]$ and $\Delta[Hb]_{Total}$ showed significant decline nearly in all breast and prostate tumors, as expected. Hydralazine administration, in principle, causes arterial dilation in normal tissue but increases the flow resistance in the tumor due to the decrease in arterial feeding pressure and an accompanying collapse of tumor vessels[43,44,45], leading to reduction of tumor blood flow, tumor blood volume, and further tumor oxygenation. Based on the response behaviors observed in this study, we can speculate that the efficacy of breast tumor treatments can be improved in most of the tumor oxygenation dependent modalities, such as radiotherapy, photodynamic therapy and chemotherapy, while the improvement of prostate tumor treatment can be achieved by only some bio-reductive drugs which will kill the tumor cells more effectively under high hypoxic conditions[Error! Bookmark not defined.46,Error! Bookmark not defined.47,Error! Bookmark not defined.48, 46,47]

The response characteristics also depend on the tumor physical size (Figs. 7(a) and 7(b)). Small tumors have better responses than the big ones, suggesting that possible necrosis have taken place within the volume of big tumors. However, for all the 9 breast tumors whoser blood volume were measured by ^{19}F MRS of PFOB, the baseline tumor blood volumes have linear relationship with tumor physical volumes, as shown in Figure 4(b). A further plot of the tumor

percentage blood volume (tumor blood volume divided by tumor physical volume) versus tumor physical volume did not show any correlation between them (*** you need to show such a figure), suggesting that no obvious necrosis has formed in those breast tumors.

In conclusion, we have firstly performed phantom experiments to validate the feasibility and accuracy of NIRS for tumor $\Delta[Hb]_{total}$ quantification by comparing with ^{19}F MRS of PFOB for the measurement of tumor blood volume. The linear correlation between tumor $\Delta[Hb]_{total}$ obtained from NIRS and tumor blood volume from MRS demonstrates the practicability and reliability of NIRS as an *in vivo*, non-invasive, real time monitoring tool for tumor vascular total hemoglobin concentration. With the reliable NIRS, we have further monitored $\Delta[HbO_2]$ and $\Delta[Hb]_{total}$ of 39 breast tumors and 21 prostate tumors with respect to different interventions. The results have shown that hyperoxic gas breathings can effectively elevate tumor vascular oxygen status in all of the breast tumors, but only in ~50% of the prostate tumors, while such respiratory interventions lead to increases in total vascular volume for some of the breast tumors (~40%) but little changes for the prostate tumors. Finally, the dynamic NIRS readings illustrate that hydralazine administration is an effective means to increase tumor vascular hyproxia in both breast tumors and prostate tumors.

Acknowledgements

This work was supported in part by the Department of Defense Breast Cancer Research grants BC000833 (YG) and BC990287 (HL), and NIH RO1 CA79515 (NCI)/ EB002762 (NIBIB) (RPM). Tumor cells were provided by the Division of Cancer Therapeutics, NIH.

Legend for the illustrations:

Figure 1 (a) Molecular structure of perfluorooctylbromide (PFOB). (b) ^{19}F NMR spectrum of PFOB emulsion in 2.5-ml Fisher rat blood, with TFA as an external label.

Figure 2 (a) A linear correlation (R=?***) between NMR spectral intensity of PFOB and the blood volume measured in the phantom study. (b) The time profiles of $[HbO_2]$ and $[Hb]_{total}$ with respect to oxygen regulation in the phantom solution. Pure O_2 gas and yeast were used to oxygenate and deoxygenate hemoglobin, respectively. Amount of 6 ml rat blood was added in the solution two times in the two cycles of oxygen regulation.

Figure 3 (a) Time course profiles of tumor vascular $\Delta[Hb]_{total}$ and $\Delta[HbO_2]$ monitored by NIRS for a representative breast tumor (2.6 cm^3), with an inhaled gas sequence of air-carbogen-air-oxygen-air. (b) Time course of tumor blood volume, $V_{T\text{-}blood}$, measured by ^{19}F MRS of PFOB for the same breast tumor (2.6 cm^3), with the gas breathing sequence same as that used in (a). (c) A linear correlation (R=***?) between the changes (with respect to the baseline signal) in $\Delta[Hb]_{total}$ and $V_{T\text{-}blood}$ at the end of each gas inhalation stage from the same breast tumor.

Figure 4 (a) A linear correlation (***R=?) between the maximal changes in $\Delta[Hb]_{total}$ and $V_{T\text{-}blood}$ for hyperoxic gas inhalations in the 9 breast tumors with (*** the equation). Triangle: carbogen intervention; Square: oxygen intervention. (b) The relationship between the baseline tumor blood volume versus tumor physical volume from 9 of the breast rat tumors.

Figure 5 (a) Time course profiles of tumor vascular $\Delta[Hb]_{total}$ and $\Delta[HbO_2]$ monitored by NIRS for a representative prostate tumor (8.9 cm^3), with respect to repeated carbogen intervention as

air-carbogen-air-carbogen-air. (b). Time course of tumor blood volume, $V_{T\text{-}blood}$, measured by ^{19}F MRS of PFOB for the same prostate tumor, with the same gas breathing sequence as air-carbogen-air-carbogen-air.

Figure 6 Time profiles of tumor vascular $\Delta[Hb]_{total}$ and $\Delta[HbO_2]$ in response to different interventions: as air-oxygen-air-carbogen-carbogen+hydralazine-air, for (a) a representative breast tumor (5.1 cm^3) and (b) a prostate tumor (8.7 cm^3) .

Figure 7 (a) The relationship between the digitized responses of $\Delta[Hb]_{total}$ and the tumor physical sizes in the 39 breast tumors. (b) The relationship between the digitized responses of $\Delta[HbO_2]$ and the tumor sizes in the 21 prostate tumors.

References:

[1] R. Cottis, N. Magee and D. J. Higgins, " Haemodynamic monitoring with pulse-induced contour cardiac output (PiCCO) in critical care", Intensive and Critical Care Nursing, 19,301-307 (2003).

[2] W. Buhre, A. Weyland, K. Buhre, S. Kazmaier, K. Mursch, M. Scmidt, M. Sydow, H. Sonntag, "Effect of the sitting position on the distribution of blood volume in patients undergoing neurosurgical procedures", British Journal of Anaesthesia. 84,354-357 (2000).

[3] A.J.G.H. Bindels, J.G. Van der Hoeven , A.D. Graafland, J. de Koning, A.E. Meinders, "Relationship between volume and pressure measurements and stroke volume in critically ill patients", Critical Care, 4,193-199 (2000).

[4] P.Vaupel, "Vascularization, blood flow, oxygneation, tissue pH, and bioenergetic status of human breast cancer", In Nemoto and Lamanna, Oxygen transport to tissue XVIII, Plenum Press, New York, 243-253(1997).

[5] R. S. Bush, R. D. T. Jenkin, W. E. C Allt, F. A. Beale, A. J. Dembo, J. F. Pringle, "Definitive evidence for hypoxic cells influencing cure in cancer therapy". Br. J Cancer 37 (suppl 3), 302-306 (1978).

[6] E. J. Hall, Radiobiology for the radiologist. 4th ed.(Lippincott, Philadelphia, PA.,1994).

[7] M. Nordsmark, J. Overgaard , "A confirmatory prognostic study on oxygenation status and loco-regional control in advanced head and neck squamous cell carcinoma treated by radiation therapy". Radiother Oncol.57, 39-43 (2000).

[8] O. Thews, D. K. Kelleher, P. Vaupel, " Erythropoietin restores the anemia-induced reduction in cyclophosphamide cytotoxicity in rat tumors," Cancer Res, 61,1358-1361 (2001).

[9] S. M. Bentzen, "Quantitative clinical radiobiology", Acta Oncol. 32,259-275 (1993).

[10] G. Lammering, U. M. Carl, H. Pape, K. A. Hartmann: "Changes in hemoglobin concentrations in combined radio- and chemotherapy in locally advanced ORL tumors", Strahlenther Onkol 175 (1999) 11, 559-562 .

[11] J. Overgaard, "Sensitization of hypoxic tumor cells-clinical experience", Int. J.Radiat. Biol. 56,801-811 (1989).

[12] B. W. Pogue, S. P. Poplack, T. O. McBride, W. A. Wells, K. S. Osterman, U. Osterberg, and K. D. Paulsen . "Quantitative hemoglobin tomography with diffuse near-infrared spectroscopy: pilot results in the breast", Radiology, Vol.218(1):261-266(2001).

[13] G. Jasdzewski, G.Strangman, J.Wagner, K.K.Kwong, R.A.Poldrack, and D.A.Boas, " Differences in the hemodynamic response to event-related motor and visual paradigms as measured by near-infrared spectroscopy", Neuroimage 20, 479-488(2003).

[14] K.J.Jeon, S.J.Kim, K.K.Park, J.W.Kim,G.Yoon, "Noninvasive total hemoglobin measurement", J.Biomedical Optics. 7(1): 45-50(2002).

[15] http://www.procrit.com/cancer/cancer_03.htm

[16] R. Tarnawski, K. Skladowski, B. Maciejewski "Prognostic value of hemoglobin concentration in radiotherapy for cancer of supraglottic larynx", Int J Radiat Oncol Biol Phys, Vol.38(5):1007-1011(1997).

[17] Höckel M, Schlenger K, Knoop C, et al. Oxygenation of carcinomas of the uterine cervix: evaluation by computerized O_2 tension measurements. Cancer Res. 1991;51:6098-6102.

[18] Braun RD, Lanzen JL, Snyder SA, et al. Comparison of tumor and normal tissue oxygen tension measurements using OxyLite or microelectrodes in rodents. AJP - Heart & Circulatory Physiology 2001;280:H2533-44.

[19] O'Hara JA, Blumenthal RD, Grinberg OY, et al. Response to radioimmunotherapy correlates with tumor pO2 measured by EPR oximetry in human tumor xenografts. Radiat. Res. 2001;155:466-73.

[20] Elas M, Williams BB, Parasca A, et al. Quantitative tumor oxymetric images from 4D electron paramagnetic resonance imaging (EPRI): Methodology and comparison with blood oxygen level-dependent (BOLD) MRI. Magn. Reson. Med. 2003;49:682-91.

[21] Zhao D, Constantinescu A, Jiang L, et al. Prognostic Radiology: quantitative assessment of tumor oxygen dynamics by MRI. Am. J. Clin. Oncol 2001;24:462-466.

[22] Zhao D, Constantinescu A, Chang C-H, et al. Measurement of tumor oxygen dynamics predicts beneficial adjuvant intervention for radiotherapy in Dunning prostate R3327-HI tumors. Radiat. Res. 2003;159:621-631.

[23] Zhao D, Ran S, Constantinescu A, et al. Tumor oxygen dynamics: correlation of in vivo MRI with histological findings. Neoplasia 2003;5:1-11.

[24] Stone HB, Brown JM, Phillips T, et al. Oxygen in human tumors: correlations between methods of measurement and response to therapy. Radiat. Res. 1993;136:422-434.

[25] Mason RP, Ran S, Thorpe PE. Quantitative assessment of tumor oxygen dynamics: Molecular Imaging for Prognostic Radiology. J. Cell. Biochem. 2002;87S:45-53.

[26] E.J.van Kampen, W.G.Zijlstra, "Spectrophotometry of hemoglobin and hemoglobin derivatives", in Advances in Clinical Chemistry, A.L.Latner and M.K.Schwartz, Eds., vol.23, 200-219, Academic, New York (1983).

[27] J.L.Schmalzel, J.M.Steinke, V.T.Randal, A.P.Shepherd, "An optical hemoglobinmeter for whole blood", Am.J.Physiol.257, H1306-H1311(1989).

[28] G.M. Tozer, and C.C. Morris, "Blood flow and blood volume in a transplanted rat fibrosarcoma: Comparison with various normal tissues", Radiother. Oncol., 17:153-166 (1990).

[29] H. Sands, S. A. Shah, B. M. Gallagher, "Vascular volume and permeability of human and murine tumors grown in athymic mice", Cancer Lett., 27:15-21 (1985).

[30] Nordsmark M, Loncaster J, Aquino-Parsons C, et al. Measurements of hypoxia using pimonidazole and polarographic oxygen-sensitive electrodes in human cervix carcinomas. Radiother. Oncol. 2003;67:35-44.

[31] Evans SM, Hahn S, Pook DR, et al. Detection of hypoxia in human squamous cell carcinoma by EF5 binding. Cancer Res. 2000;60:2018-2024.

[32] H. Liu, A. H. Hielscher, F. K. Tittel, S. L. Jacques, and B. Chance, "Influence of Blood Vessels on the Measurement of Hemoglobin Oxygenation as Determined by Time-Resolved Reflectance Spectroscopy," Med. Phys. 22, 1209-1217 (1995).

[33] M. Kameyama, T. Suto, M. Ito, T. Uehara, I. Ida, M. Fukuda, M. Mikuni, "Noninvasive Measurement of Cerebral Blood Volume Changes in Depression and Schizophrenia: A Multichannel Near-Infrared Spectroscopy Study", NeuroImage Human Brain Mapping 2002 meeting

[34]H.Liu, Y.Song, K. L.Worden, X.Jiang, A.Constantinescu, and R.P.Mason, " Noninvasive investigation of blood oxygenation dynamics of tumors by near-infrared spectroscopy," Appl. Opt. 39,5231-5243 (2000).

[35] J.G.Kim, Y.Song, D.Zhao, A.Constantinescu, R.P.Mason, and H.Liu, "Interplay of Tumor Vascular Oxygenation and pO_2 in Tumors Using NIRS, ^{19}F MR pO_2 Mapping, and pO_2 Needle Electrode," J. Biomed. Optics. 8:53-62 (2003).

[36] Y.Gu, V.Bourke, J.Kim, A.Constantinescu, R.P.Mason, H.Liu, "Dynamic response of breast tumor oxygenation to hyperoxic respiratory challenge monitored with three oxygen-sensitive parameters", Applied Optics, 42:1-8 (2003)

[37] Y.Gu, Y. Song, A. Constantinescu, H.Liu, R.P.Mason, " Vascular oxygen dynamics of breast tumors in response to physiological interventions monitored by Near Infrared Spectroscopy", submitted to Int. J. Radiat. Oncol. Biol. Phys.

[38] Y. Song, "Measurement of tumor blood volume by ^{19} F MRS of PFOB and its correlation to Δ[Hb]total by NIR", PhD dissertation in the University of Texas Southwestern Medical Center. Chapter 8, 2001.

[39] Y.Gu, Z.Qian, J.Chen, D.Blessington, N.Ramanujam ,and B.Chance, "High resolution three dimensional scanning optical image system for intrinsic and extrinsic contrast agents in tissue," Rev. Sci. Instrum.73, 172-178 (2002).

[40] N.J.Baldwin, Y.Wang, T.C.Ng, "In situ ^{19}F MRS measurement of RIF-1 tumor blood volume: Corroboration by radioisotope-labeled [^{125}I]-albumin and correlation to tumor size", Magn.Reson. Imaging, 14(3):275-280(1996).

[41] H. P. Shukla, R. P. Mason, D. E. Woessner & P. P. Antich, "A comparison of three commercial perfluorocarbon emulsions as high field NMR probes of oxygen tension and temperature", J. Magn. Reson. B, 106, 131-141 (1995).

[42]

[43] F.A.Howe, S. P.Robinson , J. R.Griffiths, " Modification of tumour perfusion and oxygenation monitored by gradient recalled echo MRI and ^{31}P MRS", NMR in biomedicine, vol 9, 208-216 (1996).

[44] B. M. Fenton, " Influence of hydralazine administration on oxygenation in spontaneous and transplanted tumor models", Int.J.Radiation Oncology Biol.Phys., vol 49, No.3, 799-808 (2001).

[45] D.G.Hirst, V.K. Hirst, K.M.Shaffi. V.E.Prise and B. Joiner. "The influence of vasoactive agents on the perfusion of tumours growing in three sites in the mouse?" Int. J. Radiat. Biol. ,60 ,211-218(1991)

[46] M.E. Fallowfield, "Vascular volume in B16 allografts and human melanoma xenografts estimated by means of Hoechst 33342", J. Pathol. 157: 249-252(1989)

[47] R.K Jain, "Physiological barriers to delivery of monoclonal antibodies and other macromolecules in tumors ", Cancer Res.(suppl)50:814-819(1990).

$$\underset{\theta}{CF_3} - \underset{\xi}{CF_2} - \underset{\eta}{CF_2} - \underset{\varepsilon}{CF_2} - \underset{\delta}{CF_2} - \underset{\gamma}{CF_2} - \underset{\beta}{CF_2} - \underset{\alpha}{CF_2Br}$$

Figure 1 (A)

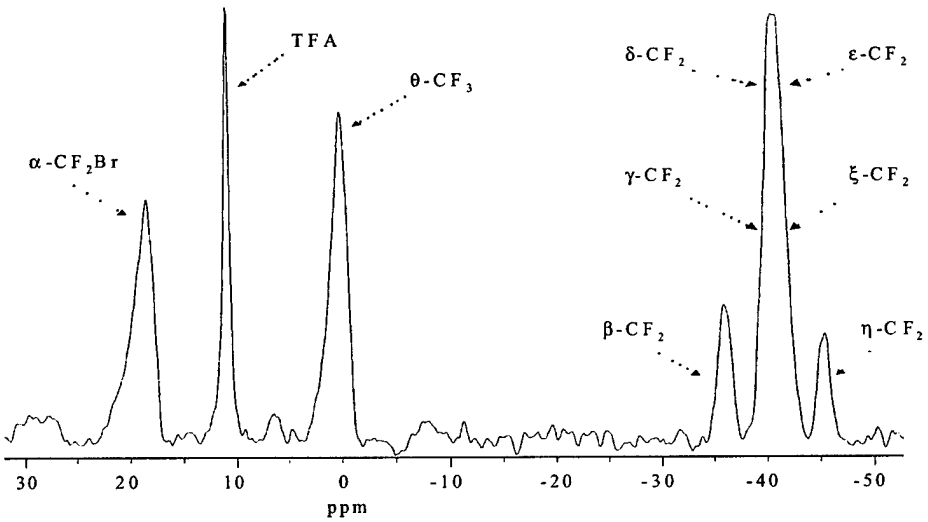

Figure 1 (B)

Figure 1 (A) Molecular structure of perfluorooctylbromide (PFOP), **(B)** ^{19}F NMR spectrum of PFOB emulsion in 2.5ml Fisher rat blood, with TFA as external label.

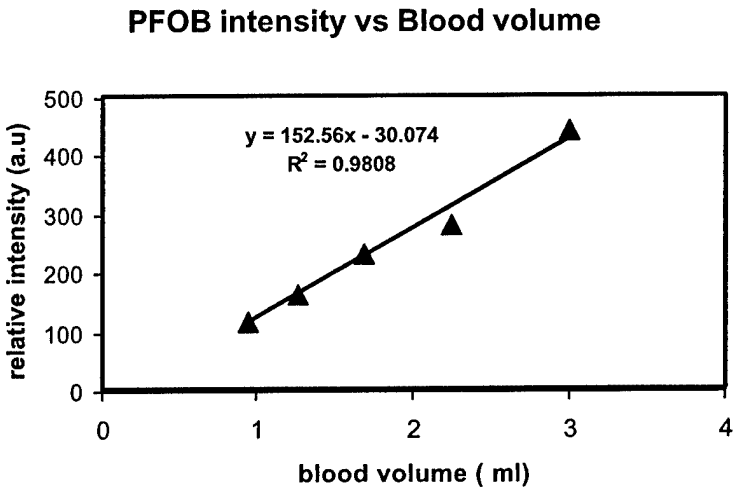

Fig. 2 (A)

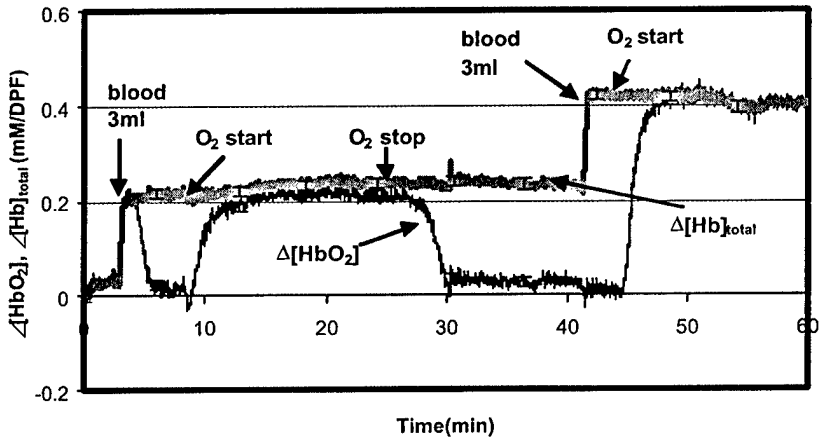

Fig. 2 (B)

Figure 2 (A) The correlation between PFOB intensity and blood volume in phantom study. (B) The time profile of $[HbO_2]$, $[Hb]_{total}$ with respect to oxygen regulation in the phantom solution. O_2 and yeast were used to oxygenate and deoxygenate hemoglobin, respectively. 6ml rat blood was added two times in the two cycles regulation.

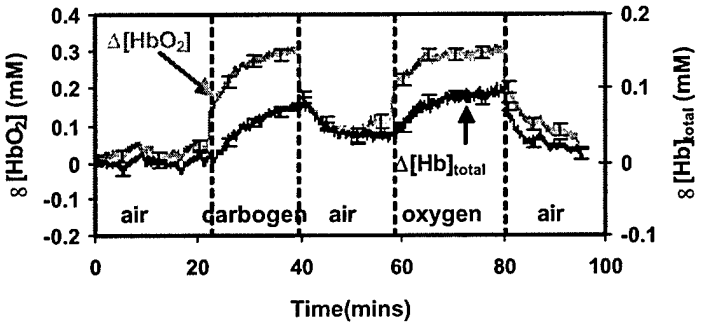

Figure 3 (A)

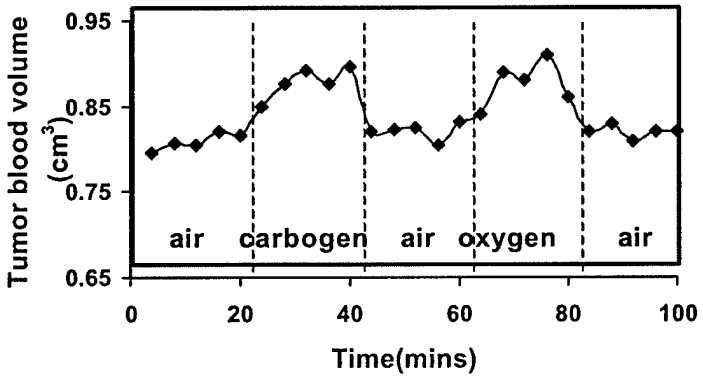

Figure 3 (B)

How about the error bars in Fig.3(B)

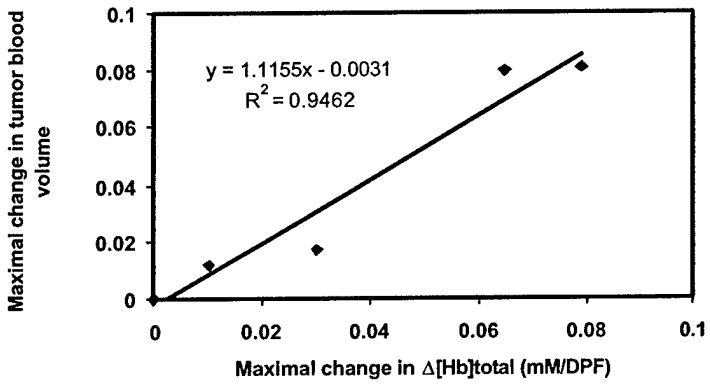

Figure 3 C

Figure 3 (A) Time course profiles of tumor vascular $\Delta[Hb]_{Total}$ and $\Delta[HbO_2]$ monitored by NIRS for a representative breast tumor (2.6 cm^3), with inhaled gas sequence of air-carbogen-air-oxygen-air. (B) Time course of tumor blood volume, $V_{T\text{-}blood}$, measured by ^{19}F MRS of PFOB for the same breast tumor(2.6 cm^3), with gas breathing sequence of air-carbogen-air-oxygen-air. (C) Correlation between the maximal changes (compared to baseline signal) in $\Delta[Hb]_{Total}$ and $V_{T\text{-}blood}$ for each gas inhalation in the breast tumor (2.6 cm^3).

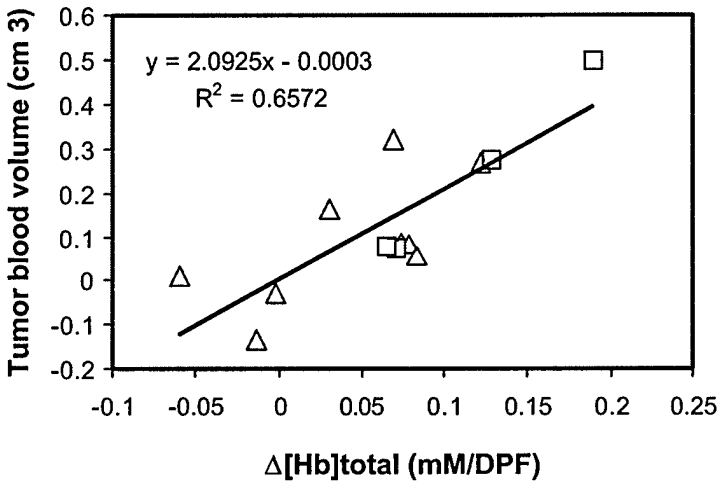

Fig.4 (A)

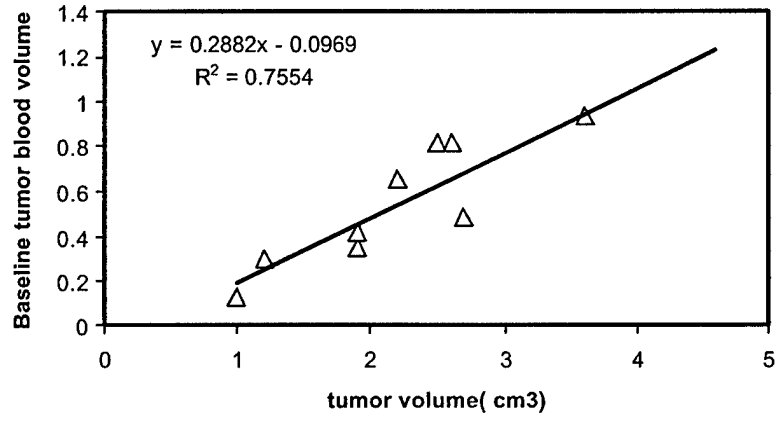

Fig.4 (B)

Figure 4 (A) Correlation between the maximal changes in $\Delta[Hb]_{Total}$ and $V_{T\text{-}blood}$ for hyperoxic gases inhalation in the 9 breast tumors. Triangle : carbogen intervention. Square: oxygen intervention.
(B) Baseline tumor blood volume versus tumor physical volume among 9 of the breast rat tumors.

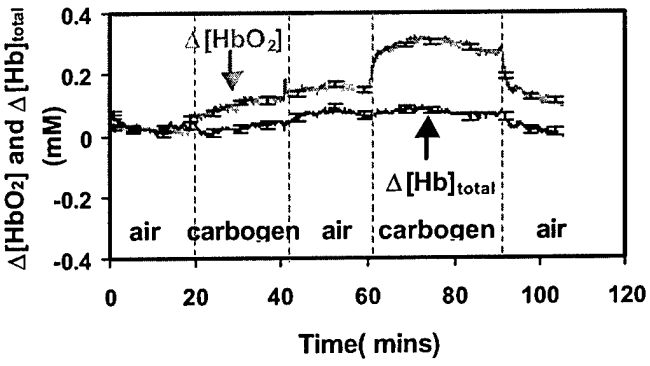

Figure 5 (A)

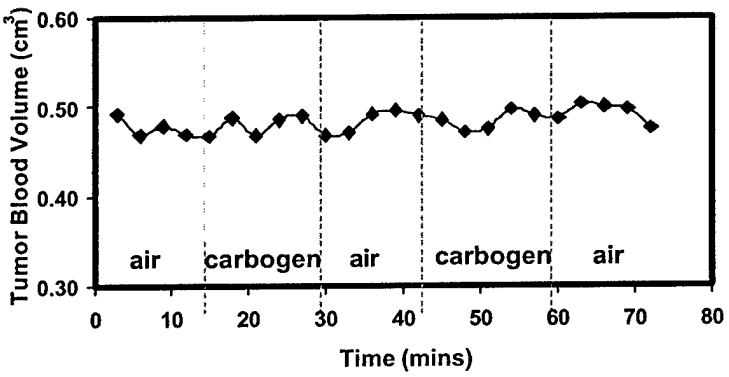

Figure 5 (B)

Figure 5 (A) Time course profile of tumor vascular $\Delta[Hb]_{Total}$ and $\Delta[HbO_2]$ monitored by NIRS for a representative prostate tumor (8.9 cm^3), with respect to repeatedly carbogen intervention as air-carbogen-air-carbogen-air. (B). Time course of tumor blood volume, $V_{T\text{-}blood}$, measured by ^{19}F MRS of PFOB for the same prostate tumor(8.9 cm^3), with gas breathing sequence of air-carbogen-air-carbogen-air.

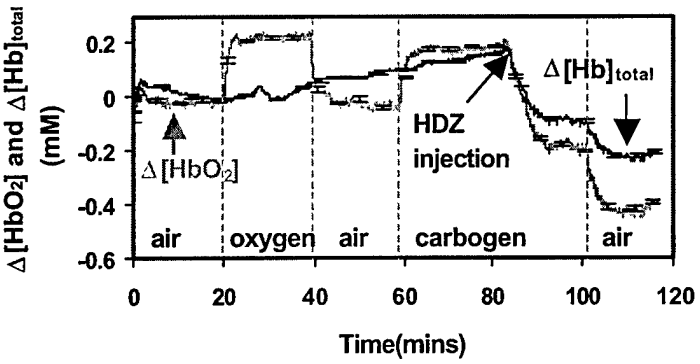

Fig.6 (A)

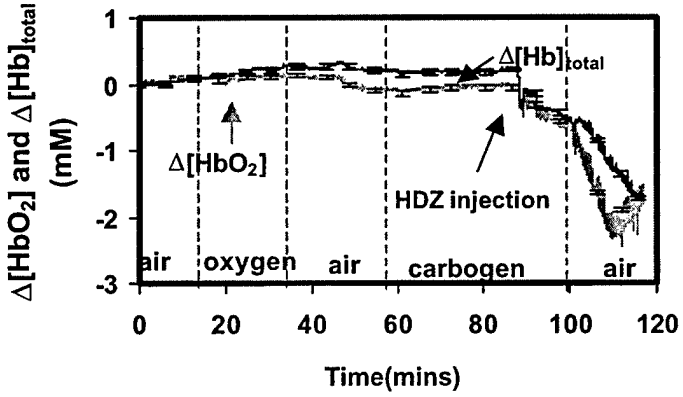

Fig. 6(B)

Fig.6 Time profile of tumor vascular $\Delta[Hb]_{Total}$ and $\Delta[HbO_2]$ in response to different interventions, with inhaled gas sequence as air-oxygen-air-carbogen-carbogen+hydralazine-air, for a representative breast tumor (5.1 cm^3) (A) and prostate tumor (8.7 cm^3) (B)

Tumor model	Total tumors	Response to hyperoxic gases in $\Delta[HbO_2]$	Response to hyperoxic gases in $\Delta[Hb]_{total}$	Response to HDZ administration in $\Delta[HbO_2]$	Response to HDZ administration in $\Delta[Hb]_{total}$
Breast tumor 13762 NF	39	39/39	15/39	19/19	19/19
Prostate tumor R3327-AT1	21	10/21	2/21	5/6	6/6

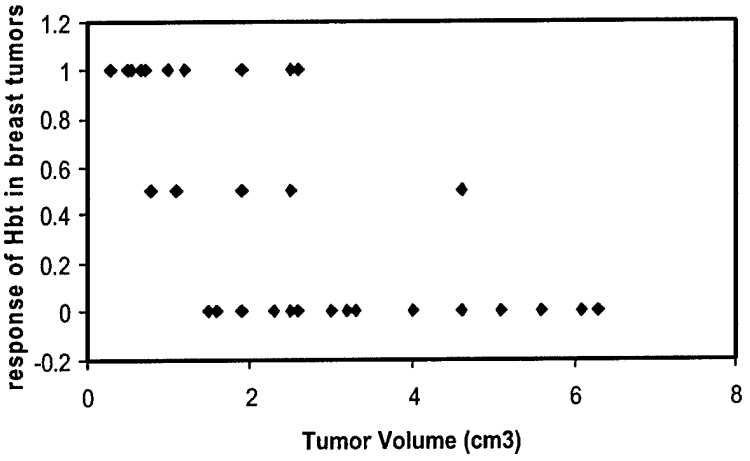

Fig.7 (A)

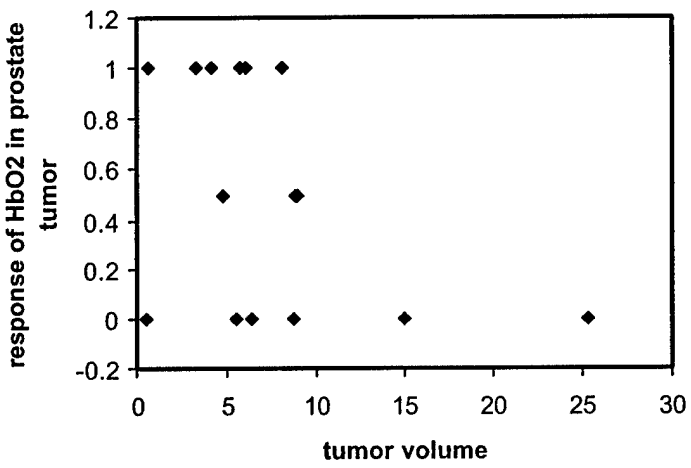

Fig. 7 (B)

Fig.7 The relationship between the response of Hbt in breast (Fig.7A) and HbO2 in prostate tumor (Fig. 7B) with tumor physical volume.